Comprehensive review of enhancement techniques and mechanisms for flow boiling in micro/mini-channels

SHANG, Huiqing, XIA, Guodong, CHENG, Lixin and MIAO, Shanshan

Comprehensive review of enhancement techniques and mechanisms for flow boiling in micro/mini-channels

Huiqing Shang [a], Guodong Xia [a, *], Lixin Cheng [a, b, *], Shanshan Miao [a]

[a] *Beijing Key Laboratory of Heat Transfer and Energy Conversion, Beijing University of Technology, Beijing 100124, China*

[b] *School of Engineering and Built Environment, Sheffield Hallam University, City Campus, Howard Street, Sheffield, S1 1WB, UK*

*Corresponding author. E-mail address: xgd@bjut.edu.cn (G. Xia), lixincheng@hotmail.com (L. Cheng)

Abstract

Due to the urgent need for heat dissipation of high heat flux devices in many engineering applications to maintain high performance and stable operation, flow boiling in micro/mini-channel heat sinks is an enabling and promising approach to tackling high heat flux cooling issues in emerging cutting-edge technology. Various enhancement techniques for flow boiling in micro/mini-channels have been investigated in recent years. These mainly include various surface modifications, enhanced channel structures and composite enhancement techniques. These techniques are able to improve flow boiling heat transfer coefficient (HTC), critical heat transfer (CHF) and mitigate two phase flow instabilities. The composite enhancement techniques take the advantage of each individual technique for flow boiling to achieve more efficient heat transfer and stable flow. However, there are challenges to optimizing these

techniques and understanding the very complex mechanisms involved in these emerging techniques. This paper presents a comprehensive review of the studies of various enhancement techniques for flow boiling and mechanisms in micro/mini-channels having hydraulic diameter of 0.1 - 3 mm over the past five years. First, the criteria for distinction of micro/mini-channels and classification of flow boiling enhancement techniques are discussed. Then, studies of flow boiling enhancement techniques using surface modification techniques and enhanced structures are critically reviewed. Next, the effects of surface modification techniques and enhanced structures on flow boiling heat transfer, CHF, two phase flow patterns, two phase flow instability and mechanisms in micro/mini-channels are discussed and analyzed. Other enhancement techniques such as using surfactants to enhance flow boiling is also mentioned. Finally, future research needs have been identified and recommended according to the comprehensive review and deep analysis. Systematic research on the physical mechanisms underlying the composite heat transfer enhancement techniques is urgently needed. Optimization design of micro/mini-channel flow boiling heat transfer enhancement techniques is a big challenge and should be focused on in future. In order to understand the mechanisms, the bubble dynamics, bubble nucleation and flow patterns of flow boiling in the composite enhancement techniques in micro/mini-channels should be systematically investigated to understand the mechanisms and optimizing the enhancement techniques. Effort should be made to develop prediction methods for flow boiling heat transfer and CHF in the long run.

Keywords: flow boiling, microchannel, minichannel, surface modification technique, enhanced structure technique, composite enhancement technique

Contents

1. Introduction

With the rapid development of advanced technology, strategic frontier areas such as micro-electromechanical systems (MEMS), electronic communication, aerospace, new energy, data center sever chips, insulated gate bipolar transistor (IGBT) modules, the flight control modules of plant protection, unmanned aerial vehicle (UAV), emerging cutting-edge technology and others have been receiving extensive attention in recent years. The large-scale application of the third-generation semiconductor materials and continuous breakthrough in core technologies have accelerated the update and iteration speed of microelectronic device in various fields. With the development trend of integrated miniaturization and high power, the heat flux of microelectronic device continues to increase. Therefore, the heat dissipation of microelectronic device becomes one of the major issues [1-5]. From air cooling scheme to liquid cooling scheme, effective thermal management solution can maintain the safe and stable operation of the device and the entire system, maximize its operating performance and reliability, and improve the service life. However, due to the rapid increase in the heat flux of electronic device, the heat flux can reach up to 100 - 500 W/cm^2 and up to 10^7 W/cm^2 in some extreme cases [6-11]. Single-phase liquid cooling can no longer meet the heat dissipation requirements of the device operation. Flow boiling two phase cooling taking the advantage of the latent heat of phase change is an enabling heat dissipation approach to cooling high heat flux and improve the heat dissipation efficiency [12].

The technology for the removal of high heat flux using flow boiling has excellent heat dissipation capacity. Micro/mini-channel heat sinks take the advantages of this heat dissipation technology even more apparent [13, 14]. HTC and CHF are the key parameters affecting the

heat dissipation performance of micro/mini-channel heat sinks. How to maximize HTC and CHF under the condition of safe operation to achieve maximum heat dissipation efficiency is one of the core challenges in the field of micro/mini-channel heat dissipation [15]. To this end, heat transfer enhancement techniques in micro/mini-channel heat sinks are enabling solutions to deal with the high heat flux cooling issue. Heat transfer enhancement techniques in micro/mini-channel heat sinks are divided into active and passive heat transfer enhancement approaches [16]. Active heat transfer enhancement approach takes external energy, such as adopting electric [17, 18], ultrasonic [19-21], magnetic [22, 23], and other energy fields to the working fluids while passive heat transfer enhancement approach does not consume external energy. Passive heat transfer enhancement techniques can be implemented through various approaches, such as optimizing the cross-sectional shape [24-28] and layout [29-33] of the heat sink channels, improving the surface wettability, using micro-/nano-structure of surfaces [34, 35], and selecting the type of coolants with excellent thermal and physical properties [36-40]. Fig. 1 shows various typical micro/mini-channels with enhanced structures for enhancing flow boiling [25, 26, 31, 33, 41, 42]: (a) triangular groove shape channels, (b) twisted tape channels, (c) embowed groove shape channels, (d) pin-fin rib channels, (e) wavy shape channels and (f) longitudinal vortex generator array channels. For instance, Fig. 1(c) shows a microchannel heat sink consisting of from-sparse-to-dense embowed groove channels which have strong capabilities in enhancing flow boiling and some shortcomings of flow boiling in a straight channel heat sink are overcome [31].

In recent years, composite passive techniques, such as combining surface modification and channel structures with micro/mini-channels, are emerging approaches to enhancing flow

boiling. Under the influence of different channel cross-sectional shapes, layouts, and micro-/nano-structures, composite enhancement techniques can break the development of the thermal boundary layer, enhance the local disturbance, promote bubble growth, and suppress rapid merging of bubbles and achieve sufficient mixing of cold and hot fluids in micro/mini-channels. This can lead to efficient heat dissipation in micro/mini-channel heat sinks. Composite passive heat transfer enhancement techniques are divided into single-type combination, such as the combination of sidewall cavities and ribs [43], and multi-type combination, such as surface wettability with ribbed channels, micro-/nano-structures combined with ribbed channels and so on [44-47]. These micro/mini-channels combine the advantages of surface modification and channel structures.

Combined structures of various types of enhanced micro/mini-channels which integrate the advantages of each individual enhancement approach have become one of the mainstream research directions for enhancing flow boiling in recent years. Compared to the smooth inner wall channels, concave cavity structures arranged on both sides of micro/mini-channel walls or rib structures placed in the middle of the channels can significantly improve flow boiling HTC and CHF. This is achieved by enhancing the disturbance to promote the rupture of large bubbles and avoiding the occurrence of drying and backflow. To a certain extent, this alleviates the instability of flow boiling in micro/mini-channels. Some studies have found that there are significant differences in the gain effects produced by different concave cavity types. The triangular concave cavity can increase the local HTC by nearly 10 times, and the elliptical concave cavity can achieve a significant advantage of reducing the wall temperature by about 6-10℃ [48-50]. The synergistic effect of porous coating structures on micro/mini-channel

sidewalls or ribs and microstructures in micro/mini-channels on flow boiling performance enhancement is significant. These composite enhancement techniques not only keep the original heat transfer advantage, but also suppress the occurrence of heat transfer deterioration.

Fig. 2 shows various surface microstructures used for flow boiling heat transfer enhancement: (a) micro-structured surfaces and micro-nano-hierarchical-structured surfaces with polydimethylsiloxane (PDMS) coatings; (b) etched surfaces and rose petal surfaces and (c) nanoscale structures on the microporous coatings. These composite structures are able to provide a large number of bubble nucleation sites, increase the density of active bubble nucleation sites, reduce the obstruction of interphase energy barrier, and promote the appearance of nucleation points in advance [54]. Just to show one example here, Fig. 3 shows the effect of the composite microchannel heat sink on the enhanced heat transfer performance and CHF. On the one hand, the treated surface has advantages over the bare surface in terms of CHF, HTC, and the degree of superheat at the onset of nucleate boiling. It shifts the boiling curve to the left and achieves higher CHF. As shown in Fig. 3(a), the required superheat degree at the onset of nucleate boiling is reduced by about 90%. On the other hand, the composite structure increases the rewetting ability in the micro/mini-channels, forms a liquid film evaporation, improves CHF and optimizes the heat transfer performance in the micro/mini-channels [55]. It is crucial to address the interface thermal resistance between the micro/mini-channel heat sink and the heating device during the heat dissipation. In addition, the durability of the micro-/nano-structure of the micro/mini-channels is a critical issue which needs to be solved. Therefore, extensive research is urgently required to alleviate the drawbacks caused by these problems. In this aspect, composite enhanced micro/mini-channels combining the surface

characteristic and channel structures have the ability to enhance the local disturbance with high surface nucleation activity of micro-/nano-structures. They can achieve effective heat dissipation under high heat flux even at lower mass flux, avoid high-temperature damage areas on the surfaces and ensure safe operation within a range of suitable temperatures [56, 57].

Modified surfaces have a significant effect on the enhancement of flow boiling heat transfer in micro/mini-channels. They are able to advance the onset of nucleate boiling and improve HTC [12, 58, 59]. Nanofluids can achieve similar heat transfer effects as a micro/nano composite heat sink when it comes into contact with the sidewall surfaces. Singh et al. [60] investigated the influence process of the convective heat transfer between a nanofluid and porous wall surfaces. According to the available studies, composite micro/mini-channel heat sinks integrating with micro/nano characteristics and channel structures can significantly inhibit this issue.

Although micro/mini-channel heat sinks have a great advantage in flow boiling heat transfer, two phase flow instability is one of the inevitable issues in flow boiling. Studies on flow instability in micro/mini-channel heat sinks have been extensively conducted to mitigate it over the past decades. Wang et al. [61] present a summary of various methods to suppressing flow boiling instability in different channels and the overall influence trend of instability on flow boiling heat transfer. Their research presents a good reference for further research on suppression of flow boiling instability in micro/mini-channels. However, limited studies have been conducted to explore and understand the mechanisms of the flow boiling in various enhanced micro/mini-channels with the aim of maximizing the effective heat dissipation performance.

So far, most of the available review studies on heat transfer enhancement using the methods of coatings and micro/nano-structures have mainly focused on pool boiling. However, there is little review available on flow boiling and two phase flow in micro/mini-channel with surface treatment technique, enhanced micro/mini-channels and composite enhancement techniques. To fully understand the current status of the research and technology development of flow boiling in enhanced micro/mini-channels, this paper presents a comprehensive review of the available studies on flow boiling enhancement techniques and mechanisms in enhanced micro/mini-channels with the surface characteristics and various structures, composite enhanced micro/mini-channels for high heat flux dissipation scenarios, highlights the challenges of the flow boiling enhancement techniques and identifies the future research and development needs.

2. Micro/mini-channel classification and types of flow boiling enhancement techniques

2.1. Criteria for classification of micro/mini-channels

The criteria for classification of macroscale and micro/mini-channels are strongly affected by the fluid types, fluid properties, intermolecular forces, gravity, surface tension, inertial forces, growth and coalescence of bubbles and suppression of nucleate boiling in the channels. The channel size has a significant effect on flow boiling heat transfer characteristics, flow patterns, CHF and the mechanisms of promoting nucleation and the essence of preventing the heat transfer deterioration. Therefore, it is essential to distinct macroscale and micro/mini-channels in investigating flow boiling and gas liquid two phase flow characteristics in channels.

Flow channels are classified as micro-channels, mini-channels or conventional channels in

the available studies by some researchers while they are also grouped into macroscale channels and micro/mini-channels by other researchers. However, there is no agreed criterion for the classification of the channels although various definitions have been proposed. For example, Mehendale and Jacobi [62] have classified different channels based on the hydraulic diameters (D_h). Channels with D_h from 1 μm to 100 μm are considered micro-channels, those with D_h between 100 μm and 1000 μm are classified as mini-channels, and channels with D_h greater than 6 mm are classified as conventional channels. Based on engineering practice and application areas such as refrigeration industry in the small tonnage units, compact evaporators employed in automotive, aerospace, air separation, and cryogenic industries, cooling elements in the field of microelectronics and MEMS, Kandlikar and Grande [63] have proposed the channel classification according to a range of D_h. When D_h is greater than 3 mm, it is considered as a conventional channel. Channels with D_h in the range of 200 μm - 3 mm are considered as mini-channels and the range of 10 - 200 μm are micro-channels. Fig. 4 shows the comparison of the channel classification criteria A by Mehendale and Jacobi [62] and criteria B by Kandlikar and Grande [63]. There are big differences between the two criteria. The classification criteria of Kandlikar and Grande have been recognized and adopted by many researchers as they are related to engineering practical applications [64]. However, these classification criteria are simply based channel hydraulic diameters and lack the physical mechanisms.

Cheng et al. [65, 66] present comprehensive reviews of the flow patterns and distribution of gas-liquid two-phase flows in micro/mini-channels. They have summarized various channel classification criteria including those by Mehendale and Jacobi [62], Kandlikar and Grande [63] and the criteria using dimensionless numbers for classifying conventional channels and

microchannels. For example, Kew and Cornwell [67] proposed the confinement number *Co* as the classification criterion for distinguishing microchannels and conventional channels as:

$$Co = \frac{1}{D_h}\sqrt{\frac{\sigma}{g\left(\rho_l - \rho_g\right)}} \tag{1}$$

where *Co* is the confinement number, σ is the surface tension, *g* is the gravitational acceleration, ρ_l and ρ_g are the density of liquid and vapor, respectively. When *Co* is less than 0.5, a channel is defined as microchannel.

Triplett et al. [68] adopted the Laplace constant L_c to distinguish a microchannel and a conventional channel as:

$$L_c = \sqrt{\frac{\sigma}{g\left(\rho_l - \rho_g\right)}} \tag{2}$$

When D_h is less than or equal to L_c, it is a microchannel.

Efforts have been made to propose various criteria for micro/mini- and macro- channels based on experimental studies over the past years. For example, the process of bubble nucleation and growth in the channels followed by their dischargement raise an important question regarding whether the channel constrains bubble growth during this process. Existing experimental data indicate that mass flux can influence the flow pattern in the channels, which subsequently affects the classification criteria for the channels. Li and Wu [69] have proposed a criterion that relates mass flux to the hydraulic diameter of channels based on their analysis

of heat transfer behavior and extensive flow boiling data. The new conventional-to-micro/mini-channel criterion is as follows:

$$BdRe_{\mathrm{l}}^{0.5} = 200,\ Bd = 4 \tag{3}$$

where Bd is the Bond number. When $BdRe_{\mathrm{l}}^{0.5} \le 200$, Nu_{tp} has a strong relationship with $BdRe_{\mathrm{l}}^{0.5}$, and the channel is classified as a micro/mini-channel. Otherwise, it is the conventional macrochannel. The proposed criterion is as follows:

$$BdRe_{\mathrm{l}}^{0.5} \le 200,\ Nu_{\mathrm{tp}} = 22.9\left(BdRe_{\mathrm{l}}^{0.5}\right)^{0.355} \tag{4}$$

Harirchian and Garimella [70] have proposed a similar dimensionless criterion for distinguishing channel types based on a large amount of flow boiling data and their experimental flow pattern map, which is related to the mass flux and the cross-sectional area. Their proposed formulas are expressed as follows:

$$Bd^{0.5}Re_{\mathrm{l}} = \frac{1}{\mu_{\mathrm{l}}}\left[\frac{g\left(\rho_{\mathrm{l}} - \rho_{\mathrm{g}}\right)}{\sigma}\right]^{0.5} GD^2 = 160 \tag{5}$$

$$D = \sqrt{A_{\mathrm{cs}}} \tag{6}$$

where $Bd^{0.5}Re_{\mathrm{l}}$ is named the convective confinement number, μ is the dynamic viscosity, G is

the mass flux, D is the length scale, and A_{cs} is the cross-sectional area of a micro/mini-channel. For $Bd^{0.5}Re_l < 160$, the channel is defined as the microchannel.

There are also other different classifications of the channels [65, 66]. So far, there is no universal classification criteria for micro/mini- and macro- channels. In this review, flow boiling enhancement techniques in channels with hydraulic diameters of 0.1 - 3 mm are focused on. This will help to understand the flow boiling enhancement techniques in a wide range of channel sizes.

2.2. Types of enhancement techniques for flow boiling in micro/mini-channels

The micro-structures of enhanced micro/mini-channels involve the expansion of surface area and the change of surface roughness. The expansion of area and the change of surface roughness can achieve good surface wettability and increase the effective heat transfer area, so as to increase the effective bubble nucleation point density. More in-depth research has been conducted on the implementation methods of channel surface characteristics in flow boiling in micro/mini-channels. Surface treatment process is becoming increasingly mature with technological advancement. Previous studies employed various techniques such as spraying [71], vapor deposition [72, 73], electrochemical deposition [74, 75], sintering [76, 77], laser etching [78-81], chemical etching [82, 83], and hot embossing [84] to modify channel surface characteristics. These techniques have been used to create modified surfaces on the sidewalls of micro/mini-channels with more nucleation active sites or micro-nano structure sidewalls with microlayers. The porous and microlayer sidewalls exhibit strong permeability and capillary wicking ability, which can enhance flow boiling, improve the surface rewetting effect and

prevent heat transfer deterioration. In the meantime, the treated channel surfaces contain numerous air pockets, which can promote bubble nucleation and increase the frequency of bubble generation and separation from the heat surface. Fig. 5 shows the summary of various techniques of porous structures on channel surfaces to enhance flow boiling in micro/mini-channels.

Structural metals are an important technique to enhancing flow boiling in micro/mini-channels. Foam metal or woven metal mesh, as a type of structural metal with high porosity, low density and high strength, has been studied for its potential to enhance flow boiling in micro/mini-channels. Addition of foam metal can also play the effect of porous structure, improve the surface wettability and surface topology, change the flow boiling mode and heat transfer mechanisms in micro/mini-channels, and greatly reduce the wall superheat required for flow boiling, so as to adapt to the increasing heat dissipation scenario [85]. Foam metal can be used as a material for manufacturing micro/mini-channel heat sinks. It can be used as a separate material for the channel walls or the channel bottoms and can even be used as a filler in micro/mini-channels. However, appropriate structural metal heat sink preparation methods should be chosen based on the actual heat dissipation requirements of the occasion [86-90].

There are other treatment processes such as increasing the surface roughness of micro/mini-channels or forming the surface of the channels. Various processes have been developed over the past decades, such as wire-arc thermal spray [91], grayscale lithography [92], deep reactive ion etching (DRIE) [93, 94], electrospinning [95], and electrical-discharge machining (EDM) [96]. For instance, EDM technology is used to develop a microstructure on the heated boiling surface [97], which forms a surface coating with the characteristics required

for flow boiling enhancement, such as increased porosity and enhanced capillary wicking capacity. Therefore, as control technology precision continues to improve, use of those treatment processes to enhance micro/mini-channel flow boiling becomes increasingly wide applications.

3. Research on flow boiling enhancement in micro/mini-channels

Flow boiling heat transfer performance is affected by the dynamics of bubbles in micro/mini-channels due to different wetting patterns. Table 1 lists the selected studies of flow boiling and two-phase flow in enhanced micro/mini-channels with microstructures or coatings. These studies show that adjusting the characteristics of the inner channel surfaces of the heat sink has a positive effect on enhancing flow boiling performance in the micro/mini-channels, achieving enhancement amplitudes ranging from 10% to 200%. In the meanwhile, these processing techniques also provide strong data support for future research on new heat transfer enhancement techniques using microstructures and coatings in micro/mini-channels.

Kim et al. [98] proposed three non-uniform wetting patterns: crosswise pattern, parallel pattern and dotted pattern, and studied the heat transfer performance and bubble movement mode under different conditions. These non-uniform wetting patterns are shown in Fig. 6. The difference between these patterns results in varying nucleation point densities and rewetting abilities, leading to non-uniform wetting patterns. There should be an optimal value of heat transfer. In the non-uniform wetting patterns, the proportion of hydrophilic and hydrophobic stripes is a crucial research content. If the hydrophobic fringe pattern is too wide or too narrow, it can negatively impact the heat transfer process. If the hydrophobic stripe is too narrow, it can reduce the nucleation density point of the bubble. Conversely, if the hydrophobic stripe is too

wide, the bubbles will be confined to this region and may not be discharged in time, which is detrimental to the heat transfer process. Experimental analysis shows that the optimal proportion of hydrophobic area in parallel pattern is the same as that in dotted pattern, at approximately 32%. However, the optimal proportion in crosswise pattern is much smaller, at only about 16.5%. In addition, significant difference in bubble merging behaviors exists between different patterns. The rewetting liquid required by the hydrophobic region can be replenished from the hydrophilic region due to the alternating distribution of hydrophilic and hydrophobic stripes, and the bubbles formed in the hydrophobic region can be separated in time. This can prevent the growth of bubbles without limit and effectively inhibit the merger between bubbles. Moreover, when the stripe direction is perpendicular to the flow direction, the non-uniform wetting surface can increase the heat transfer coefficient by almost 40%, and this represents a significant improvement compared to previous studies [99]. In the non-uniform wetting, a gradient wettability surface can enhance flow boiling heat transfer and suppress flow instability. Tan et al. [100] prepared gradient wetting surfaces using 1.0 M sodium hydroxide / 0.05 M ammonium persulfate solution and 1 wt% fluorosilane ethanol solution. This surface has a gradient wetting property, with hydrophobicity upstream and hydrophilicity downstream, and it can increase the disturbance frequency in the microchannel under high heat flux, preventing the rapid aggregation and merging of bubbles, which leads to enhance flow boiling heat transfer. Gradient wetted surfaces can improve the comprehensive enhancement benefit by over 50% due to their upstream enhanced nucleation and downstream enhanced fluid supplement, making it become a widely applicable enhancement method in the field of flow boiling heat transfer. Lioger-Arago et al. [101] applied a hexagonal-shaped mask to deposit

SiOC coating on the substrate surface, creating a non-uniform wettability surface as shown in Fig. 7. By comparing the heat transfer coefficient changes at different channel positions and mass flow rates, it shows that the heat transfer coefficient appears a peak value with the increase of heat flux. This means that it gradually increases before the drying occurs during the heat transfer process. In addition, the HTCs at the upstream position in the mini-channel are generally higher than those at the downstream. However, the HTCs do not always follow the afore-mentioned trend at all heat fluxes, excessively high or low heat flux can negatively impact heat transfer in the channel, preventing it from reaching optimal conditions. Compared to the porous coating surface of polymer-derived ceramics (PDC), the SiOC coating is less sensitive to flow boiling enhancement. The CHF is increased by about 10% at low mass fluxes, and is only a quarter of that on the PDC porous coating surface. Therefore, the porous structure plays an import role in flow boiling heat transfer enhancement.

Flow boiling heat transfer in micro/mini-channels can be enhanced by modifying the surface wettability. There are some differences in the nature of bubble nucleation from alternating hydrophilic and hydrophobic surfaces to porous coated surfaces. The former uses hydrophobic surfaces to reduce the barriers of bubble nucleation, while the latter increases the bubble nucleation density. When studying the enhancement of flow boiling heat transfer on a porous surface coating, it is important to ensure that the thickness and coverage of the coating are uniform, the adhesion is strong, and the coating does not easily fall off. The ABM (‘A’ is aluminum particles, ‘B’ is brushable ceramic epoxy, ‘M’ is methyl ethyl ketone)) coating used in the surface does not show any signs of falling off after 110 hours of boiling. The use of porous coatings can easily increase the average HTC by 1.5 times while the HTC and CHF can be

increased by 2.5 times and 2 times respectively when the coating pore size and thickness are optimized. This demonstrates the substantial benefits of utilizing such coatings [102]. However, experimental research has shown that not all porous coatings can enhance boiling heat transfer. The process depends on the coating thickness and the size of the surface coating micropore, which in turn is affected by the particle size. Therefore, the performance of boiling heat transfer is also affected by the size of the coating pore. Zhang et al. [76, 103] and Mao et al. [104] prepared a porous structured coating with different dendritic copper particle sizes on the microchannel surfaces. Copper particles of different sizes were selected in the size range of 10 μm - 150 μm to be coated on the surfaces. Fig. 8 displays the SEM pictures of the porous surfaces created by sintering copper particles with varying diameters. It can be seen that the surfaces formed by larger particle diameters contain more large-sized pores. The experimental results show that the sizes of the particles have a significant effect on flow boiling HTC and CHF in the microchannels. There is an optimum value of the particle sizes. If the size exceeds this, the overall performance of boiling heat transfer in micro/mini-channels cannot reach the expected effect and the opposite trend occurs. By comparing the heat transfer behaviors of on the coatings having different copper particle sizes, it is found that boiling at high heat flux is mainly capillary evaporation, that is, thin liquid film evaporation, which is different from nuclear boiling at low heat flux. The coating with a particle size in the range of 90 μm - 120 μm shows the expected effect and achieves the highest CHF as shown in Fig. 9. The timely supply of liquid in the channel is the essence of the effect of size on boiling heat transfer. It is also the effect of the interaction between particle diameter and coating thickness. Although the porous metal coating plays a very important role in improving the heat transfer, there is a problem

which needs to be considered with this type of coating. Whether the metal coating particles will be oxidized during the use of this process and its enhancement effect will be weakened, or even be failed. The range of optimal particle size for efficient heat transfer in the micro/mini-channel is also affected by the cooling medium [105]. The basis for optimizing the heat transfer characteristics in the micro/mini-channel is the change of wettability and the presence of microporous structure [106]. Not only the cooling medium affects the heat transfer, but also the influence of the coating type is very obvious, which is mainly due to the difference in the pore structures of the coatings, and the larger particle size has more advantages. Compared with the smooth surface, the TiO_2 coating surface can increase the CHF by about 20% while the Al_2O_3 coating surface can increase the proportion to about 25%, showing a better heat transfer improvement effect [107]. Fig. 10 shows the SEM pictures of the surface microstructures of the two coatings. The flow boiling heat transfer is enhanced by filling the porous structures in the micro/mini-channels, which is consistent with that by using the porous inner-wall in the channels. The presence of a large number of cavities and gaps creates favorable conditions for activating bubble nucleation [108]. Therefore, designing multifunctional structures is crucial to enhancing flow boiling performance in micro/mini-channels. Ahn et al. [109] utilized the advantages of carbon nanotubes to form the two-tier vertically aligned multiwalled carbon nanotube (VAMWNT). The number of bubble nucleation microcavities increases with the aggregation of carbon nanotubes while also limiting the growth of bubbles. This structure creates a distinct channel that efficiently separates vapor from the liquid flow area. This prevents vapor from deteriorating the heat transfer phenomenon and enhances heat transfer performance within the channel. The structure exhibits excellent heat transfer performance

under various heat flow and steam quality conditions. The structure exhibits excellent heat transfer performance under most various heat flux and vapor quality conditions. Even when the CHF is not reached, the HTC is significantly higher than that using other heat transfer enhancement techniques.

The two main methods to enhancing the thermal performance in micro/mini-channel heat sinks are to improve heat transfer efficiency and suppress flow boiling instability. The main methods to improving heat transfer efficiency are to increase the overall flow boiling HTC, the CHF and reduce the wall superheat required at the beginning of boiling. However, preventing nucleation bubbles from growing and merging quickly is the key to inhibiting flow boiling instability in the micro/mini-channel heat sink, and the generated vapor must be discharged promptly. Therefore, the surface microstructure is undoubtedly one of the main factors to enhance boiling heat transfer in micro/mini-channels. Both the coating microstructure and the etched microstructure play the same role in enhancing flow boiling essentially. Modifying the microstructures of micro/mini-channel surfaces increases the number of tiny cavities or gaps, providing more vaporization core, promoting nucleation separation of the bubble, and inhibiting rapid growth of the bubble. In addition, this method can increase the direct heat transfer area between the channels and the flowing liquid to improve the flow boiling performance in the micro/mini-channels. In the meanwhile, the modified microstructures can also improve the capillary wicking ability of the contact surface to some extent and promote rewetting, significantly delaying the formation of the vapor film and preventing the formation of continuous drying areas in the micro/mini-channels [110, 111]. Alternatively, the microstructures may exhibit micro layers, which can trigger a more efficient mechanism of thin

liquid film boiling in the channels. As electronic devices generate higher heat flux, the space available for heat dissipation becomes limited. Consequently, the requirements for micro/mini-channel flow boiling heat dissipation become increasingly stringent. Enhancing flow boiling heat transfer needs to adopt a more effective improvement of new ways. Inspired by the nature case of efficient heat dissipation, periodic changes may be a very promising development direction. Porous microstructures such as carbon nanotube coatings and sintered metal particle porous coatings are selected through segmentation in the micro/mini-channels to achieve the gradient wetting mentioned by Tan et al. [100] or to form a circulating microstructure, keeping the liquid film in the development stage without the occurrence drying. However, different treatment processes can increase the difficulty of processing the micro/mini-channel heat sink, which may become the key to controlling the increase of flow boiling heat transfer in the future. So far, significant improvements of heat transfer performance in channels have been achieved by using some enhancement techniques. These enhancement effects can fulfil the necessary heat dissipation requirements of micro/mini-channel heat sinks.

3.1. Research on flow boiling in enhanced micro/mini-channels with surface modification techniques

3.1.1. CHF enhancement in micro/mini-channels

Table 2 summarizes the selected studies of the surface modification techniques to flow boiling heat transfer enhancement in micro/mini-channels. The advantages of surface modification techniques in flow boiling heat transfer enhancement are obvious according these studies. In particular, the enhancement effect is almost doubled through the superposition of the

treatment methods or the mixing of surface materials. CHF enhancement is crucial to flow boiling in micro/mini-channels. Research of CHF enhancement using surface modification techniques in micro/mini-channels has been extensively conducted in recent years. Wang et al. [71] created porous 316L coatings ranging from 80 μm to 120 μm in size on the surface of SA508 steel using a direct spraying process. The cooling time of heating surface is significantly reduced as compared to that of an ordinary surface under the same conditions, with a reduction of over 56%. The heat transfer performance has been significantly improved by the porous coating and the CHF has increased by about 30%. Surface wettability is a crucial parameter in micro/mini-scale boiling heat transfer. The dynamics of bubbles in micro/mini-channels is affected by heat transfer performance due to the surface wettability. Modifying the surface wettability at the solid-liquid interface can significantly improve the CHF. Khanikar et al. [73] developed a type of carbon nanotubes (CNTs) coating for copper-based microchannels to improve flow boiling heat transfer and CHF. They added the multilayer metal catalysts in coating. It shows that the addition of catalyst can reduce the thermal resistance between the CNTs coating and the copper-based surface, thereby enhancing the durability. However, during a long period of flow boiling heat transfer experiments, the surface morphology of the CNTs coating was changed as the carbon nanotubes was washed by the fluid. Fig. 11(a) shows obvious bending and overlapping, forming a unique “fish scale” shape. Although the durability of the coating has been improved, its rigidity may limit its performance. After repeated experiments, it was found that CNTs gradually lost their enhancement effect on the CHF due to the strong shear force, and the maximum decrease in the CHF exceeds 30% compared to that in the first test. Therefore, the rigidity of this coating under the experimental conditions of high mass

flowrate needs further strengthening. Kumar et al. [112] improved the adhesion between the copper surface and the CNTs coating by using sandblasting treatment and a diamond intermediate layer to alleviate the durability. Fig. 11(b) illustrates the diamond intermediate layer and the CNTs coating attached to its surface. Flow boiling experiments were conducted at different mass flow rates to investigate the effect of CNTs coating on flow boiling heat transfer. The coating can significantly enhance flow boiling heat transfer, particularly at low mass fluxes when the CNTs remain in a vertical state which provides a higher bubble nucleation density and enhances the local disturbances, resulting in enhancing flow boiling performance and increasing CHF by 21.9% at the mass flux of 283 kg/(m^2s). Fig. 12 shows the trend of enhanced heat transfer of CNTs coatings with various mass fluxes. It shows the same trend as that of Khanikar et al. [73] and the enhancement effect is reduced as the mass flux continues to increase. Kousalya et al. [113] prepared a CNTs coating with a non-uniform wetting region that has alternating superhydrophilic and superhydrophobic streaks. The relevant coating microstructures and the alternating non-uniform wetting patterns of the superhydrophilic/superhydrophobic surfaces are shown in Fig. 11(c). This coating is formed by graphitic petal-decorated carbon nanotubes (GPCNTs). The graphitic petals are a carbon nanostructure comprising of stacks of graphene layers standing vertically on a substrate. By adjusting the area fraction of the superhydrophilic region, the flow boiling heat transfer performance can be improved. It indicates that a non-uniform wetting coating surface can significantly enhance flow boiling heat transfer performance as compared to a uniform wetting surface. When the area fraction of the superhydrophilic region is between 66% and 85%, higher heat transfer performance can be achieved, and bubble nucleation can be triggered earlier. On

the one hand, the hydrophobic property reduces the nucleation barrier, while the porous structure increases the bubble nucleation density. On the other hand, addition of a higher proportion of hydrophilic streaks greatly enhances the coating rewetting ability, which stimulates the thin liquid film boiling and improves the CHF by regulating this area fraction.

Porous coatings not only increase the density of nucleation points but also promote liquid penetration. When the liquids penetrating the cavities can be connected together, they can stimulate a thin liquid film boiling with higher efficiency. Graphene nanoplatelets (GNPs) coatings are one of them, and their ultrafast liquid permeability is the main factor in enhancing heat transfer and their tunable wettability makes them one of the highly popular coating materials. Sia et al. [114] combined graphene nanoplatelets with silver-filled epoxy (GNPs/SE) and carbon-filled epoxy (GNPs/CE) respectively, to achieve tunable wettability (superhydrophilic, hydrophobic and superhydrophobic) in the minichannel surfaces by the thermal curing process. Then, they investigated the enhancing effect of this coating on flow boiling heat transfer performance. Fig. 13 shows the schematic diagram of the heat transfer enhancement mechanisms of the coatings. The superhydrophilic surface has a higher density of nucleation sites than other surfaces. The enhanced heat transfer trend is due to the nano capillary network of the superhydrophilic GNPs/SE coating, which accelerates liquid permeability to form the rapid rewetting action and efficient thin liquid film boiling heat transfer. This avoids drying up during flow boiling, resulting in increasing the CHF by up to 59.5% at lower mass flowrates. Therefore, the coating is more conducive to flow boiling heat transfer. The ultrafast liquid permeability of the GNPs coating is a unique phenomenon in the research of enhancing flow boiling heat transfer. While the liquid permeability can create an efficient thin liquid film

boiling for heat transfer, but it is not that the faster the permeability, the better the heat transfer. However, if the liquid penetration rate is too fast, it can hinder the timely discharge of vapor between the interlayers, leading to discontinuity of thin liquid film boiling and a reduction in boiling heat transfer performance. Subsequently, the preparation process for hydrophobic and superhydrophobic coatings was altered, and the effect of flow boiling in the coating channels was investigated [115]. However, the performance of the superhydrophobic coating with improved process contradicts conventional understanding, which is superior to that of the superhydrophilic surface. It can increase the CHF by 134% at the mass flowrate of 57 kg/(m^2s) while the superhydrophilic surface can only achieve about half of it, which is about 71.8%. This interesting trend is caused by the pressure-induced wetting transition of the superhydrophobic coating from the Cassie-Baxter to the Wenzel states, and this can easily achieve the detachment of pinning bubbles, resulting in lower wall temperatures. This process is illustrated in Fig. 14.

Selecting an appropriate coating treatment process can improve the durability of the porous coating, enhance adhesion between the coating and surface, and extend the lifespan of the porous coating. Cu-TiO_2 nanocomposite coating was prepared on a copper surface using electrochemical deposition technology and the heat transfer characteristics of flow boiling were studied using deionized water as the cooling medium [116]. The coating was obtained by applying different current density deposition, and then the porous structure was increased at a lower current density to form the final nano-composite coating. The coating exhibits good adhesion to the copper surface and is very suitable for practical heat transfer environments. The experimental results indicate that the CHF increases by up to 92% when compared to that on the bare copper surface. Addition of a porous coating surface greatly improves the surface

roughness and the density of nucleation sites, as well as the surface wettability, which makes the onset of nucleate boiling (ONB) appear earlier. Therefore, the flow boiling heat transfer performance is enhanced. This technology involves applying an electric field twice for coating deposition, and the comparison of microstructure created by the bare copper surface as shown in Fig. 15. However, a different electrochemical deposition technology has been proposed in subsequent research. In this new technique, the low current density deposition coating in the second step is replaced with a sintering treatment method. By using this new electrodeposition technology, a Cu-TiO_2 coating with higher thermal conductivity, greater stability and higher porosity can be obtained. After once sintering, the coating can increase the CHF by 143%, approximately 1.5 times, and the wall temperature decreases by more than half, demonstrating excellent flow boiling heat transfer performance [117]. Therefore, this new technique is currently a cutting-edge technology for enhancing flow boiling. Porous metal oxide coatings are a suitable option for enhancing flow boiling heat transfer. Gupta et al. [118-120] prepared a Cu-Al_2O_3 coating with different processing techniques. It reduces the wall superheat required for boiling initiation and achieve a similar flow boiling heat transfer enhancing effect as the former. When this coating prepared using a single-step electrodeposition method which is required sintering treatment after once electrodeposition, the surface nanoparticles expand and improve adhesion after the sintering step. The performance of the coating is significantly affected by the current density during this process. Increasing the current density effectively improves the CHF. The maximum augmentation in the CHF on this coated surface is achieved up to 86% as compared to that on the bare surface, which is mainly attributed to the sharp increase in bubble nucleation sites. While this coating surface prepared using a new four-step

electrochemical technique (two-step of deposition and two-step of sintering in reducing atmosphere) exhibits several advantageous properties, especially in terms of adhesion. First, a deposition-sintering process is used to generate a porous coating on the substrate surface. Second, the deposition-sintering process is again used to deposit a layer of porous coating on top of the existing coating. However, using a lower current density during the first treatment process results in better surface performance during flow boiling. This is because some particles did not deposit in the micropores of the existing porous surface during the second deposition. As shown in Fig. 16, the growth of nanoparticles on the surface is more pronounced and the right is more obvious. The surface of the right coating can increase the CHF by about 176%. On the one hand, the surface porosity increases by about 14.5% as compared to that on the left coating surface, which significantly increases the density of nucleation sites. On the other hand, the increase of porosity promotes the reduction of drying areas with this structure, improves the wettability of the coating surface and enhances the boiling heat transfer performance in the minichannels. In their recent research, a two-step approach was used. The microstructure of the coating surface becomes more prominent with the porous coating prepared by the two-step electrochemical deposition method. This results in better heat transfer performance and up to a 93% increase in the CHF. The improvement of the porosity and the CHF with different processing techniques is shown in Fig. 17. The Cu-Al_2O_3 porous coating exhibits highly stable hydrothermal properties. It can be effectively prepared through a combined process, making a more practical option with promising application prospects.

Laser etching is one of the surface treatment processes [121, 122]. Laser etching technology is a high-precision and high-efficiency processing method and uses the high energy

density of a laser beam to process the surface of metals or non-metals. This non-polluting process creates grooves or microstructures which can improve nucleation density, increase surface wettability and enhance the flow boiling heat transfer performance. Lim et al. [81] proposed a new technique for enhancing flow boiling heat transfer in minichannels using femtosecond lasers. They prepared three surfaces with different nano-structures, including laser-induced periodic surface structure (LIPSS), micro-groove covered clustered cavity by low fluence (MGCC-LF), and micro-groove covered clustered cavity by high fluence (MGCC-HF) as shown in Fig. 18(a). The laser-induced boiling surfaces exhibit micro-/nano-structural characteristics. However, there are significant differences in the characteristics of different surfaces and these can be clearly seen from Fig. 18(b). For instance, LIPSS exhibits a dense surface structure while MGCC-HF has a surface structure with a large number of cavities and gaps. Despite having significantly more nucleation sites than the bare surface, LIPSS is not very active in promoting bubble growth. This results in a significantly shorter detachment diameter and growth cycle compared to the bare surface. The surface only increases the number of cavities required for bubble nucleation but does not promote bubble growth. This is why the CHF on the surface decreases instead of increasing. The density of bubble nucleation sites on the surface of MGCC-LF is significantly higher than that on the bare surface. This activates the surface cavities, promotes the growth of bubbles and increases the CHF by over 30%. However, the strong hydrophobicity prevents the nucleation site from replenishing liquid in time after bubble detachment, resulting in a significantly lower heat transfer coefficient than other surfaces. While MGCC-HF exhibits a unique explosive nucleation phenomenon during the boiling process, which can significantly enhance its heat transfer performance. As compared

with the plain copper in Fig. 19, the trend of the CHF variation on the surface formed after laser induction and the change in CHF can be obviously reflected. The laser etching process can create numerous additional nucleation sites in microchannel surfaces. The micro/mini-channel surfaces can be modified by adjusting the properties and power of the laser, creating numerous nucleation cavities and enhancing the re-wetting ability. Laser etching technology is highly applicable to metal surfaces and has become an important method for the surface treatment of metal micro/mini-channel heat sinks [123]. Surface wettability is a crucial parameter in microscale flow boiling phenomena in micro/mini-channels, where the characteristics differ from those in macrochannels. Laser etching can create the desired microstructure in metal- or non-metal-based channels, increasing nucleation sites or promoting rewetting. Furthermore, the creation of microstructure surface by laser etching does not require the consideration of adhesion. To some extent, this increases the lifespan of micro/mini-channel heat sinks. The increasing popularity of bionics in heat dissipation has led to widespread attention in the industry towards laser etching technology due to its many advantages, including high precision, process controllability, and low thermal effects. Surface morphology can be affected by various factors such as energy density, laser wavelength, duration time, and laser overlap, which in turn can alter the wettability of the micro/mini-channel surfaces [124, 125]. The excellent parameter adjustability of this technology further enhances its practicality in this field.

The treatment of the metal micro/mini-channel microstructures also involves chemical etching method. The micro-/nano-structures formed by this treatment can significantly enhance the thermal performance of micro/mini-channel heat sinks and even the system as a whole. In the meanwhile, those structures facilitate bubble nucleation and improve the heat transfer

mechanism, thereby maintaining the system in a relatively stable and efficient state [83, 126, 127]. The surface treated with acid base solution etching provides numerous nucleation cavities for vaporization and exhibits good rewetting ability during boiling heat transfer. However, as the heat flux increases, this advantageous mode is disrupted, and the rewetting cycle increases sharply, even making it impossible to perform secondary wetting and leading to a decline in heat transfer performance [128].

One ideal way to ensure optimal flow boiling heat transfer performance is to regulate the microstructure in the micro/mini-channels. This maintains boiling in the nucleating boiling stage for an extended period and in a regular cyclic state in the micro/mini-channels. Both chemical etching treatment and laser etching treatment technologies can significantly enhance durability and extend service life. For instance, using hydrochloric acid (HCl) to etch the aluminum surface is a highly scalable and cost-effective method for preparing highly durable superhydrophilic surfaces. The etched surface exhibits greater structural strength, enabling it to withstand high-strength impacts from high mass flow rates. Furthermore, it is not as fragile as some nanowires structural, and it does not result in adhesion failure or interface thermal resistance [129-133].

3.1.2. Flow boiling heat transfer enhancement in micro/mini-channels

Flow boiling heat transfer in micro/mini-channels strongly depend on the surface characteristics of the channels. Using porous surfaces is a promising flow boiling heat transfer enhancement technique. The rapid liquid replenishment on the nanocomposite porous coating surface accelerates the detachment frequency of bubbles while the ultrafast liquid permeability

speeds up the nucleation of bubbles in cavities, thereby enhancing flow boiling heat transfer. Aravinthan et al. [134] prepared a nano-roughened silver surface on the inner surface of the copper tube through a simple chemical reaction, and then dipped it in a 1-mM solution of heptadecafluoro-1-decanethiol with hydrophobic groups to create hydrophobic tails projecting outwards from the surface. This technique increased the surface roughness by approximately 120%, therefore this surface has more noticeable surface particles. The surface structure provides favorable conditions for bubble nucleation and is positively correlated with experimental comparisons between treated and untreated surfaces. The maximum HTC of the hydrophobic coating is increased by over 20% at low mass flow rates, but the increase of HTC declines with increasing the mass flux. Mass flux significantly influences flow boiling heat transfer in micro/mini-channels. A high mass flow rate can reduce part of the benefits of the enhanced heat transfer on the porous surface. Therefore, it is essential to maintain the enhanced heat transfer capacity of the porous coating at high mass flow rates and strengthen the research on the practical applications of micro/mini-channel heat sinks using modified porous coatings.

Porosity is one important parameter in evaluating flow boiling on porous surfaces. The porosity of the porous sintering coating is defined as the ratio of the volume of voids in coating to the volume of the entire coating, which is gained by the mass difference before and after sintering [135]. The formula is as follows:

$$\varphi = 1 - \frac{\delta_m}{\rho_{\mathrm{Cu}} V_{\mathrm{Cu}}} \tag{7}$$

where φ is the porosity, δ_m is the mass difference of a material before and after sintering, and

$\rho_{Cu}V_{Cu}$ represents the mass of dense material with the same volume as the porous coating.

Fig. 9 shows that the porosity increases with increasing the average particle diameter, following a monotonically increasing trend. However, the porosity trend of the porous coating prepared by Zhang et al. [135] differs, as shown in Fig. 20, showing a trend of first decreasing and then increasing with the increase of particle diameter. The difference between the two trends is primarily in the preparation of the coatings. In the former, pressure is applied to ensure complete contact between the copper powder and the copper base before sintering. In the latter, copper powder is mixed with anhydrous ethanol to form a slurry that is spread evenly over a copper substrate, the required coating thickness is achieved through gravity, followed by evaporation of anhydrous ethanol. In addition, there is also variation in the sintering temperature for coatings with different particle sizes. There are significant variation of the porosity and surface microstructures. After sintering, small particles agglomerate, which instead increases the porosity of the coating. The SEM images of various porous surfaces are shown in Fig. 20(a). Experimental analysis demonstrates that a coating of 75 μm can increase HTC up to 114.5%. The coating of 75 μm has fast permeability and high liquid storage capacity, while the surface coating of 13 μm penetrates slowly but has a high liquid storage capacity and a long penetration time, so that both types of surface coatings exhibit good heat transfer ability. Furthermore, sintering porous coatings can easily solve the issue of the porous coating thickness which is key parameter in enhancing flow boiling heat transfer.

Due to the significant impact of particle diameter on the heat transfer enhancement performance, the selection of coating particle diameter and thickness is crucial to the heat transfer enhancement. It is important to comprehensively consider these factors to meet the

enhanced heat transfer needs in practical scenarios. Research has shown that porous thin coatings are effective in enhancing flow boiling when the coating thickness is smaller than the thermal boundary layer [136, 137]. Porous coatings can provide adequate vaporization cores during boiling heat transfer, which can be divided into internal pores and surface cavities. The internal pores generate thin liquid film boiling, resulting in high heat transfer performance. In addition, the surface cavity is very advantageous in increasing the density of vaporization cores and reducing wall superheat when compared to that of conventional surfaces [138]. Therefore, when studying the enhancement of flow boiling heat transfer on the porous coatings, it is necessary to implement external interventions or improvement measures to increase the number of internal pores in the coatings. This can achieve higher bulk porosity and reduce the number of ineffective closed pores in the coatings, and this is of great significance for further improving the flow boiling heat transfer performance [139-141]. The surface of micro/mini-channels can have a porous structure not limited to a coating, and a porous woven tape structure. A complete heat sink sintered with metal particles can also enhance flow boiling heat transfer. He et al. [77, 142] proposed a bi-porous minichannel heat sink (BPM) sintered with the copper woven tape on the surface of the copper woven tape. As shown in Fig. 21(a), there are two kinds of pore structures, comprising cavities formed by copper strands and crevices formed by copper wires. This structure enables liquid to penetrate the woven tape, increase the density of bubble nucleation sites and further enhance the heat transfer capacity in minichannels. Experimental research has shown that the wall superheat required for bubble nucleation during flow boiling heat transfer of this structure is significantly lower than that of plain surface minichannels (PSM). It results in an increase of the HTC by over 2.5 times, and after converting energy

efficiency, an improvement of about 1.2 times can be achieved. In the meanwhile, the diameter at which bubbles nucleate in the channels is significantly smaller than in smooth surface channels. As shown in Fig. 21(b), the diameter of bubbles formed on the surface of BPM is significantly smaller at G = 253 kg/(m^{2}s) and the effective heat flux q_{eff} = 11.2 kW/m^2. Another possible explanation is that the uneven surface of the copper woven tape increases the local disturbance during flow boiling in the channel. This promotes the rapid detachment of bubbles from the surface, increases the frequency of bubble detachment and reduces the possibility of merging between bubbles. As a result, the heat transfer performance of flow boiling is effectively improved. Yin et al. [143] investigated the effect of a complete heat sink sintered with copper particles on the flow boiling heat transfer enhancement. Fig. 22(a) illustrates the comparison of the surface microstructures between a porous heat sink and a solid heat sink, and the SEM image on the right displays the microchannel surface that is randomly distributed with a large number of cavities. The boiling curve in the sintered porous microchannel heat sink shifts to the left as compared to that in the solid copper heat sink. The wall temperature is reduced by about 15℃ at the high heat flux which demonstrates a significant advantage in the flow boiling heat transfer for the heat dissipation. Fig. 22(b) shows the schematic diagrams of the bubble nucleation and growth in the two microchannels. The capillary wicking ability of the porous wall is enhanced due to the numerous internal pores in the channel ribs after sintering, enhancing its rewetting ability. This prevents local drying by ensuring timely replenishment of the flowing liquid. In addition, it increases the nucleation sites of bubbles, thereby improving their nucleation rate. At high heat fluxes, the pores deep within the rib walls are also activated, and the HTC is improved up to 2 times than that of the solid copper heat sink. The channel size

also has a significant impact on the enhanced heat transfer performance of copper powder sintered porous structures. Selecting an appropriate channel size can result in heat transfer enhancement [144]. Furthermore, porous structures can enhance efficient thin liquid film boiling heat transfer during flow boiling in micro/mini-channels. The porosity of these structures can be increased by mixing particles with different diameters or applying external energy, which can reduce the number of ineffective closed pores, enhances the liquid storage capacity of internal cavities and ensures the continuity of thin liquid film boiling.

Several studies have attempted to sinter metal fibers. Surface adhesion with an appropriate thickness of sintered metal fibers can effectively reduce the wall superheat required for the bubble nucleation and achieve higher porosity at the same thickness [145, 146]. This characteristic is very beneficial to flow boiling heat transfer. Therefore, sintered metal fibers are expected to become one of the main techniques for flow boiling heat transfer enhancement in micro/mini-channels. Furthermore, the CHF enhancement techniques discussed in the previous section can improve the flow boiling HTC. For instance, as compared the GNPs coatings to the uncoated surface [114, 115], the superhydrophilic coating has a higher flow boiling HTC than the uncoated surface. The superhydrophobic surface with unique properties has the ability to increase HTC up to 135%. Moreover, the Cu-TiO_2 coating can increase HTC by 94% to 153% [116, 117]. The Cu-Al_2O_3 coating can increase HTC by up to 200% [118-120]. Fig. 23 shows the comparison of CHF enhancement with different Cu-Al_2O_3 coatings formed by three different methods including single-set electrodeposited technique, two-step electrodeposited technique and four-step electrochemical technique.

According to the available studies, the mechanism of coating-enhanced heat transfer is due

to the porous structure on the coating surfaces. This structure increases the nucleation active site density and the rewetting ability in micro/mini-channels. As a result, the frequency of bubble generation during the flow boiling heat transfer increases and thus accelerates the detachment rate of bubbles. This process does not result in continuous drying areas in the micro/mini-channels and thereby enhancing the flow boiling heat transfer. There are two potential enhancement methods to enhancing flow boiling heat transfer through porous structures. One is the layered structure coatings which create an ultra-thin interlayer structure to achieve efficient interlayer thin liquid film boiling. Therefore, future research should focus on the coating materials which can generate layered structures, such as graphene nanoplatelets and other two-dimensional materials with interlayer structures. The other one is high porosity coatings, such as sintered metal fibers. The coatings can achieve a higher wetting surface area and nucleation site density at the same volume, and thus enhance flow boiling heat transfer in micro/mini-channels. These composite techniques have enormous potential to enhancing flow boiling heat transfer. Future research should be focused on the mechanism of the composite enhancement techniques to determine the coordinated proportion of each individual technique in flow boiling heat transfer enhancement in micro/mini-channels. As the utilization of fluorinated fluids becomes increasingly prevalent and porous coating technologies are continuously advanced, it is meaningful to establish the correlation pertinent to these composite techniques. Furthermore, new composite enhancement techniques should be researched and developed in future.

3.1.3. Two phase flow patterns in enhanced micro/mini-channels

Surface coatings not only affect heat transfer but also significantly impact the flow patterns of flow boiling in micro/mini-channels. Flow patterns are intrinsically related to flow boiling heat transfer and CHF and can explain the underneath mechanisms. Lee et al. [147] compared the flow boiling heat transfer and flow patterns in microchannels with porous coatings to the channels without coatings. The coated surface has more nucleation sites and a higher frequency of bubble generation. In addition, no significant differences in the types of flow patterns are observed on the coated surface and the uncoated surface. However, the porous coating advances the transition time of flow patterns in the microchannels, causes the local disturbance effects and increases the actual contact surface area. As a result, continuous wall drying region does not occur in the annular flow regime. Choi et al. [148] observed elongated bubbles accounting for more than half of the entire channel length as shown in Fig. 24. In addition, the wettability of the channel surface significantly affects the heat transfer. The thin liquid film boiling heat transfer mechanism can suppress the occurrence of local drying points, thereby improving heat transfer at the same level. Sia et al. [114] have found that there is a notable difference in boiling condition between the uncoated channels and those with superhydrophilic or superhydrophobic coatings as shown in Fig. 25. As compared to the uncoated surfaces, the hydrophobic surfaces are easier to produce bubbles. However, these bubbles tend to merge together and form larger bubbles that stick to the channel surface and are difficult to detach, leading to a sharp decrease in the number of effective nucleation sites. Lu et al. [149] studied flow boiling in enhanced microchannels formed by sintering of mixed copper powders with different particle sizes. It shows that the mixed coating can achieve a higher effective heat flux, and more nucleating

bubbles appear in the microchannel with coating of mixed particle sizes. Even when the heat flux exceeds 90 W/cm^2, the channel is still dominated by the annular flow. However, the local drying phenomenon has already occurred in microchannels with coating of single particle size, showing a trend towards heat transfer deterioration. Therefore, it is important to consider the different particle size components in the mixed particles when studying the improved flow boiling performance in the sintering coatings.

Certain nanoscale surface structures can rapidly enhance the capillary wicking ability and thus facilitate liquid rewetting. However, some of these structures may not be suitable for timely vapor discharge. Conversely, micro/mini-scale structures exhibit opposite trends. They can discharge vapor timely, but lack significant capillary wicking ability in such structures, which results in the inability to rewet in time after discharge the vapor. This leads to drying regions and a decline in heat transfer as the boiling process continues. Therefore, combination between nanoscale and microscale structures becomes an important approach to enhancing flow boiling. Flow boiling heat transfer has certain drawbacks when using a single wetted surface. Under specific laser etching conditions, a super-wettability surface is formed. It has raised microstructures near the treated micro grooves as shown in Fig. 26. The microstructures can provide favorable conditions to enhance flow boiling. Subsequent treatment leads to the formation of a biphilic surface, which can further enhance the flow boiling heat transfer. The surface with mixed wetting properties shows better flow boiling heat transfer performance because of biphilic surfaces extend bubbly/slug flow over a wider range of heat fluxes, suppressing bubble merging. Up to 28% heat transfer increase can be obtained by this method with the biphilic surfaces [150]. The relationship between the flow patterns and vapor quality

in the channels is significant. Vapor quality serves as an indicator of the transition of flow patterns in micro/mini-channels. Timely adjustment of the relevant influencing parameters based on the amount of vapor quality in the channel can prevent the occurrence of heat transfer deterioration. The vapor quality can be determined according to thermal balance as follows:

$$x_i = \frac{Q_{\text{eff}} - c_p m(T_i - T_{\text{in}})}{m h_{\text{fg}}} \tag{8}$$

where Q is the heat exchange capacity, m is the mass flow rate of liquid, c_p is the specific heat capacity of the cooling liquid, T_{in} and T_i are the inlet temperature of the micro/mini-channel and the local temperature in the channel, respectively, h_{fg} is the latent heat of vaporization.

3.2. Research on flow boiling in micro/mini-channels with enhanced structures

3.2.1. CHF enhancement using foam metals and woven metal meshes in micro/mini-channels

Enhanced structures can be roughly divided into structural metals and geometrical structures. Table 3 lists the selected studies of the enhanced flow boiling heat transfer using in the micro/mini-channels with enhanced structures. Structural metals including the foam metal and woven metal mesh have unique characteristics and can enhance flow boiling heat transfer. Increasing the density of bubble nucleation sites in micro/mini-channels can also balance the pressure in the channels, avoiding the occurrence of flow instability. Fu et al. [151] designed a copper foam fin heat sink which increased the CHF by 25% as compared to that of a solid fin heat sink. The CHF enhancement is because the former achieves pressure balance between the

adjacent channels and reduces the occurrence of backflow phenomenon. In addition, the porous fins can minimize the appearance of drying areas in the microchannels. The capillary wicking ability of porous foam facilitates rapid liquid penetration while the internal cavity provides optimal conditions for bubble nucleation, and this changes the position of bubble nucleation and the distribution of heat flux, resulting in a more uniform wall temperature distribution during the heat dissipation process [152, 153]. However, the repeated results under various experimental conditions indicate that the liquid supplement rate is far lower than the evaporation rate, ultimately leading to the occurrence of heat transfer deterioration. The reason for this is because the liquid film evaporation rate in the porous foam copper fins is too fast and limits the capillary wicking ability in the flow boiling heat transfer at high heat fluxes and low mass fluxes. Therefore, further enhancing the heat transfer performance mainly involves breaking the restriction of the capillary wicking ability.

Gradient metal foam is an advanced heat transfer material which offers great advantages in improving the fluid replacement mechanism and promoting vapor discharge [154]. Ahmadi and Bigham [155] proposed a gradient wick channel heat sink with woven copper mesh to overcome the limitations of the capillary wicking ability. This structure enhances the permeation of liquid into the gradient wick channels, improving the flow boiling HTC and CHF. The structure and the liquid-vapor interface formed by this structure are depicted in Fig. 27. The flow boiling behaviors of the gradient wick heat sink are significantly outperform than those of the homogenous wick structure minichannel heat sink and the pure copper minichannel heat sink. The interaction between the layers of copper mesh in the copper mesh wall of the gradient wick structure is crucial to enhancing flow boiling heat transfer. The heat transfer

performance is significantly improved when the rib wall is made up of coarse, medium and fine copper mesh from top to bottom. 60% enhancement in CHF is achieved. This is due to the transition from nuclear boiling to thin liquid film boiling. Although the merged slender bubbles occupy the channel, this structure results in the liquid interface that penetrates into the rib much lower than the vapid-liquid interface. But the liquid penetrating into the rib can still stimulate efficient thin liquid film boiling at high heat fluxes. The other two types of woven copper mesh can still achieve an efficient rewetting effect at high heat fluxes even though the capillary wicking ability of the fine copper mesh is limited. Furthermore, at low mass fluxes, the capillary wicking ability of coarse copper mesh on the upper layer can greatly promote liquid penetration, resulting in better performance than the pure copper minichannel heat sink. The optimization process is implemented by adjusting the rib height and filling gradient foam metal in channels which are effective methods. With the optimization of the enhancement techniques, it is possible to improve flow distribution, enhance mixing frequency, promote timely vapor discharge, and balance the pressure distribution at the end of the micro/mini-channels. Therefore, HTC can be increased. In addition, use of foam metal fins can reduce the flow resistance in the micro/mini-channels to a certain extent, which is conducive to stable heat transfer [156-158]. Addition of foam metal to the micro/mini-channels serves two purposes. One is that it disperses pressure drop by preventing bubble merging in the channel and can alter the flow pattern transformation at specific conditions. Furthermore, it facilitates the heat transfer from the ribs on both sides and thus excites the liquid in the porous structure to form a thin liquid film boiling [159-161]. The heat transfer performance increases as the volume ratio of foam metal in the channels increases, it can adapt to different mass fluxes and vary vapor

qualities in the channels by optimizing the ratio.

3.2.2. Flow boiling heat transfer enhancement using foam metals and woven metal meshes in micro/mini-channels

Structural metals can enhance flow boiling heat transfer in micro/mini-channels, depending on its powerful wicking capability and effective nucleation sites [162, 163]. Compared to the pure copper fin channel heat sinks, the foam copper heat sinks can increase flow boiling HTC by around 60% which increases with the increase in fin width [164]. Foam copper was used as the inlet device of a microchannel heat sink by Hong et al. [165]. It was designed to ensure continuous wetting in the microchannels. This heat sink is similar to a vapor-liquid separation device, which prevents vapor from occupying the channels for an extended period and causing drying, thereby improving the HTC up to 170%. Furthermore, addition of foam copper results in an 80% increase in the HTC [151]. The gradient woven metal mesh minichannels can increase the HTC by 3 times as compared to that of the plain minichannels [155]. However, using structural metals to enhance flow boiling heat transfer is an “middle” technique. Structural metals provide a large number of nucleation sites to make sufficient nucleation probability. In addition, the staggered structure in structural metals acts as micro-ribs and enhances the local disturbances in flow boiling. Furthermore, structural metals can transit from the nucleate boiling to thin film evaporation in micro/mini-channels and therefore effectively suppresses the occurrence of dryout in the channels.

3.2.3. CHF enhancement in micro/mini-channels with geometrical structures

Adjusting the channel geometrical structure is one of the main approaches to improving the CHF. In this type of flow boiling heat transfer enhancement technique, the channel geometrical structure has been focused on to achieve higher heat transfer and effectively improve the heat dissipation capacity of micro/mini-heat sinks, such as the saw-tooth shape micro/mini-channels or gradient wick micro/mini-channels. Designing the micro-pinfin fences into both sides of channel can enhance the CHF by 80% [166]. Combining the micro-nozzle with reentry cavities can increase the CHF by 37% as compared to that without cavities [167]. Adjusting the rib shape to the saw-tooth on the microchannel sidewalls can significantly increase the CHF of the microchannel heat sink by 87% [168]. Using a new Tesla-type microchannel can increase the CHF by 88.4% [169]. There is a distinction between forward flow and backward flow in this new type of microchannel heat sink. With increasing the mass flow rate, the inhibition of backflow in the forward direction can gradually increase the enhancement effect, resulting in the final heat transfer enhancement.

3.2.4. Flow boiling heat transfer enhancement in enhanced micro/mini-channels with geometrical structure

Using various micro/mini-channel types is a typical technique to enhancing flow boiling heat transfer. The essence of enhancing flow boiling heat transfer by different channel geometrical structures is to increase the heat transfer area, change the flow patterns and increase the local disturbance and thereby achieving high heat transfer performance. Hajialibabaei et al. [170] studied the effect of a wavy-shaped channel heat sink on the cooling process of a system.

The presence of an open area above the channel heat sink would affect the final heat transfer performance, and the height of the wavy-shaped channel rib had an optimum value in the process of affecting heat dissipation. Wen et al. [171] compared the heat dissipation of two rectangular channel heat sinks of different sizes. The nucleation and growth of bubbles in the channels are greatly affected by the channel size. In addition, vapor quality has an objective critical value of 0.6 in flow boiling heat transfer. When the vapor quality is less than 0.6, flow boiling heat transfer in the channel is favorable, otherwise, the heat transfer deteriorates due to the expansion of the drying area. Deng et al. [172, 173] investigated the effect of the channel types on flow boiling heat transfer and found that the significance of the channel type on flow boiling heat transfer due to the variation of various flow patterns in the channels.

The aspect ratios of non-circular micro/mini-channels have a significant effect on flow boiling heat transfer. Marseglia et al. [174] studied flow boiling heat transfer in microchannels with different aspect ratios at fixed channel heights and their results show that narrow channels have higher HTC than others. The alteration in any aspect such as channel size or shape forces the local heat transfer mechanism in micro/mini-channels to change, thereby affecting the operating performance of the entire heat dissipation system [175]. Lin et al. [176] investigated the impact of channel microstructure, such as micro-fin and micro-cavity, on the flow boiling in microchannels. The microchannels with micro-fins have a significantly smaller drying area due to the capillary wetting effect and the HTC is increased by about 62% in as compared to that of smooth surface while the HTC in the channel with micro-cavity is increased by olny17.2%. Flow boiling in micro/mini-channels is influenced by the channel size and the effect of surface tension becomes dominant. When the micro-pin-finned surfaces are manufactured in

micro/mini-channels, the intensive micro-pin-finned arrangements increase the contact area and the wicking effect, thereby promoting the liquid replenishment, which breaks the liquid boundary and enhances the local disturbance to suppress appearance of drying regions [177-179]. Li et al. [166] utilized a new strategy from the purpose of transform the channel boundary layer structure to improve the performance. They designed micro-pin fin fences along the inner wall of the microchannel, which can achieve excellent heat transfer performance even at high heat fluxes. Compared to conventional plain wall microchannels, the HTC is improved by around 170%. Subsequently, they integrated nanowires into the micro-pin fin fences and the HTC is further increased. But the drawback of suppressed onset of nucleate boiling in the channel is addressed [180].

Suppressing two phase flow instability and disrupting the flow boundary layer can enhance flow boiling heat transfer in micro/mini-channels. The orifice design represents one of the structures and can achieve the suppression of two phase flow instability. The presence of the orifice results in a specific flow separation, which in turn exerts an influence on the heat transfer in the micro/mini-channels [181]. Clark et al. [182] used this design to ascertain whether the stability of the flow boiling in microchannels would be affected. The microchannels with an orifice restrictor demonstrated a stable flow under the conditions set in the experiment, whereas the microchannels without this structure exhibited significant oscillations. Furthermore, the micro-nozzle structure is also conducive to flow boiling heat transfer. It can disrupt the boundary layer and ensure a timely supply of liquid, thus facilitating the mixing of the boundary layer and the mainstream area of the microchannels. In the meanwhile, it can promote thin liquid film evaporation at high heat fluxes, thereby enhancing the heat transfer [183]. Li et al.

[167, 184] proposed a four-nozzle configuration integrated with the concave cavities and the capillary micro-pinfin fences along the sidewalls of the microchannels, respectively. The presence of cavities in the microchannels results in a significant increase in the effective HTC by 200%. This is achieved through a strategic interplay between the timely supply of liquid from micro-nozzles and the facilitation of the liquid rewetting process by cavities. Moreover, the micro-pinfin fence also displays a notable capacity for liquid rewetting and the formation of a new boundary layer. The combination with micro-nozzles produces sufficient mixing and promotes the thin liquid film evaporation, achieving heat transfer enhancement under their experimental conditions. Han et al. [168, 185] proposed a saw-tooth microchannel including symmetrical and staggered structures. The essence of the symmetric saw-tooth channel structure is to use the principle of gradually shrinking and gradually expanding to fully integrate the fluid in the channel while preventing the complete development of the boundary layer in the channel and causing periodic interruptions. By modifying the shape of the saw-tooth, it is possible to enhance the flow boiling performance in the channel, leading to an increase in the HTC by 110%. In theory, the heat transfer is periodically maintained at a relatively high level, thereby achieving enhanced flow boiling heat transfer. Although it has obvious advantages over straight channels, there are some local areas with insufficient heat transfer due to the strong periodicity while the staggered layout can better overcome this disadvantage with generating eddy currents and breaking the thermal boundary layer [186, 187]. Lan et al. [188] designed a minichannel heat sink which induces swirling flow through twisted tapes inserted into the minichannels. The twisted tapes contact with the inner wall of the minichannel and act as nucleation sites for bubbles to increase the nucleation density. The swirling flow created by the

twisted tapes inhibits the growth and merging of bubbles, effectively suppressing two phase flow instability in the mini-channel. Moreover, bubbles in the channel are more likely to detach due to the presence of disturbance. This approach increases the HTC by up to 80.9%, greatly improving the overall performance of the heat sink. The length of the twisted tape also has a significant effect on the overall heat transfer, and the swirling flow generated by too short twisted tapes cannot improve the heat transfer at the end of the channel.

Passive enhancement techniques, such as the foam metal and woven metal mesh, are employed to mitigate two phase instability in micro/mini-channels. Other effective enhancement techniques are used to ensure adequate thermal performance of the heat sink. Priy et al. [189] designed a microchannel heat sink with secondary flow path based on hydrophobic porous materials to mitigate two phase flow instabilities in the channels and thus enhance flow boiling heat transfer. Fig. 28 shows the schematic diagram of the structure of the heat sink. To prepare the hydrophobic substrate required for the secondary flow path, citric acid monohydrate (CAM) particles are dissolved in the PDMS solution in varying proportions. The porosity of this PDMS structure depends upon the amount of CAM particles. The vapor generated in the microchannels is timely discharged through the secondary flow path. It can effectively reduce the temperature and pressure fluctuations. The experimental results show that this structure can improve the rewetting ability of the microchannels, significantly shorten the interval time of boiling between bubbles, and increase HTC by 32% as compared to those of conventional configurations.

Double-layer or manifold micro/mini-channel heat sinks have been designed and investigated to effectively remove high heat flux and to further improve the heat dissipation

performance through enough mixing, reverse flow or local jet flow [190-193]. For instance, fluids vertically flow into and out of microchannels to make effective heat transfer by forming local jet effect in manifold the microchannel (MMC) heat sinks. More uniform flow distribution and smaller temperature difference on the surface are achieved [194]. Short flow distance and sufficient liquid replenishment make partial drying less likely. Therefore, MMC heat sinks have attracted more attention due to their high heat dissipation. Luo et al. [194-196] conducted comprehensive research on the manifold ratios (inlet/outlet width ratios), different channel widths and fin widths, as well as manifold arrangements of various types (Z-type, C-type, H-type, and U-type) for MMC heat sinks. When the manifold ratio is less than 1, a considerable thermal resistance is generated, which impedes the heat dissipation of the heat sink. Once the manifold ratio has been established, the favorable heat transfer performance appears just at the width of the fins less than that of the channel. In the meanwhile, the manifold arrangements have a significant effect on uniform surface temperatures.

New structures of micro/mini-channels are used to enhance flow boiling heat transfer, such as the channel structures with sector bump, diamond bump and others [169, 197-199]. These new structures can maintain an alternating process of development interruption and redevelopment of the thermal boundary layer in micro/mini-channels. In addition, the ribs in the middle of the Tesla-type structure can inhibit the vapor backflow, prevent the occurrence of flow instability, and promote the occurrence of thin liquid film boiling, thereby enhancing flow boiling heat transfer. While the local flow velocity of the sector bump is higher, it is more conducive to the bubble separation. However, if the ribs are too compact, they can create a heat transfer blind spot, which can have adverse effects. For instance, when compared to straight

channels at a mass flux of 360 kg/(m^2s), the new Tesla-type structural channel can increase HTC by 86.8% in forward direction [169]. However, further studies are required to understand the heat transfer enhancement mechanism and the factors which influence the new structured micro/mini-channel heat sinks, such as reducing the pressure drop or resolving non-uniformity of temperature distribution in the heat sinks from a bionic perspective [200-202].

3.2.5. Two phase flow patterns in enhanced micro/mini-channels

The enhancement of flow boiling heat transfer in micro/mini-channels is dependent on the flow patterns such as continuous nucleate boiling mode and liquid film evaporation. Porous structures of foam metal and the channel types have been proved to significantly enhance flow boiling heat transfer in micro/mini-channels. The ability to activate nucleation sites and balance pressure in the channel is extremely important. Flow patterns are used to explain the flow boiling heat transfer behaviors. Previous studies or reviews on flow boiling have focused on flow patterns and their relations to flow boiling behaviors and mechanisms [203-207]. By predicting or explaining the transition mechanism of flow patterns, adverse states that occur during flow boiling can be alleviated, thus ensuring the stability of effective flow boiling heat transfer.

Wang et al. [208] manufactured an aluminum-based porous rib minichannel heat sink using foam copper with 85% porosity. To verify the superior heat transfer performance of the porous rib minichannel heat sink, they also included a solid fin minichannel heat sink for comparison as shown in Fig. 29(a). The special porous structure of foam copper rib focuses on two aspects: contact area and nucleation cavity. The stationary or slow-moving liquid within

the porous ribs triggers high-frequency, small-sized bubble nucleation driven by heat flow. As shown in Fig. 29(b), with increasing the effective heat flux, the process of flow pattern transformation in the porous rib minichannels is significantly lower than that in the solid rib minichannels. The porous rib minichannels can provide local disturbances under annular flow. The connection between channels helps to suppress the two phase flow instability. As shown in Fig. 30, although the main channel is occupied by slender bubbles, a thin liquid film is also attached near the wall and the surface of the micropores. The thin liquid film can prevent the occurrence of drying areas in the channels, thereby slowing down the decrease in heat transfer performance during the evolution of the flow patterns. Kim et al. [209] also obtained similar trends in the flow pattern transitions and concluded that are not significantly affected by the material of the porous media.

The channel geometrical structure significantly affects the flow patterns in micro/mini-channels by suppressing liquid backflow and preventing the merging of elongated bubbles, or breaking the bigger bubble [210-212]. Inserting twisted tapes in minichannels can cause high disturbance, which can break slender bubbles such as in slug flow and annular flow and increase the rewetting ability in the channels as in shown Fig. 31(a). The rate of bubble coalescence is mitigated due to the better fluid mixing, the separation and extrusion effects caused by the twisted tape inserts [188, 213] as in shown Fig. 31(b). For the micro/mini-channels with ribs, the vapor slug is easily segmented by the ribs. Smooth geometric characteristics of the channel ribs are more conducive to the stability of the flow patterns than other structures such as the smooth concave arc surface as shown in Fig. 32.

The channel geometrical structures can suppress instability and prevent backflow to some

extent. However, parallel micro/mini-channels are not connected and cannot achieve pressure balance in the channels while structural metals can achieve this goal. Structural metals, such as copper foam, woven copper mesh, and aluminum foam exhibit excellent heat transfer and strengthening performance in micro/mini-channel heat dissipation. These metals have lightweight and possess good stiffness, making them ideal for use in heat dissipation systems for medical health, unmanned flight, new energy batteries and other fields. In particular, through the segmented gradient wick design, the structural metal heat sinks can meet the heat dissipation requirements at various heat fluxes and develop more efficient and stable heat sinks [214, 215].

3.3. Research on flow boiling with surfactants in micro/mini-channels

3.3.1. CHF enhancement with surfactants in micro/mini-channels

Nanofluids and surfactants have been extensively investigated to enhance the CHF in flow boiling. It is crucial to select the appropriate concentrations of nanoparticles and surfactants to prevent particle precipitation due to improper proportions. Incorporating surfactants into coatings used in micro/mini-channels presents a promising technique for future research, which have a beneficial effect on flow boiling. The extent of enhancement in flow boiling heat transfer and CHF achieved solely through surfactants is relatively limited. Therefore, it is essential to consider the combination of surfactants with other enhancement techniques. Table 4 lists the selected studies of the enhanced flow boiling using surfactants in micro/mini-channels.

Incorporation of surfactants into working fluids or coatings is beneficial to the CHF. Kumar et al. [216] demonstrated that adding 4 wt.% SDS surfactant into a ZnO-Al_2O_3 coating resulted in a maximum CHF enhancement of 44.6%. This improvement is attributed to the

increase of hydrophilicity imparted by SDS. In the meantime, the increased hydrophilicity in conjunction with the inherent microcavity structure of the coating can significantly enhance the heat transfer performance. Wang et al. [217] reported a maximum CHF increase of 70% by adding SDS to deionized water and R113. An optimal mass concentration of 0.1 ‰ CTAC/NaSal solution increases the CHF by 26% as compared to that of pure water, demonstrating a significant strengthening effect [218]. Flow patterns responsible for CHF in pure water and CTAC/NaSal solutions are different and can elucidate the physical processes underlying surfactant-enhanced flow boiling heat transfer [219]. Zhang et al. [220] investigated the effects of surfactant SDBS and SiO_2 particle concentrations on flow boiling heat transfer and found that any variation in these components would lead to changes in the CHF. When the concentration of SDBS is kept constant, the CHF initially increases and then decreases as the concentration of SiO_2 particles increases. However, compared to deionized water, the increase in CHF of this aqueous solution is 18%, which is relatively moderate.

3.3.2. Flow boiling heat transfer enhancement with surfactants

Surfactants can be incorporated into coatings to create composite coatings, as well as into nanofluids. Recent studies have focused on working fluids with addition of surfactants to regulate the surface tensions. Addition of surfactants to working fluids presents a swift and effective technique to heat transfer enhancement. Surfactants can significantly enhance the nucleation of bubbles on the channel surface and facilitate the timely detachment of bubbles from the channel wall, thereby improving HTC. In addition, adding surfactants into nanofluids not only enhances their stability but also effectively reduces their surface tension [221-223].

Kumar et al. [216] utilized spray pyrolysis technique to obtain ZnO-Al_2O_3 coatings with sodium dodecyl sulfate (SDS) surfactants of different mass concentrations. The hydrophilicity of the coating is enhanced by the addition of SDS surfactant. In the meanwhile, the roughness of the coating surface exhibits a corresponding increase. This phenomenon contributes to enhancement of flow boiling heat transfer due to the effect of the surfactant. Notably, compared to pure ZnO coatings, ZnO-Al_2O_3 composite coatings containing 4 wt.% surfactants can enhance the HTC by 30%.

Inclusion of surfactant solutions can mitigate the formation of elongated vapor in micro/mini-channels and enhance the rewetting of the channel surface [224]. However, there exists an optimal concentration for surfactants. Either excessive or insufficient amount of surfactants can lead to detrimental effects, such as precipitation and flocculation. Wang et al. [218] demonstrated that an aqueous of cetyltrimethyl ammonium chloride (CTAC) and sodium salicylate (NaSal) at a suitable concentration of 0.1 ‰ exhibited favorable flow boiling performance. The HTC was be increased by 36% as compared to pure water at the same conditions. As illustrated in Fig. 33, the flow visualization revealed a significantly higher number of nucleation sites at this concentration as compared to other concentrations at which no discernible large bubbles are presented. At appropriate concentrations, low surface energy activates a substantial volume air pockets which are able to generate bubbles and facilitate flow boiling heat transfer enhancement. Zhang et al. [225] investigated the influence of various types (including sodium dodecyl benzene sulfonate (SDBS), cetyl trimethyl ammonium bromide (CTAB) and sorbitan monooleate (Span80)) and concentrations of surfactants on Al_2O_3/R141b nanofluids. Their results show that the surfactants have a significant effect on the heat transfer

enhancement. Addition of SDBS can enhance HTC by over 30%. At low mass concentrations, the diffusion rate of surfactant molecules is relatively high, leading to a greater number of surfactant molecules adhering to the surfaces of bubbles. The adherence can reduce the surface energy and facilitate the bubble detachment. In contrast, an increase in fluid viscosity adversely affects the heat transfer performance. A similar trend is observed using the TiO_2 nanoparticles. In addition, incorporation of surfactants can enhance the stability of the nanofluid and prevent the aggregation of the nanoparticles in the inlet region under the influence of the electric field [226]. Addition of SDS into deionized water and R113 can significantly improve the wettability in the channel walls [217]. At a mass concentration of 2 ‰, the heat transfer enhancement reaches the peak, resulting in a 140% increase in the HTC. Flow boiling enhancement using surfactants primarily due to improving the bubble nucleation and rewetting effects in micro/mini-channels. However, there is an optimal mass concentration which can maximize the enhancement of flow boiling heat transfer. In addition, it is important to ensure that the two phase pressure drop remains within a reasonable range when using surfactant solutions in flow boiling in micro/mini-channels [227]. In general, Further research is needed to optimize the concentrations and understand the enhancement mechanisms. Selecting proper surfactants is also a critical aspect.

3.3.3. The effects of surfactants on two phase flow patterns in micro/mini-channels

Addition of surfactants significantly alters the flow patterns in micro/mini-channels. Fig. 34 illustrates the comparison of flow patterns for water and a 0.1 ‰ CATC/NaSal surfactant solution in a channel over 4 ms [218]. Addition of the surfactants results in insignificant

merging of bubbles in the channel at the conditions: $q = 2.9 \times 10^5$ W/m^2, $G = 152$ kg/(m^{2}s) and $\Delta T_{sub,\,in} = 20$ K. It has the substantial potential to mitigate the formation of elongated bubbles, thereby suppressing the occurrence of dry spots in the channel. As illustrated in Fig. 35(a), the trend of change shows that water is thermally nucleated in a straight microchannel, leading to the formation of bubbles to grow and merge. The bubbles gradually evolve into slug flow, annular flow, and local drying. However, addition of surfactant into water results in bubbles clustered together and forming bubble clusters in relatively dispersed locations of the channels. As the bubbles grow, they do not exhibit significant merging phenomena. The vapor bubble clusters maintain the flow stability of the channels. The high hydrophilicity and low surface tension of the SDS surfactant solution facilitate adequate wettability during the bubble growth and ensure independence of the bubbles. It attributes to the distribution of surfactant molecules [224]. A significant number of vapor clusters are presented in the channels, primarily formed by the mutual extrusion of stacking among the bubbles. Furthermore, the specific surface area of the bubbles is considerably larger than that of the merged bubbles. Consequently, the flow boiling heat transfer in the micro/mini-channels can be enhanced to a certain extent due to the change of flow patterns.

4. Research on flow boiling in composite enhanced micro/mini-channels

In recent years, composite enhanced micro/mini-channels have been increasingly investigated to enhance flow boiling heat transfer and CHF. Composite enhanced micro/mini-channels are generally formed by integrating two or more types of heat transfer enhancement techniques. Fig. 36 illustrates various composite heat transfer enhancement techniques used in

the available studies. Deng et al. [228] proposed a composite structure heat sink which has a type of Ω-shaped reentrant porous channels with multi-scale rough surface. The composite structure heat sink can easily achieve the advantages of flow boiling enhancement and maintain more uniform heat sink base temperatures as compared to those of a reentrant copper microchannel heat sink. Li et al. [229] used porous structures on the ribs in microchannels to increase the fluid mixing. This helps to break the continuous development of the thermal boundary layer and effectively avoid the heat transfer blind zone formed behind the ribs, resulting in more conducive to convective boiling heat transfer. Yu et al. [230] designed a pin fin wall structure by gradient distributed micro pin fin arrays in microchannels. The flow instabilities can be completely suppressed by this structure, thereby reducing the occurrence of dryout region by facilitating the high-frequency bubble detachment. In addition, the rib-elliptical groove complex structure has positive effects in increasing the local disturbance and suppressing blind spots behind ribs [231].

Although much research into the channel surface wettability focuses on flow boiling in straight micro/mini-channels, the benefits of irregular micro/mini-channels are promising in enhancing flow boiling. These methods work together by cooperative interaction to suppress the rapid growth and merging of bubbles, and increase the amount of nucleation in the channels to a relatively high level. The continuous development of technology makes the composite enhanced micro/mini-channel heat sinks as one of mainstream directions in flow boiling enhancement [45, 232]. However, there are challenges in developing and investigating composite enhanced microchannel heat sinks which include porous surfaces and irregular channels. When setting up interval symmetric or interval staggered porous surfaces in irregular

channels, the position of nucleation sites is a key issue affecting the flow boiling characteristics. For example, the nucleation sites may move forward. In addition, the double-layer porous wick structure is an effective approach to enhancing flow boiling in micro/mini-channels [46]. This type of composite enhancement technique should be extensively studied in the studies of flow boiling in micro/mini-channels to understand the mechanisms and optimized design methods.

5. Challenges for flow boiling prediction methods in micro/mini-channels

A large number of correlations and models have been developed for saturated flow boiling in macroscale channels over the past 70 years. The HTC correlations of flow boiling are generally classified into three groups: (i) The summation correlations: The HTC is considered to be the addition of the nucleate and convective boiling contribution such as the Chen correlation [233]; (ii) The asymptotic model: The heat transfer coefficient is assumed as one of the two mechanisms to be dominant such as the Steiner and Taborek model [234]; (iii) The flow pattern based model: This model consists of a flow pattern map and flow pattern specific models and correlation for the heat transfer such as the prediction methods by Kattan et al. [235], Wojtan et al. [236, 237], Cheng et al. [238, 239] and Moreno Quibén et al. [240, 241] which are based on the asymptotic model and the relevant flow patterns. However, there are big challenges for developing prediction methods for flow boiling in micro/mini-channels as pointed out by Cheng and Xia [207] in their comprehensive review. Some correlations for micro/mini-channel flow boiling heat transfer have been developed on the basis of these for macroscale channel flow boiling. Most of these consider the contribution of two flow boiling heat transfer mechanisms: nucleate boiling dominant and convective boiling dominant. Furthermore, efforts

have been made to develop the mechanistic heat transfer models for flow boiling heat transfer in micro/mini-channels such as the three-zone heat transfer model in microchannels by Thome et al. [242, 243] and annular flow heat transfer model developed by Cioncolini and Thome [244] and Thome and Cioncolini [245]. However, the actual heat transfer mechanisms are much more complex than the two mechanisms and should be well understood.

A number of heat transfer models and correlations have also been developed based on micro/mini-channel flow boiling experimental data. From the analysis and comparison of the experimental data from different studies [207], it is concluded that well performed and documented experimental studies on microchannel flow boiling are still needed. The channel size effect on the flow boiling heat transfer behaviours and mechanisms have not yet well been understood. In general, the available heat transfer correlations and models poorly predict independent data. No universal prediction methods are available for micro/mini-channel flow boiling heat transfer so far. Most of the available heat transfer correlations and models lack the heat transfer mechanism basis which should be based on the flow structures and micro/mini-channel sizes and structures. Furthermore, there is little studies regarding the prediction methods for flow boiling in enhanced micro/mini-channels.

Description of experimental phenomena and mechanism analysis are crucial in investigating very complex flow boiling phenomena and mechanisms in enhanced micro/mini-channels. Flow boiling correlations and prediction methods for both HTC and CHF should be developed based on the carefully experimental studies of flow boiling phenomena and mechanisms. Cheng and Xia [207] present a comprehensive review of flow boiling in micro/mini-channels and have evaluated 12 models and correlations for flow boiling heat

transfer in micro/mini-channels with a database including 2336 data points of 8 test fluids including R410A, R141b, R134a, R245fa, R12, R123, R22 and N_2, tube diameter: 0.19 - 3.69 mm, mass flux: 20 - 1471.2 kg/(m^2s), heat flux: 5 - 150 kW/m^2 and both horizontal and vertical arrangements. It shows that adopting flow pattern based heat transfer model combining the three-zone model and the annular flow model together with the corresponding flow patterns by Thome and Cioncolini [245] gives much better results than the three-zone model alone. As summarized by Cheng and Xia [207], the flow pattern based heat transfer model for flow boiling in micro/mini-channel predict the database reasonably well. However, mechanistic prediction methods and models are needed to be well developed and improved. Relating the heat transfer behaviors to the corresponding flow regimes is promising methods to understand the heat transfer mechanisms and to develop new prediction models for flow boiling covering both macroscale and micro/mini-channels. Furthermore, systematic experimental, analytical and modelling studies of unstable and transient flow boiling phenomena in microchannels should be focused on.

The prediction methods should not only reflect the evolving trends in flow boiling but also support the selection of actual engineering applications. Flow boiling in parallel micro/mini-channels represents a significant foundation in this field of study. Fang et al. [246] conducted an analysis to evaluate the predictive accuracy of the existing HTC correlations for their flow boiling experimental data in the parallel micro/mini-channel heat sinks. Their results demonstrated that different correlations exhibit varying degrees of accuracy within the different position of the channels. A comparative analysis of the correlations reveals that the correlations proposed by Liu and Winterton [247] and Li and Wu [248] exhibit the most accurate predictions.

These models obtained the lowest mean absolute error (MAE), namely 12.9% and 9.1%, respectively. However, the conclusion lacks generality of the applications of these two correlations. Their experimental conditions are very narrow with a mass flux from 50 - 300 kg/(m^2s), vapor quality from 0.1 to 0.2, heat flux is up to 21 kW/m^2 and only one working fluid. An effective prediction value is a crucial element in ensuring the safe and stable operation of micro/mini-channel systems in practical engineering applications. Fang et al. [249] proposed a correlation formula that can be utilized in a broader range of operational contexts. Through their analysis of different databases, they discovered that the new correlation formula enhanced the mean absolute deviation (MDA) to approximately 10%, thereby demonstrating enhanced precision in predicting the HTC for individual fluid data, which exhibited notable reliability. Furthermore, Ma et al. [250] improved a new correlation based on Liu and Winterton's model, which is able to predict more than 80% of the data within ± 30% error band. This demonstrates a good predictive ability.

The effective prediction methods of CHF can give a broad range of actual environments for engineering applications. Cheng et al. [251] conducted a detailed comparison of the experimental CHFs with the predicting result by previous correlations. They have concluded that the differences exhibited by different correlations within different micro/mini-channels are relatively large. Furthermore, they observed that the values given by the correlations are generally high than the measured data. This indicates that these correlations only work in some specific channel sizes. Therefore, when developing new correlation formula, they not only consider the influence of the hydraulic diameters of micro/mini-channels, but also take the additional geometric metrics such as the aspect ratios of the channels as important parameters.

Furthermore, optimization of the correlations is essential. Koşar et al. [252] have proposed below CHF correlations:

$$q''_{\mathrm{CHF}} = 0.0035 G h_{\mathrm{fg}} We^{-0.12} \tag{9}$$

$$We = \frac{\left(G^2 D_{\mathrm{h}}\right)}{\sigma \rho_{\mathrm{f}}} \tag{10}$$

They have further developed the following correlation equation after optimization as:

$$q''_{\mathrm{CHF}} = 0.00472 G h_{\mathrm{fg}} We_{\mathrm{HL}}{}^{-0.0671} \left(\frac{W}{D_{\mathrm{h}}}\right)^{3.19} \tag{11}$$

where G is the mass flux, h_{fg} is the latent heat, We is the Webber number based on the hydraulic diameter of the channel and We_{HL} is the Webber number based on the channel heated length, W is the width of micro/mini-channels.

There are a number of studies on CHF prediction methods for flow boiling in micro/mini-channels, which are needed to be evaluated but are not the focus of this review. However, for enhanced micro/mini-channels, no general prediction method is available so far.

Overall, there lack prediction methods for flow boiling HTC and CHF in enhanced micro/mini-channels due to the very complex flow boiling phenomena and mechanisms for various enhancement techniques. Advanced experimental methods and accurate measurement techniques are urgently needed to obtain reliable experimental data and reasonable mechanisms

which are intrinsically related to the complex flow patterns in micro/mini-channels with various enhancement techniques. Therefore, the flow boiling HTC and CHF measurements and flow pattern observation should be simultaneously taken. On the basis of the accurate database, effort should be made to develop mechanistic prediction models based on flow patterns in future.

6. Analysis and discussion

6.1. Flow boiling enhancement by increasing the nucleation density

One of the effective methods to enhancing flow boiling in micro/mini-channels is to increase the nucleation rate of bubbles. For homogeneous or heterogeneous surfaces, surface modifications can reduce the wettability of the surfaces to make it hydrophobic and reduce the potential barrier for bubble nucleation. Therefore, change of the surface properties plays a crucial role in increasing the number of active nucleation sites. It also serves as a bridge to balance the CHF and HTC [253]. Mixed wettability (heterogeneous surfaces) is considered an effective technique to enhancing flow boiling heat transfer. Biphilic surfaces with mixed the wettability have more nucleation sites and higher boiling heat transfer performance as compared to those of uniformly hydrophobic surfaces. There is an optimal state to maximize the heat transfer enhancement [254, 255]. Therefore, it is important to further investigate the arrangement of patterns and the proportion of pattern area on mixed wettability surfaces to increase nucleation density.

While porous coating surfaces contain numerous cavities which can act as nuclei at the beginning of boiling and accelerate the nucleation rate of bubbles. These surfaces have a positive effect on improving nucleation density and enhancing the channel rewetting ability.

However, it is important to note that porous coatings are not a permanent solution for enhancing flow boiling heat transfer. The first is the issue of strength, it is a concern for porous coatings formed by vertically arranged nanowires or nanotubes. At high mass flow rates, their strength cannot withstand the impact which may bend and lose their advantages, resulting in a considerable number of microcavities unable to exert their benefits. But silicon nanowires are an exception as the nanowire coatings have their robustness under the shear stress of two-phase flow [256]. The second issue to consider is adhesion. A layer of functional coating is applied to the channel surface through various techniques, and its adhesion is a crucial aspect. For instance, after simple spraying and drying, a porous coating is formed. However, after repeated use, the full coverage of the coating on the channel surface cannot be guaranteed, and the peeling off of the coating cannot ensure the original enhancement effect. In the meanwhile, in some micro/mini-channels with smaller hydraulic diameters, there is a higher risk of channel blockage. The third issue concerns pore closed. Some of the micropores or pores in porous coatings originate from the material itself, such as the inherent micropores on the surface of carbon nanotubes, or from the formed coatings, such as sintered porous coatings which can effectively solve the two aforementioned problems. However, when preparing sintered porous coatings, it is inevitable that some “closed pores” may appear inside the coating due to the fact that it is formed by sintering multiple specifications of metal particles. Therefore, controlling the number of closed pores is crucial in achieving the expected performance.

6.2. Flow boiling enhancement by increasing the local disturbance or the contact area

Enhancing flow boiling heat transfer in micro/mini-channels can be achieved by changing

channel types or using structural metals to increase the local disturbance or the contact area. Addition of staggered fins in micro/mini-channels can improve the heat transfer performance to some extent, and then addition of fins ahead of the channels have a more significant enhancement effect [257]. When using alternating porous coatings in micro/mini-channels with slightly larger dimensions to form a composite enhanced structure, it is important to consider the issue controlling the position of the generated disturbance according to actual requirements. In order to further enhance heat transfer, it is important to ensure that the area where the disturbance applied to does not flush out the unformed bubbles. If the coordination between the channel type and the porous coating is inappropriate, it may inhibit the bubble nucleation, or even result in no nucleation in the channels. Therefore, it is essential to fully utilize the benefits of both techniques and create an enhanced heat transfer mechanism as illustrated in Fig. 37.

6.3. Suppression of flow boiling instability

Flow boiling instability in micro/mini-channels is a critical issue. Selecting appropriate methods based on the different types may suppress flow boiling instability. The methods to suppressing the flow boiling instability can be classified into two principal categories: active separation of vapor and change of the channel geometrical structures. Enhancing flow boiling can also be achieved indirectly by the methods of suppressing flow instability. Specific methods to suppressing the flow boiling instability in micro/mini-channels have been extensively studied and identified, such as vapor-liquid separation (rapid separation of vapor in upward secondary paths), pressure balancing (connecting the end of the channels to balance the pressure inside the channels), throttling (adding throttling devices at the channel inlets), and backflow

suppression (adding fin structures in the channels). Zhang et al. [258] developed a membrane-venting microchannel heat sink. This is a novel optimization technique to enhancing flow boiling heat transfer in microchannels. It employs a porous membrane to facilitate the discharge of vapor by an additional vapor path. The unique structure can reduce the vapor quality in the microchannels, thereby ensure stable flow boiling in the channels. He et al. [259] developed a novel interconnected bi-porous minichannel heat sink. When the confined elongated bubbles are formed in the channels, this configuration enables the separation of partial vapor to the adjacent channels through connected regions, and effectively inhibits the occurrence of backflow phenomenon and improves flow stability. Shah et al. [260] used an inlet plenum flow restrictor to suppress flow boiling instability in microchannels. It can reduce the maximum oscillation amplitude of the pressure fluctuation by 66.7% at lower mass flux. Xia et al. [261, 262] investigated change of continuous flow instability in straight and triangular corrugated microchannels. The triangular corrugated microchannels can suppress flow boiling instability and achieve better heat transfer performance.

Extending the length of micro/mini-channels and enhancing axial thermal conduction can significantly reduce oscillation fluctuations. Xia et al. [263] conducted experimental study on suppressing the flow boiling instability in a novel type of semi-open microchannel heat sink. It achieves connectivity in the downstream region of the channels. The elongated bubbles in the microchannels merge without moving back to the upstream and therefore enhance the heat transfer performance of the microchannel heat sink. Furthermore, the manifold micro/mini-channels have a distinctive advantage in reducing two phase pressure drop in the channels [264, 265]. The pressure drop can be reduced by 43.3% under a heat flux of 400 W/cm^2 [195], which

can create favorable conditions for suppressing flow boiling instability the channels. Real-time monitoring of the temperature changes on the heat sinks bottom surface is crucial to comprehending the physical processes such as flow pattern transition and dryout identification in micro/mini-channels. Measurement of the local pressure and temperature distribution can accurately provide more accurate data to understand the mechanism of heat transfer enhancement [266]. Therefore, it is significant to understand the heat transfer mechanism by accurate experimental data, flow pattern observations and a reliable fitting model through a large of test database under a wide range of experimental conditions.

Although numerous studies have focused on creating micro/nano-structures with varying roughness to improve heat transfer performance, the heat transfer mechanisms and the bubble dynamics still remain incompletely understood. Li [267] carried out experiments of R410A flow boiling in an enhanced tube. They visualized the flow regimes and measured the corresponding HTCs. In the meanwhile, they identified four flow regimes, namely annular flow, intermittent flow, stratified-wavy flow, and stratified flow. Then, the equation of continuity is adopted to address the physical mechanism of the two-phase flow phenomenon. A new concept, potential fluctuation at the flow interface between vapor and liquid has been proposed based on the analytical solution of differential equation of continuity. It has oscillatory wave behaviors along spatial dimensions and temporal dimension governed by the continuity relationships, and acts as the “inside gene” to control two-phase flow development and instability. The fluctuations influenced by the densities and velocities of vapor and liquid in flow boiling. The theoretical analysis has provided a good basis to further understand the physical processes and mechanisms in enhancing flow boiling heat transfer using micro/nano-structures. Potential fluctuation can

be used in flow boiling in micro/mini-channels to suppress flow instability and should be considered in studying micro/mini-channel flow boiling and instability in future.

6.4. Optimization of enhanced micro/mini-channels

Flow boiling enhancement techniques in micro/mini-channels include surface modification enhancement techniques, enhanced structures, enhancement using surfactants, and composite enhancement techniques. There is a critical issue of optimization of the heat transfer enhancement techniques in micro/mini-channels. Although optimization of enhancement techniques has been concerned [135], there lacks systematical knowledge and theory regarding optimization of enhancement techniques in micro/mini-channels due to the limited studies. For instance, when selecting the particle size and coating thickness in sintered porous coatings, it is essential to optimize the particle size, and coating thickness to achieve optimized heat transfer enhancement effect. However, seldom did researchers consider to optimize the particle size and coating thickness. The emerging composite enhancement techniques are promising methods to enhancing flow boiling but need to be optimized to ensure the harmonious integration of each individual enhancement technique. As illustrated in Fig. 37, the composite enhancement technique includes the integration of channel fins and porous surfaces. However, the “forward movement” of the nucleation sites is a significant challenge. In recent years, there are some optimization studies of the emerging enhancement techniques, such as innovative design of the vapor secondary channel [189]. This novel structure effectively optimizes the vapor discharge to maintain the pressure drop and achieve enhanced heat transfer. Priy et al. [268] proposed a microchannel heat sink with a condensing cover plate, which can mitigate the vapor clogging

in the channels. This approach offers a promising solution for improving flow boiling heat transfer and achieving superior thermal performance without increasing the pressure drop in the microchannels. Consequently, this can be integrated with porous sidewalls or micro fences to facilitate thin liquid film boiling in the micro/mini-channels and optimize the enhancement techniques applied to the micro/mini-channels. However, optimization of enhanced micro/mini-channels is very limited in the available studies and need to be concerned as a mainstream research topic when developing or applying enhancement techniques in micro/mini-channels. It is obvious that optimization of enhancement techniques requires in-depth research. Effort should be made to achieve systematic knowledge, methods, mechanism and theory of optimization of enhanced micro/mini-channels in future studies.

7. Summary and recommendation for future research needs

This comprehensive review provides a complete summary and detailed analysis of the available studies regarding flow boiling enhancement techniques and mechanisms in micro/mini-channels in recent 5 years. Flow boiling heat transfer, CHF, flow instability, flow patterns, mechanisms and optimization in enhanced micro/mini-channels are critically reviewed and discussed. Various enhancement techniques such as non-uniform wetting surfaces, porous coatings, nanowire coatings, porous walls, oven metal meshes, and addition of surfactants have been discussed and analyzed. Of the available techniques in micro/mini-scale, surface modification techniques and enhanced structures have broad prospects for flow boiling enhancement. According to the review and analysis, the following conclusions and future research recommendations have been obtained:

(1) Mixed hydrophobic and hydrophilic surfaces are a promising enhancement technique for flow boiling in micro/mini-channels. The hydrophobic part of a non-uniform wetting surface has a lower surface energy, which can promote bubble nucleation. The hydrophilic part can promote rewetting and suppress the large drying regions in the channels. The synergy between two types of surfaces can effectively improve flow boiling HTC and CHF in micro/mini-channels while Single hydrophilic or hydrophobic type has certain drawbacks and limitations.

(2) Porous structures with a high porosity can result in a large number of cavities in micro/mini-channels and provide sufficient nucleation sites for the bubble nucleation. Due to the enhancement of the capillary wicking ability and continuous penetration of liquid in the porous structures, the liquid inside the cavities is easily excited to form a thin liquid film evaporation to achieve high flow boiling heat transfer performance and suppress the occurrence of dryout in micro/mini-channels.

(3) In practical scenarios with high mass fluxes, the strength of some nanowires may not be sufficient to resist the shear stress in flow boiling, resulting in a decrease in heat transfer enhancement effect and even failure whereas the silicon nanowire coatings show a good ability to resist the shear stress. The gradient wick structures can adapt to a wider range of heat fluxes and mass fluxes.

(4) Sintering coatings are promising heat transfer enhancement technique for flow boiling in micro/mini-channels. They can achieve high porosity on thinner thickness coatings and significantly improve the bubble nucleation and the channel rewetting, thereby improving flow boiling heat transfer and CHF in micro/mini-channels.

(5) Integrating irregular channel structures with porous microstructures in micro/mini-channels is a promising technique to enhancing flow boiling. On the one hand, irregular structures of the channels are able to disrupt the thermal boundary layer and increase the local turbulence through ribs or sidewall cavities. On the other hand, porous microstructure can generate significant bubble nucleation, and therefore improve flow boiling HTC and CHF. Porous coatings in periodic cavities on the sidewalls of micro/mini-channels can effectively promote the nucleation of boiling. In the meantime, the pressures in micro/mini-channels are balanced through vapor-liquid separation device at the end of the channels and thus can suppresses the flow boiling instability. This composite enhancement technique is very promising for flow boiling in micro/mini-channels. Further studies should focus on the optimization of the composite enhanced microchannels and flow boiling mechanisms.

(6) Promoting the occurrence and maintenance of thin liquid film evaporation in micro/mini-channels is one of the most efficient techniques to enhancing flow boiling. The techniques of coatings or structures with layers are crucial to improving flow boiling HTC and CHF. In the meanwhile, timely liquid penetration and narrow gaps between layers are two important aspects to ensure the triggering of thin liquid film evaporation. With the continuous development of new technology such as the coatings of MXenes two-dimensional materials, using layered surfaces in micro/mini-channels is a promising enhancement technique for flow boiling. Research and development of this new enhancement technique should be conducted to understand the mechanism and optimization of the techniques in future.

(7) The synergy of the composite enhancement technique using the enhancing effect generated by irregular structures and the effect of thin liquid film boiling needs to be investigated and

optimized to achieve maximized the heat transfer enhancement. Furthermore, the enhancement mechanisms of the composite technique should be investigated according to the bubble dynamics, bubble nucleation and flow patterns of flow boiling in composite enhanced micro/mini-channels. However, understanding the function of each individual technique adopted in composite enhancement techniques should be clarified but presents a big challenge due to the complex phenomena. Optimization of the composite enhancement techniques is critical but a big challenge. Future research should focus on all these aspects.

(8) There lack the prediction methods for flow boiling HTC and CHF in enhanced micro/mini-channels, all the available models are not for enhanced micro/mini-channels. Although it is a great challenge due to the very complex flow boiling phenomena involved and lack of systematic experimental data and mechanisms, it is the time to start to develop the relevant prediction methods. Effort should be made to conduct careful and systematical experiments to provide accurate experimental data of HTC and CHF under a wide range of experimental conditions. It is essential to relate the measured the data to the corresponding flow patterns in order to understand the underneath mechanisms. It must be pointed out that advanced experimental methods should be specially designed and developed for flow boiling in enhanced micro/mini-channels.

Acknowledgments

This work was supported by Beijing Natural Science Foundation (No. 3242014).

References

[1] M. C. Gorur, D. Doganay, M. B. Durukan, M. O. Cicek, Y. E. Kalay, C. Kincal, N. Solak, H. E. Unalan, 3D printing of hexagonal boron nitride nanosheets/polylactic acid nanocomposites for thermal management of electronic devices, Compos. Part B-Eng. 265 (2023) 110955.

[2] J. Ma, Y. Sun, S. Zhang, J. Li, S. Li, Experimental study on the performance of vehicle integrated thermal management system for pure electric vehicles, Energ. Convers. Manage. 253 (2022) 115183.

[3] Y. Li, L. Gong, B. Ding, M. Xu, Y. Joshi, Thermal management of power electronics with liquid cooled metal foam heat sink, Int. J. Therm. Sci. 163 (2021) 106796.

[4] T. Kang, Y. Ye, Y. Jia, Y. Kong, B. Jiao, Enhanced thermal management of GaN power amplifier electronics with micro-pin fin heat sinks, Electronics 9(11) (2020) 1778.

[5] T. G. Karayiannis, M. M. Mahmoud, Flow boiling in microchannels: Fundamentals and applications, Appl. Therm. Eng. 115 (2017) 1372-1397.

[6] N. Hu, Q. Wang, S. Liu, J. Gu, L. Li, J. Lyu, A narrow shape double-layer microchannel heat sink (DL-MCHS) designed for high-power laser crystal, Appl. Therm. Eng. 211 (2022) 118456.

[7] Q. Yang, J. Zhao, Y. Huang, X. Zhu, W. Fu, C. Li, J. Miao, A diamond made microchannel heat sink for high-density heat flux dissipation, Appl. Therm. Eng. 158 (2019) 113804.

[8] L.-Y. Zhang, Y.-F. Zhang, J.-Q. Chen, S.-L. Bai, Fluid flow and heat transfer characteristics of liquid cooling microchannels in LTCC multilayered packaging substrate, Int. J. Heat Mass Tran. 84 (2015) 339-345.

[9] S. G. Kandlikar, Review and projections of integrated cooling systems for three-dimensional integrated circuits, J. Electron Packaging 136(2) (2014) 024001.

[10] H. Herwig, High heat flux cooling of electronics: the need for a paradigm shift, J. Heat Transfer 2013, 135: 111011-111013.

[11] A. S. El-dean, O. Hassan, H. M. Shafey, Heat transfer characteristics of two-phase flow in a double-layer microchannel heat sink, Int. Commun. Heat Mass 132 (2022) 105899.

[12] G. Liang, I. Mudawar, Review of channel flow boiling enhancement by surface modification, and instability suppression schemes, Int. J. Heat Mass Tran. 146 (2020) 118864.

[13] D. B. Tuckerman, R. F. Pease, Optimized convective cooling using micromachined structure, J. Electrochem. Soc. 129(3) (1982) 98-100.

[14] D. B. Tuckerman, R. F. Pease, High-performance heat sinking for VLSI, IEEE Electr. Device L. 2(5) (1981) 126-129.

[15] S. Nukiyama, The maximum and minimum values of the heat q transmitted from metal to boiling water under atmospheric pressure, Int. J. Heat Mass Tran. 27(7) (1984) 959-970.

[16] A. E. Bergles, The implications and challenges of enhanced heat transfer for the chemical process industries, Chem. Eng. Res. Des. 79(4) (2001) 437-444.

[17] Y. Wang, G. Xia, R. Li, Q. Li, Z. Yan, Heat transfer enhancement in porous wall mini-channel heat sinks utilizing electric field: An experimental study, Int. J. Heat Mass Tran. 203 (2023) 123803.

[18] T. Li, X. Luo, B. He, L. Wang, J. Zhang, Q. Liu, Flow boiling heat transfer enhancement in vertical minichannel heat sink with non-uniform microcavity arrays under electric field, Exp. Therm. Fluid Sci. 149 (2023) 110997.

[19] J. Zhou, X. Luo, C. Li, L. Liang, G. Wang, B. He, Z. Tian, Flow boiling heat transfer enhancement under ultrasound field in minichannel heat sinks, Ultrason. Sonochem. 78 (2021) 105737.

[20] F. Yu, X. Luo, B. He, J. Xiao, W. Wang, J. Zhang, Experimental investigation of flow boiling heat transfer enhancement under ultrasound fields in a minichannel heat sink, Ultrason. Sonochem. 70 (2021) 105342.

[21] J. Xiao, J. Zhang, Experimental investigation on flow boiling bubble motion under ultrasonic field in vertical minichannel by using bubble tracking algorithm, Ultrason. Sonochem. 95 (2023) 106365.

[22] S. A. Zonouzi, R. Khodabandeh, H. Safarzadeh, H. Aminfar, M. Mohammadpourfard, M. Ghanbarpour, Experimental study of the subcooled flow boiling heat transfer of magnetic nanofluid in a vertical tube under magnetic field, J. Therm. Anal. Calorim. 140 (2020) 2805-2816.

[23] K. Guo, H. Li, Y. Feng, T. Wang, J. Zhao, Coupling enhancement effect of the magnetic field and wall superheat on boiling heat transfer characteristics of magnetic nanofluid (MNF) under reduced gravity, Microgravity Sci. Tec. 35 (2023) 4.

[24] G. D. Xia, J. Jiang, J. Wang, Y. L. Zhai, D. D. Ma, Effects of different geometric structures on fluid flow and heat transfer performance in microchannel heat sinks, Int. J. Heat Mass Tran. 80 (2015) 439-447.

[25] L. Chai, L. Wang, X. Bai, Thermohydraulic performance of microchannel heat sinks with triangular ribs on sidewalls – Part 1: Local fluid flow and heat transfer characteristics, Int. J. Heat Mass Tran. 127 (2018) 1124-1137.

[26] A. M. Ali, A. Rona, H. T. Kadhim, M. Angelino, S. Gao, Thermo-hydraulic performance of a circular microchannel heat sink using swirl flow and nanofluid, Appl. Therm. Eng. 191 (2021) 116817.

[27] J. Song, F. Liu, Y. Sui, D. Jing, Numerical studies on the hydraulic and thermal performances of trapezoidal microchannel heat sink, Int. J. Therm. Sci. 161 (2021) 106755.

[28] A. Manoj, U. V. Goddumarri, R. A, S. Chakraborty, Heat transfer and fluid flow characteristics of a microchannel heat sink with microplates – A critical computational study, Appl. Therm. Eng. 226 (2023) 120309.

[29] D. Jing, S. Song, L. He, Reexamination of Murray's law for tree-like rectangular microchannel network with constant channel height, Int. J. Heat Mass Tran. 128 (2019) 1344-1350.

[30] G. Hedau, M. Qadeer, N. P. Gulhane, R. Raj, S. K. Saha, On the importance of fluidic manifold design and orientation on flow boiling instability in microchannel heat sinks, Int. J. Heat Mass Tran. 209 (2023) 124120.

[31] Q. Zhu, Y. Cui, J. Zeng, S. Zhang, Z. Wang, T. Zhao, Local hydrothermal characteristics and temperature uniformity improvement of microchannel heat sink with non-uniformly distributed grooves, Case Stud. Therm. Eng. 47 (2023) 103113.

[32] R. A, S. Chakraborty, Microchannel heat sink with microstructured wall – A critical study on fluid flow and heat transfer characteristics, Therm. Sci. Eng. Prog. 38 (2023) 101613.

[33] C. Li, X. Li, H. Huang, Y. Zheng, Hydrothermal performance analysis of microchannel heat sink with embedded module with ribs and pin-fins, Appl. Therm. Eng. 225 (2023) 120167.

[34] B. Markal, A. Evcimen, O. Aydin, Effect of inlet temperature on flow boiling behavior of

expanding micro-pin-fin type heat sinks, Int. Commun. Heat Mass 149 (2023) 107143.

[35] Z. Yao, M. Derikvand, M. S. Solari, J. Zhang, F. M. A. Altalbawy, A. H. D. Al-Khafaji, O. A. Akbari, D. Toghraie, I. M. Mohammed, Numerical assessment of the impacts of non-Newtonian nanofluid and hydrophobic surfaces on conjugate heat transfer and irreversibility in a silicon microchannel heat-sink, J. Taiwan Inst. Chem. E. 142 (2023) 104642.

[36] C. J. Ho, J.-K. Peng, T.-F. Yang, S. Rashidi, W.-M. Yan, On the assessment of the thermal performance of microchannel heat sink with nanofluid, Int. J. Heat Mass Tran. 201 (2023) 123572.

[37] Z. Chen, P. Qian, Z. Huang, W. Zhang, M. Liu, Study on flow and heat transfer of liquid metal in the microchannel heat sink, Int. J. Therm. Sci. 183 (2023) 107840.

[38] H. Wang, X. Chen, Performance improvements of microchannel heat sink using Koch fractal structure and nanofluids, Structures 50 (2023) 1222-1231.

[39] Z. Tan, P. Jin, Y. Zhang, G. Xie, Flow and thermal performance of a multi-jet twisted square microchannel heat sink using CuO-water nanofluid, Appl. Therm. Eng. 225 (2023) 120133.

[40] C. Qu, J. Zheng, S. Wu, R. Dai, J. Zhang, Multi-objective optimization of thermal and hydraulic performance with various concentrations of hybrid Fe_3O_4 / graphene nanofluids in a microchannel heat sink, Case Stud. Therm. Eng. 45 (2023) 102963.

[41] G. D. Xia, Y. X. Tang, L. X. Zong, D. D. Ma, Y. T. Jia, R. Z. Rong, Experimental investigation of flow boiling characteristics in microchannels with the sinusoidal wavy sidewall, Int. Commun. Heat Mass 101 (2019) 89-102.

[42] J.-F. Zhang, Y. K. Joshi, W.-Q. Tao, Single phase laminar flow and heat transfer characteristics of microgaps with longitudinal vortex generator array, Int. J. Heat Mass Tran.

111 (2017) 484-494.

[43] Y. Li, Z. Wang, J. Yang, H. Liu, Thermal and hydraulic characteristics of microchannel heat sinks with cavities and fins based on field synergy and thermodynamic analysis, Appl. Therm. Eng. 175 (2020) 115348.

[44] L. Gao, J. Lyu, M. Bai, Y. Li, D. Gao, L. Shi, The microchannel combined hydrophobic nanostructure for enhancing boiling heat transfer, Appl. Therm. Eng. 194 (2021) 116962.

[45] L. Liu, L. Yu, B. Yuan, B. Liu, J. Wei, Flow boiling heat transfer enhancement via micro-pin-fins/ZnO nanorods hierarchical surface, Int. J. Heat Mass Tran. 203 (2023) 123810.

[46] Y. Cheng, J. Wang, J. Yuan, J. Xu, Experimental studies on boiling heat transfer and friction characteristics in evaporator with double-layer micro/nano porous wick, Appl. Therm. Eng. 221 (2023) 119901.

[47] X. Yuan, Y. Du, C. Wang, Experimental study on pool boiling enhancement by unique designing of porous media with a wettability gradient, Appl. Therm. Eng. 321 (2023) 120893.

[48] Y. Li, G. Xia, Y. Jia, Y. Cheng, J. Wang, Experimental investigation of flow boiling performance in microchannels with and without triangular cavities – A comparative study, Int. J. Heat Mass Tran. 108 (2017) 1511-1526.

[49] Y. F. Li, G. D. Xia, D. D. Ma, J. L. Yang, W. Li, Experimental investigation of flow boiling characteristics in microchannel with triangular cavities and rectangular fins, Int. J. Heat Mass Tran. 148 (2020) 119036.

[50] D. Zhang, Q. Zhao, J. Zhou, Y. Li, Q. Li, X. Chen, Experimental study of flow boiling characteristics of open microchannels with elliptical cavities and elliptical ribs, Appl. Therm. Eng. 236 (2024) 121821.

[51] J. Kim, U. P. Kumar, S.-J. Lee, C.-L. Kim, J.-W. Lee, Implementation of endurable superhydrophobic surfaces through dilution rate control of the PDMS coating on micro-nano surface structures, Polymer 275 (2023) 125929.

[52] T. P. Allred, J. A. Weibel, S. V. Garimella, The petal effect of parahydrophobic surfaces offers low receding contact angles that promote effective boiling, Int. J. Heat Mass Tran. 135 (2019) 403-412.

[53] X. Wang, D. Fadda, J. Godinez, J. Lee, S. M. You, Effect of wettability on pool boiling heat transfer with copper microporous coated surface, Int. J. Heat Mass Tran. 194 (2022) 123059.

[54] W. Zhang, Y. Chai, J. Xu, G. Liu, Y. Sun, 3D heterogeneous wetting microchannel surfaces for boiling heat transfer enhancement, Appl. Surf. Sci. 457 (2018) 891-901.

[55] B. Chu, C. Fang, F. Zheng, W. Cheng, R. Wang, W. Zhang, J. Tao, L. Huai, P. Tao, C. Song, W. Shang, B. Fu, T. Deng, Hybrid graphene oxide/crumpled graphene film via subcooled boiling-induced self-assembly for highly efficient boiling heat transfer, Mater. Today Energy 22 (2021) 100868.

[56] Y. Tang, J. Cao, S. Wang, Experimental research on thermal performance of ultra-thin flattened heat pipes, J. Therm. Sci. 31(6) (2022) 2346-2362.

[57] S. C. Zhao, Z. Zhang, R. Zhao, T. Wu, X. Zhang, Z. C. Liu, W. Liu, An R1234zeI loop heat pipe with flat-plate evaporator for cooling electronic devices, Therm. Sci. Eng. Prog. 42 (2023) 101935.

[58] B. P. Benam, A. K. Sadaghiani, V. Yağcı, M. Parlak, K. Sefiane, A. Koşar, Review on high heat flux flow boiling of refrigerants and water for electronics cooling, Int. J. Heat Mass Tran. 180 (2021) 121787.

[59] D. Deng, L. Zeng, W. Sun, A review on flow boiling enhancement and fabrication of enhanced microchannels of microchannel heat sinks, Int. J. Heat Mass Tran. 175 (2021) 121332.

[60] S. K. Singh, D. Sharma, Review of pool and flow boiling heat transfer enhancement through surface modification, Int. J. Heat Mass Tran. 181 (2021) 122020.

[61] B. Wang, Y. Hu, Y. He, N. Rodionov, J. Zhu, Dynamic instabilities of flow boiling in micro-channels: A review, Appl. Therm. Eng. 214 (2022) 118773.

[62] S. S. Mehendale, A. M. Jacobi, R. K. Shah, Fluid flow and heat transfer at micro- and meso-scales with application to heat exchanger design, Appl. Mech. Rev. 53(7) (2000) 175-193.

[63] S. G. Kandlikar, W. J. Grande, Evolution of microchannel flow passages-thermohydraulic performance and fabrication technology, Heat Transfer Eng. 24(1) (2003) 3-17.

[64] Y. Gan, J. Xu, J. Zhou, Y. Chen, Key issues related to microscale phase change heat transfer, Adv. Mech. 34(3) (2004) 399-407.

[65] L. Cheng, D. Mewes, Review of two-phase flow and flow boiling of mixtures in small and mini channels, Int. J. Multiphas. Flow 32 (2006) 183-207.

[66] L. Cheng, G. Xia, Flow patterns and flow pattern maps for adiabatic and diabatic gas liquid two phase flow in microchannels: fundamentals, mechanisms and applications, Exp. Therm. Fluid Sci. 148 (2023) 110988.

[67] P. A. Kew, K. Cornwell, Correlations for the prediction of boiling heat transfer in small-diameter channels, Appl. Therm. Eng. 17(8-10) (1997) 705-715.

[68] K. A. Triplett, S. M. Ghiaasiaan, S. I. Abdel-Khalik, D. L. Sadowski, Gas-liquid two-phase flow in microchannels Part I: two-phase flow patterns, Int. J. Multiphas. Flow 25 (1999)

377-394.

[69] W. Li, Z. Wu, A general criterion for evaporative heat transfer in micro/mini-channels, Int. J. Heat Mass Tran. 53 (2010) 1967-1976.

[70] T. Harirchian, S. V. Garimella, A comprehensive flow regime map for microchannel flow boiling with quantitative transition criteria, Int. J. Heat Mass Tran. 53 (2010) 2694-2702.

[71] J. Wang, X. Fei, H. Liu, L. Zhang, Cooling time and CHF enhancement of reactor vessel cooling process by flame sprayed porous coating in different orientations, Nucl. Eng. Des. 390 (2022) 111706.

[72] M. Nedaei, A. R. Motezakker, M. C. Zeybek, M. Sezen, G. O. Ince, A. Kosar, Subcooled flow boiling heat transfer enhancement using polyperfluorodecylacrylate (pPFDA) coated microtubes with different coating thicknesses, Exp. Therm. Fluid Sci. 86 (2017) 130-140.

[73] V. Khanikar, I. Mudawar, T. Fisher, Effects of carbon nanotube coating on flow boiling in a micro-channel, Int. J. Heat Mass Tran. 52 (2009) 3805-3817.

[74] W. Cui, S. K. Mungai, C. Wilson, H. Ma, B. Li, Subcooled flow boiling on a two-step electrodeposited copper porous surface, J. Enhanc. Heat Transf. 23(2) (2016) 91-107.

[75] P. A. Milani, M. Mahdi, A. Abarghooei, Experimental investigation of the effect of copper electrodeposition on the aluminum surface and addition of ethylene glycol on boiling heat transfer coefficient, Heat Mass Transfer 58 (2022) 801-812.

[76] D. Zhang, J. Mao, J. Qu, Q. Lei, Ch. Li, Y. Chen, Characterizing effect of particle size on flow boiling in sintered porous-microchannels, Appl. Therm. Eng. 229 (2023) 120571.

[77] B. He, X. Luo, F. Yu, J. Zhou, J. Zhang, Flow boiling characteristics in bi-porous minichannel heat sink sintered with copper woven tape, Int. J. Heat Mass Tran. 158 (2020)

119988.

[78] M. C. Vlachou, C. Efstathiou, A. Antoniadis, T. D. Karapantsios, Micro-grooved surfaces to enhance flow boiling in a macro-channel, Exp. Therm. Fluid Sci. 108 (2019) 61-74.

[79] T. Liu, W. Yan, W. Wu, S. Wang, Thermal performance enhancement of vapor chamber with modified thin screen mesh wick by laser etching, Case Stud. Therm. Eng. 28 (2021) 101525.

[80] H. Zhou, J. Lee, M. Kang, H. Kim, H. Lee, J. B. In, All laser-based fabrication of microchannel heat sink, Mater. Design. 221 (2022) 110968.

[81] K. Lim, K. Lee, H. Ki, J. Lee, Enhancement of flow boiling heat transfer by laser-induced periodic surface structures using femtosecond laser, Int. J. Heat Mass Tran. 196 (2022) 123229.

[82] J. K. Mendizábal, B. P. Singh, K. F. Rabbi, N. V. Upot, K. Nawaz, A. Jacobi, N. Miljkovic, Enhanced internal condensation of R1233zdI on micro- and nanostructured copper and aluminum surfaces, Int. J. Heat Mass Tran. 207 (2023) 124012.

[83] N. V. Upot, K. F. Rabbi, A. Bakhshi, J. K. Mendizabal, A. M. Jacobi, N. Miljkovic, Etching-enabled ultra-scalable micro and nanosculpturing of metal surfaces for enhanced thermal performance, Appl. Phys. Lett. 122 (2023) 031603.

[84] X. Wang, X. Li, Y. Liu, D. Shan, B. Guo, J. Xu, Surface wettability regulation on the miniaturized V-shaped channels fabricated by hot-embossing, Surf. Coat. Tech. 451 (2022) 129069.

[85] X. Yuan, Y. Du, Q. Xu, C. Li, C. Wang, Synergistic effect of mixed wettability of micro-nano porous surface on boiling heat transfer enhancement, Therm. Sci. Eng. Prog. 42 (2023) 101933.

[86] W. Gao, X. Xu, X. Liang, Flow boiling of R134a in an open-cell metal foam mini-channel evaporator, Int. J. Heat Mass Tran. 126 (2018) 103-115.

[87] H.-W. Li, G.-B. Wei, Y.-C. Wang, D. Yang, B. Sun, W.-P. Hong, Investigation on the phase split characteristics of slug and annular flow in a metal foam-filled T-junction, Exp. Therm. Fluid Sci. 109 (2019) 109878.

[88] H.-W. Li, C.-Z. Zhang, D. Yang, B. Sun, W.-P. Hong, Experimental investigation on flow boiling heat transfer characteristics of R141b refrigerant in parallel small channels filled with metal foam, Int. J. Heat Mass Tran. 133 (2019) 21-35.

[89] H. Hu, Z. Lai, Y. Zhao, Heat transfer and pressure drop of refrigerant flow boiling in metal foam filled tubes with different wettability, Int. J. Heat Mass Tran. 177 (2021) 121542.

[90] H. Hu, Y. Zhao, J. Sheng, Y. Li, Influence of surface wettability on heat transfer and pressure drop characteristics of R1234zeI flow boiling in metal foam filled tubes, Int. J. Refrig. 146 (2023) 366-374.

[91] J. Palumbo, S. Chandra, Additive manufacturing of complex structures and flow channels using wire-arc thermal spray, J. Manuf. Process. 107 (2023) 459-471.

[92] C. Salmean, H. Qiu, Gradient microstructures for flow-boiling enhancement, Int. J. Heat Mass Tran. 215 (2023) 124467.

[93] H. Wang, Y. Yang, Y. Wang, C. Y. H. Chao, H. Qiu, Effects of non-wetting fraction and pitch distance in flow boiling heat transfer in a wettability-patterned microchannel, Int. J. Heat Mass Tran. 190 (2022) 122753.

[94] K. Luo, W. Li, J. Ma, W. Chang, G. Huang, C. Li, Silicon microchannels flow boiling enhanced via microporous decorated sidewalls, Int. J. Heat Mass Tran. 191 (2022) 122817.

[95] M. Freystein, F. Kolberg, L. Spiegel, S. Sinha-Ray, R. P. Sahu, A. L. Yarin, T. Gambaryan-Roisman, P. Stephan, Trains of Taylor bubbles over hot nano-textured mini-channel surface, Int. J. Heat Mass Tran. 93 (2016) 827-833.

[96] M.-Y. Wen, K.-J. Jang, C.-Y. Ho, Boiling heat transfer and pressure drop of R-600a flowing in the mini-channels with fillisters, Heat Mass Transfer, 51 (2015) 49-58.

[97] A. Bharadwaj, R. D. Misra, Study of pool boiling on hydrophilic surfaces developed using electric discharge coating technique, Appl. Therm. Eng. 234 (2023) 121267.

[98] J. Kim, J. Y. Cho, J. S. Lee, Flow boiling enhancement by bubble mobility on heterogeneous wetting surface in microchannel, Int. J. Heat Mass Tran. 153 (2020) 119631.

[99] Y. Lin, Y. Luo, J. Li, W. Li, Heat transfer, pressure drop and flow patterns of flow boiling on heterogeneous wetting surface in a vertical narrow microchannel, Int. J. Heat Mass Tran. 172 (2021) 121158.

[100] K. Tan, Y. Hu, Y. He, Enhancement of flow boiling in the microchannel with a bionic gradient wetting surface, Appl. Therm. Eng. 230 (2023) 120784.

[101] R. Lioger-Arago, P. Coste, N. Caney, Study of flow boiling in a vertical mini-channel with surface structuring: Heat transfer analysis using inverse method, Int. J. Therm. Sci. 192 (2023) 108392.

[102] T. Semenic, S. M. You, Two-phase heat sinks with microporous coating, Heat Transfer Eng. 34(2-3) (2013) 246-257.

[103] D. Zhang, H. Xu, Y. Chen, L. Wang, W. Cao, M. Wang, Z. Zhou, Experimental study on flow boiling heat transfer characteristics of porous microchannels, Energ. Conserv. Tech. 39(1) (2021) 20-25.

[104] J. Mao, D. Zhang, L. Sun, Q. Lei, J. Qu, Boiling heat transfer and resistance characteristics of two types of sintered structures, Chem. Ind. Eng. Prog. 41(7) (2022) 3483-3492.

[105] P. Bai, T. Tang, B. Tang, Enhanced flow boiling in parallel microchannels with metallic porous coating, Appl. Therm. Eng. 58 (2013) 291-297.

[106] J. Sun, Y. Lin, J. Li, W. Tang, W. Li, W. Ahmad, J. Zhao, Heat transfer and visualization of flow boiling on nanowire surfaces in the microchannel, Appl. Therm. Eng. 256 (2024) 124064.

[107] M. S. Sarwar, Y. H. Jeong, S. H. Chang, Subcooled flow boiling CHF enhancement with porous surface coatings, Int. J. Heat Mass Tran. 50 (2007) 3649-3657.

[108] T. Y. Liu, P. L. Li, C. W. Liu, C. Gau, Boiling flow characteristics in microchannels with very hydrophobic surface to super-hydrophilic surface, Int. J. Heat Mass Tran. 54 (2011) 126-134.

[109] J. Ahn, W. Jeon, H.-G. Kim, S.-M. Kim, S. Baik, Dryout suppression and significantly enhanced flow boiling heat transfer through the two-tier vertically aligned carbon nanotube channel, Int. J. Heat Mass Tran. 214 (2023) 124438.

[110] J.-L. Luo, D.-C. Mo, Y.-Q. Wang, S.-S. Lyu, Biomimetic copper forest wick enables high thermal conductivity ultrathin heat pipe, ACS Nano, 15 (2021) 6614-6621.

[111] D. I. Shim, W.-T. Hsu, M. Yun, D. Lee, B. S. Kim, H. H. Cho, Superbiphilic patterned nanowires with wicking for enhanced pool boiling heat transfer, Int. J. Mech. Sci. 249 (2023) 108280.

[112] C. S. S. Kumar, S. Suresh, L. Yang, Q. Yang, S. Aravind, Flow boiling heat transfer enhancement using carbon nanotube coatings, Appl. Therm. Eng. 65(1-2) (2014) 166-175.

[113] A. S. Kousalya, K. P. Singh, T. S. Fisher, Heterogeneous wetting surfaces with graphitic petal-decorated carbon nanotubes for enhanced flow boiling, Int. J. Heat Mass Tran. 87 (2015) 380-389.

[114] G. D. Sia, M. K. Tan, G. M. Chen, Y. M. Hung, Performance enhancement of subcooled flow boiling on graphene nanostructured surfaces with tunable wettability, Case Stud. Therm. Eng. 27 (2021) 101283.

[115] G. D. Sia, C. S. Lim, M. K. Tan, G. M. Chen, Y. M. Hung, Anomalously enhanced subcooled flow boiling in superhydrophobic graphene-nanoplatelets-coated microchannels, Int. Commun. Heat Mass 146 (2023) 106932.

[116] S. K. Gupta, R. D. Misra, An experimental investigation on flow boiling heat transfer enhancement using Cu-TiO_2 nanocomposite coating on copper substrate, Exp. Therm. Fluid Sci. 98 (2018) 406-419.

[117] S. K. Gupta, R. D. Misra, Flow boiling performance analysis of Copper-Titanium Oxide micro-/ nanostructured surfaces developed by single-step forced convection electrodeposition technique, Arab. J. Sci. Eng. 46 (2021) 12029-12044.

[118] S. K. Gupta, R. D. Misra, Enhancement of flow boiling heat transfer performance using single-step electrodeposited Cu-Al_2O_3 nanocomposite coating on copper substrate, IJST – T. Mech. Eng. 44 (2020) 481-496.

[119] S. K. Gupta, R. D. Misra, Flow boiling heat transfer performance of copper-alumina micro-nanostructured surfaces developed by forced convection electrodeposition technique, Chem. Eng. Process. 164 (2021) 108408.

[120] S. K. Gupta, R. D. Misra, Experimental investigation on flow boiling heat transfer

characteristics of water inside micro/nanostructured-coated minichannel, Int. J. Thermophys. 44 (2023) 148.

[121] J. Long, P. Fan, M. Zhong, H. Zhang, Y. Xie, C. Lin, Superhydrophobic and colorful copper surfaces fabricated by picosecond laser induced periodic nanostructures, Appl. Surf. Sci. 311 (2014) 461-467.

[122] M. Zupančič, D. Fontanarosa, M. Može, M. Bucci, M. Vodopivec, B. Nagarajan, M. R. Vetrano, S. C. I. Golobič, Enhanced nucleate boiling of Novec 649 on thin metal foils via laser-induced periodic surface structures, Appl. Therm. Eng. 236 (2024) 121803.

[123] A. D. Sommers, K. L. Yerkes, Using micro-structural surface features to enhance the convective flow boiling heat transfer of R-134a on aluminum, Int. J. Heat Mass Tran. 64 (2013) 1053-1063.

[124] Y. Chen, Y. Shao, X. Xiao, A new method for predicting the morphology and surface roughness of micro grooves in aluminum alloy ablated by pulsed laser, J. Manuf. Process. 96 (2023) 193-203.

[125] S. S. Sunderlal, G. L. Samuel, Near-infrared femtosecond laser direct writing of microchannel and controlled surface wettability, Opt. Laser Technol. 170 (2024) 110214.

[126] N. V. Upot, A. Bakhshi, K. F. Rabbi, F. Lu, A. M. Jacobi, N. Miljkovic, Enhanced refrigerant flow boiling heat transfer in microstructured finned surfaces, Int. J. Heat Mass Tran. 207 (2023) 123999.

[127] Y. Kubo, S. Yamada, H. Murakawa, H. Asano, Correlation between pressure loss and heat transfer coefficient in boiling flows in printed circuit heat exchangers with semicircular and circular mini-channels, Appl. Therm. Eng. 204 (2022) 117963.

[128] Q. Zhao, J. Qiu, J. Zhou, M. Lu, Q. Li, X. Chen, Visualization study of flow boiling characteristics in open microchannels with different wettability, Int. J. Heat Mass Tran. 180 (2021) 121808.

[129] J. Ma, D. G. Cahill, N. Miljkovic, Condensation induced blistering as a measurement technique for the adhesion energy of nanoscale polymer films, Nano Lett. 20 (2020) 3918-3924.

[130] N. V. Upot, A. Mahvi, K. F. Rabbi, J. Li, A. M. Jacobi, N. Miljkovic, Scalable and resilient etched metallic micro- and nanostructured surfaces for enhanced flow boiling, ACS Appl. Nano Mater. 4 (2021) 6648-6658.

[131] P. Zhao, Y. Wang, Q. Ren, Y. Dong, X. Zhai, G. Zhu, Hydrophilic aluminum prepared by chemical etching and its wettability change rule, Surf. Tech. 46(5) (2017) 171-176.

[132] M. Sattari, A. Olad, F. Maryami, I. Ahadzadeh, K. Nofouzi, Facile fabrication of durable and fluorine-free liquid infused surfaces on aluminum substrates with excellent anti-icing, anticorrosion, and antibiofouling properties, Surf. Interfaces 38 (2023) 102860.

[133] K. F. Rabbi, K. S. Boyina, W. Su, S. Sett, A. Thamban, S. Shahane, S. Wang, N. Miljkovic, Wettability-defined frosting dynamics between plane fins in quiescent air, Int. J. Heat Mass Tran. 164 (2021) 120563.

[134] M. Aravinthan, S. Sarkar, P. Dhar, S. K. Das, A. R. Balakrishnan, Flow boiling heat transfer characteristics in minitubes with and without hydrophobicity coating, Heat Transfer Eng. 41 (2020) 288-301.

[135] Z. Zhang, Y. Wu, K. He, X. Yan, Experimental investigation into flow boiling heat transfer and pressure drop in porous coated microchannels, Int. J. Heat Mass Tran. 218 (2024)

124734.

[136] C. S. S. Kumar, G. U. Kumar, M. R. M. Arenales, C.-C. Hsuc, S. Suresh, P.-H. Chen, Elucidating the mechanisms behind the boiling heat transfer enhancement using nano-structured surface coatings, Appl. Therm. Eng. 137 (2018) 868-891.

[137] J. Chen, S. Zhang, Y. Tang, H. Chen, W. Yuan, J. Zeng, Effect of operational parameters on flow boiling heat transfer performance for porous interconnected microchannel nets, Appl. Therm. Eng. 121 (2017) 443-453.

[138] M. Sun, L. Jia, L. Yin, C. Dang, Y. Xue, Experimental study on visualization of flow boiling in porous microchannels, J. Eng. Thermophys. 43(1) (2022) 226-232.

[139] A. Rahimian, H. Kazeminejad, H. Khalafi, A. Akhavan, M. Mirvakili, Effect of gamma irradiation on the critical heat flux of sintered nano-coated surfaces, Radiat. Phys. Chem. 199 (2022) 110297.

[140] Z. Tian, D. Zhang, G. Zhou, S. Zhang, M. Wang, Compaction and sintering effects on scaling law of permeability-porosity relation of powder materials, Int. J. Mech. Sci. 256 (2023) 108511.

[141] J. Zhou, X. Luo, Y. Pan, D. Wang, J. Xiao, J. Zhang, B. He, Flow boiling heat transfer coefficient and pressure drop in minichannels with artificial activation cavities by direct metal laser sintering, Appl. Therm. Eng. 160 (2019) 113837.

[142] B. He, X. Luo, F. Yu, T. Li, L. Wang, J. Zhou, Y. Fan, Effects of inlet subcooling on the flow boiling heat transfer performance of bi-porous mini-channels, Appl. Therm. Eng. 229 (2023) 120577.

[143] L. Yin, M. Sun, P. Jiang, C. Dang, L. Jia, Heat transfer coefficient and pressure drop of water

flow boiling in porous open microchannels heat sink, Appl. Therm. Eng. 218 (2023) 119361.

[144] S. Zhang, Y. Sun, W. Yuan, Y. Tang, H. Tang, K. Tang, Effects of heat flux, mass flux and channel width on flow boiling performance of porous interconnected microchannel nets, Exp. Therm. Fluid Sci. 90 (2018) 310-318.

[145] Y. Otomo, E. S. Galicia, K. Enoki, Enhancement of subcooled flow boiling heat transfer with high porosity sintered fiber metal, Appl. Sci. 11 (2021) 1237.

[146] E. S. Galicia, Y. Otomo, T. Saiwai, K. Takita, K. Orito, K. Enoki, Subcooled flow boiling heat flux enhancement using high porosity sintered fiber, Appl. Sci. 11 (2021) 5883.

[147] V. Y. S. Lee, G. Henderson, A. Reip, T. G. Karayiannis, Flow boiling characteristics in plain and porous coated microchannel heat sinks, Int. J. Heat Mass Tran. 183 (2022) 122151.

[148] C. Choi, J. S. Shin, D. I. Yu, M. H. Kim, Flow boiling behaviors in hydrophilic and hydrophobic microchannels, Exp. Therm. Fluid Sci. 35 (2011) 816-824.

[149] J. Lu, W. Cao, D. Zhang, Y. Chen, Z. Zhou, H. Xu, Boiling heat transfer characteristics of mixed particle porous microchannels, Ship Sci. Tech. 43(7) (2021) 162-167.

[150] V. E. Ahmadi, T. Guler, S. Celik, F. Ronshin, V. Serdyukov, A. Surtaev, A. K. Sadaghiani, A. Koşar, Effect of mixed wettability surfaces on flow boiling heat transfer at subatmospheric pressures, Appl. Therm. Eng. 236 (2024) 121476.

[151] K. Fu, W. Gao, X. Xu, X. Liang, Flow boiling heat transfer and pressure drop characteristics of water in a copper foam fin microchannel heat sink, Appl. Therm. Eng. 218 (2023) 119295.

[152] G. Xia, Y. Wang, R. Li, Z. Yan, Q. Li, Experimental study of boiling heat transfer characteristics of metal foam porous-wall mini-channels, Int. J. Refrig. 151 (2023) 278-289.

[153] M. Cen, S. Deng, C. Hu, J. Luo, S. Tan, C. Wang, Y. Wu, Enhanced boiling heat transfer of

HFE-7100 on copper foams under overflow conditions, Appl. Therm. Eng. 224 (2023) 120083.

[154] H. Wang, Q. F. Ying, E. Lichtfouse, C. G. Huang, Boiling heat transfer in copper foam bilayers in positive and inverse gradients of pore density, J. Appl. Fluid Mech. 16(5) (2023) 973-982.

[155] M. Ahmadi, S. Bigham, Gradient wick channels for enhanced flow boiling HTC and delayed CHF, Int. J. Heat Mass Tran. 167 (2021) 120764.

[156] H.-W. Li, H.-Y. Li, L.-T. Zheng, D.-W. Fu, Z.-Y. Li, Research on the effect of bubble dynamics and turbulent kinetic energy on heat transfer in mini-channels filled with metal foam, J. Therm. Anal. Calorim. 141 (2020) 69-81.

[157] H.-W. Li, T.-L. Chang, C.-H. Du, D.-W. Fu, W.-P. Hong, Experimental study on flow boiling heat transfer characteristics of multi-channel modified filled foam metal small channel, Int. Commun. Heat Mass 127 (2021) 105588.

[158] S. Azizifar, M. Ameri, I. Behroyan, Experimental study of the effect of metal foams on subcooled flow boiling heat transfer of water and developing a correlation for predicting heat transfer, Chem. Eng. Sci. 262 (2022) 118032.

[159] R. Dyga, M. Płaczek, Influence of hydrodynamic conditions on the type and area of occurrence of gas-liquid flow patterns in the flow through open-cell foams, Materials 13 (2020) 3254.

[160] M. Płaczek, R. Dyga, Void fraction prediction method in gas-liquid flow through channel packed with open-cell metal foams, Energies, 14 (2021) 2645.

[161] S. Nam, D. Y. Kim, Y. Kim, K. C. Kim, Effect of metal foam insert configurations on flow

boiling heat transfer and pressure drop in a rectangular channel, Materials, 14 (2021) 4617.

[162] R. Wen, S. Xu, Y.-C. Lee, R. Yang, Capillary-driven liquid film boiling heat transfer on hybrid mesh wicking structures, Nano Energy 51 (2018) 373-382.

[163] S. Sivasankaran, F. O. M. Mallawi, Numerical study on convective flow boiling of nanoliquid inside a pipe filling with aluminum metal foam by two-phase model, Case Stud. Therm. Eng. 26 (2021) 101095.

[164] W. Gao, K. Fu, X. Xu, X. Liang, Flow boiling heat transfer in copper foam fin microchannels with different fin widths using R134a, Sci. China Technol. Sc. 66(11) (2023) 3245-3258.

[165] S. Hong, C. Dang, E. Hihara, A 3D inlet distributor employing copper foam for liquid replenishment and heat transfer enhancement in microchannel heat sinks, Int. J. Heat Mass Tran. 157 (2020) 119934.

[166] W. Li, Z. Wang, F. Yang, T. Alam, M. Jiang, X. Qu, F. Kong, A. S. Khan, M. Liu, M. Alwazzan, Y. Tong, C. Li, Supercapillary architecture-activated two-phase boundary layer structures for highly stable and efficient flow boiling heat transfer, Adv. Mater. 32 (2020) 1905117.

[167] W. Li, J. Ma, T. Alam, F. Yang, J. Khan, C. Li, Flow boiling of HFE-7100 in silicon microchannels integrated with multiple micro-nozzles and reentry micro-cavities, Int. J. Heat Mass Tran. 123 (2018) 354-366.

[168] Q. Han, Z. Liu, C. Zhang, W. Li, Enhanced single-phase and flow boiling heat transfer performance in saw-tooth copper microchannels with high L/D_h ratio, Appl. Therm. Eng. 236 (2024) 121478.

[169] Q. Han, Z. Liu, Y. Chen, W. Li, Enhance flow boiling in Tesla-type microchannels by

inhibiting two-phase backflow, Int. J. Heat Mass Tran. 214 (2023) 124471.

[170] M. Hajialibabaei, M. Z. Saghir, I. Dincer, Y. Bicer, Experimental and numerical study on heat transfer performance of wavy channel heat sink with varying channel heights, Int. Commun. Heat Mass 148 (2023) 107044.

[171] T. Wen, H. Zhan, L. Lu, D. Zhang, Experimental investigation and development of new correlation for flow boiling heat transfer in mini-channel, Int. J. Therm. Sci. 129 (2018) 209-217.

[172] D. Deng, Y. Xie, Q. Huang, W. Wan, On the flow boiling enhancement in interconnected reentrant microchannels, Int. J. Heat Mass Tran. 108 (2017) 453-467.

[173] D. Deng, L. Chen, W. Wan, T. Fu, X. Huang, Flow boiling performance in pin fin-interconnected reentrant microchannels heat sink in different operational conditions, Appl. Therm. Eng. 150 (2019) 1260-1272.

[174] G. Marseglia, M. G. D. Giorgi, D. S. Carvalho, P. Pontes, R. R. Souza, A. L. N. Moreira, A. S. Moita, Experimental investigation on the effects of the geometry of microchannels based heat sinks on the flow boiling of HFE-7100, Appl. Therm. Eng. 236 (2024) 121479.

[175] P. Guo, S. Zheng, J. Yan, Q. Zhou, S. Wang, W. Li, Experimental investigation on heat transfer of subcooled flow boiling of water in mini channels under high heat fluxes, Exp. Therm. Fluid Sci. 142 (2023) 110831.

[176] Y. Lin, Y. Luo, W. Li, W. J. Minkowycz, Enhancement of flow boiling heat transfer in microchannel using micro-fin and micro-cavity surfaces, Int. J. Heat Mass Tran. 179 (2021) 121739.

[177] X. Ma, X. Ji, J. Wang, J. Fang, Y. Zhang, J. Wei, Flow boiling heat transfer characteristics

on micro-pin-finned surfaces in a horizontal narrow microchannel, Int. J. Heat Mass Tran. 194 (2022) 123071.

[178] S. W. Chang, T. H. Cheng, Thermal performance of channel flow with detached and attached pin-fins of hybrid shapes under inlet flow pulsation, Int. J. Heat Mass Tran. 164 (2021) 120554.

[179] J. Li, D. Zhang, Y. Wang, W. Chen, G. Zhu, Pressure drop of R134a in mini channels with micro pin fins during flow boiling, Appl. Therm. Eng. 217 (2022) 119195.

[180] W. Chang, K. Luo, W. Li, C. Li, Enhanced flow boiling of HFE-7100 in silicon microchannels with nanowires coated micro-pinfins, Appl. Therm. Eng. 216 (2022) 119064.

[181] C. Anderson, Z. Gao, M. Hanchak, T. Bandhauer, Experimental and computational investigation of flow boiling in a 52 μm hydraulic diameter microchannel evaporator with inlet restrictions and heat spreading, ASME J. Heat Mass Trans. 146 (2024) 061601.

[182] M. D. Clark, J. A. Weibel, S. V. Garimella, Impact of pressure drop oscillations and parallel channel instabilities on microchannel flow boiling and critical heat flux, Int. J. Multiphas. Flow 161 (2023) 104380.

[183] W. Li, X. Qu, T. Alam, F. Yang, W. Chang, J. Khan, C. Li, Enhanced flow boiling in microchannels through integrating multiple micro-nozzles and reentry microcavities, Appl. Phys. Lett. 110 (2017) 014104.

[184] W. Li, J. Ma, C. Li, Enhanced flow boiling in microchannels by incorporating multiple micro-nozzles and micro-pinfin fences, Int. J. Heat Mass Tran. 165 (2021) 120695.

[185] Q. Han, Z. Liu, W. Li, Enhanced thermal performance by spatial chaotic mixing in a saw-like microchannel, Int. J. Therm. Sci. 186 (2023) 108148.

[186] G. Wang, N. Qian, G. Ding, Heat transfer enhancement in microchannel heat sink with bidirectional rib, Int. J. Heat Mass Tran. 136 (2019) 597-609.

[187] Z. Feng, C. Zhou, F. Guo, J. Zhang, Q. Zhang, Z. Li, The effects of staggered triangular ribs induced vortex flow on hydrothermal behavior and entropy generation in microchannel heat sink, Int. J. Therm. Sci. 191 (2023) 108331.

[188] Y. Lan, Z. Feng, Z. Hu, S. Zheng, J. Zhou, Y. Zhang, Z. Huang, J. Zhang, W. Lu, Experimental investigation on the effects of swirling flow on flow boiling heat transfer and instability in a minichannel heat sink, Appl. Therm. Eng. 219 (2023) 119512.

[189] A. Priy, S. Raj, M. Pathak, M. K. Khan, A hydrophobic porous substrate-based vapor venting technique for mitigating flow boiling instabilities in microchannel heat sink, Appl. Therm. Eng. 216 (2022) 119138.

[190] R. Loganathan, A. Mohiuddin, S. Gedupudi, Experimental investigation of the effect of bypass inlet on flow boiling in a mini/micro-channel, Int. Commun. Heat Mass 110 (2020) 104405.

[191] J. Zhou, X. Chen, Q. Zhao, M. Lu, D. Hu, Q. Li, Flow thermohydraulic characterization of hierarchical-manifold microchannel heat sink with uniform flow distribution, Appl. Therm. Eng. 198 (2021) 117510.

[192] J. Zhou, Q. Li, X. Chen, Micro pin fins with topologically optimized configurations enhance flow boiling heat transfer in manifold microchannel heat sinks, Int. J. Heat Mass Tran. 206 (2023) 123956.

[193] R. Erp, R. Soleimanzadeh, L. Nela, G.s Kampitsis, E. Matioli, Co-designing electronics with microfluidics for more sustainable cooling, Nature 585 (2020) 211-216.

[194] Y. Luo, J. Zhang, W. Li, A comparative numerical study on two-phase boiling fluid flow and heat transfer in the microchannel heat sink with different manifold arrangements, Int. J. Heat Mass Tran. 156 (2020) 119864.

[195] Y. Luo, J. Li, K. Zhou, J. Zhang, W. Li, A numerical study of subcooled flow boiling in a manifold microchannel heat sink with varying inlet-to-outlet width ratio, Int. J. Heat Mass Tran. 139 (2019) 554-563.

[196] Y. Luo, W. Li, J. Zhang, W. J. Minkowycz, Analysis of thermal performance and pressure loss of subcooled flow boiling in manifold microchannel heat sink, Int. J. Heat Mass Tran. 162 (2020) 120362.

[197] L. Sun, J. Li, H. Xu, J. Ma, H. Peng, Numerical study on heat transfer and flow characteristics of novel microchannel heat sinks, Int. J. Therm. Sci. 176 (2022) 107535.

[198] Z. Rui, F. Zhao, H. Sun, L. Sun, H. Peng, Experimental research on flow boiling thermal-hydraulic characteristics in novel microchannels, Exp. Therm. Fluid Sci. 140 (2023) 110755.

[199] Q. Han, W. Lai, Z. Liu, L. Li, W. Li, A comparative study of enhanced thermal performance in Tesla-type microchannels, Appl. Therm. Eng. 239 (2024) 122157.

[200] K. Hu, C. Lu, B. Yu, L. Yang, Y. Rao, Optimization of bionic heat sinks with self-organized structures inspired by termite nest morphologies, Int. J. Heat Mass Tran. 202 (2023) 123735.

[201] Y. Xu, L. Li, Z. Yan, Experimental investigations of the flow boiling characteristics of green refrigerants in a novel petaloid micropin-fin heat sink, Int. J. Heat Mass Tran. 212 (2023) 124243.

[202] Q. Gao, H. Zou, J. Li, Numerical investigations of heat transfer and fluid flow characteristics in microchannels with bionic fish-shaped ribs, Processes 11 (2023) 1861.

[203] S. G. Kandlikar, Fundamental issues related to flow boiling in minichannels and microchannels, Exp. Therm. Fluid Sci. 26 (2002) 389-407.

[204] S. Szczukiewicz, N. Borhani, J. R. Thome, Two-phase flow operational maps for multi-microchannel evaporators, Int. J. Heat Fluid Fl. 42 (2013) 176-189.

[205] C. B. Tibiriçá, G. Ribatski, Flow boiling in micro-scale channels – Synthesized literature review, Int. J. Refrig. 36 (2013) 301-324.

[206] S.-M. Kim, I. Mudawar, Review of databases and predictive methods for heat transfer in condensing and boiling mini/micro-channel flows, Int. J. Heat Mass Tran. 77 (2014) 627-652.

[207] L. Cheng, G. Xia, Fundamental issues, mechanisms and models of flow boiling heat transfer in microscale channels, Int. J. Heat Mass Tran. 108 (2017) 97-127.

[208] L. Wang, X. Luo, J. Zhang, Improved flow boiling characteristics in minichannel with open-cell porous ribs, Appl. Therm. Eng. 239 (2024) 121994.

[209] Y. Kim, D. Y. Kim, K. C. Kim, Flow pattern map of flow boiling in a rectangular channel filled with porous media, Energies 14 (2021) 2440.

[210] S. Raj, M. Pathak, M. K. Khan, Flow boiling characteristics in different configurations of stepped microchannels, Exp. Therm. Fluid Sci. 119 (2020) 110217.

[211] B. Markal, B. Kul, M. Avci, R. Varol, Effect of gradually expanding flow passages on flow boiling of micro pin fin heat sinks, Int. J. Heat Mass Tran. 197 (2022) 123355.

[212] D. Wang, D. Wang, F. Hong, C. Zhang, J. Xu, Improved flow boiling performance and temperature uniformity in counter-flow interconnected microchannel heat sink, Appl. Therm. Eng. 241 (2024) 122370.

[213] A. Shishkin, F. Kanizawa, G. Ribatski, S. Tarasevich, A. Yakovlev, Experimental investigation of the heat transfer coefficient during convective boiling of R134a in tubes with twisted tape insert, Int. J. Refrig. 92 (2018) 196-207.

[214] M. Iasiello, N. Bianco, W. K. S. Chiu, V. Naso, The effects of variable porosity and cell size on the thermal performance of functionally-graded foam, Int. J. Therm. Sci. 160 (2021) 106696.

[215] A. Tikadar, S. Kumar, Investigation of thermal-hydraulic performance of metal-foam heat sink using machine learning approach, Int. J. Heat Mass Tran. 199 (2022) 123438.

[216] C. S. Sujith Kumar, S. Suresh, A. S. Praveen, M. C. Santhosh Kumar, V. Gopi, Effect of surfactant addition on hydrophilicity of ZnO-Al_2O_3 composite and enhancement of flow boiling heat transfer, Exp. Therm. Fluid Sci. 70 (2016) 325-334.

[217] P.-Y. Wang, X.-L. Zhao, Z.-H. Liu, Experimental study on boiling performance of wetting fluids in three-dimensional rectangle microchannels, Heat Mass Transfer 56 (2020) 2639-2652.

[218] J. Wang, H. Sakashita, F.-C. Li, M. Mori, Heat transfer and CHF in subcooled flow boiling of aqueous surfactant solutions, Exp. Therm. Fluid Sci. 93 (2018) 131-138.

[219] J. Wang, S. Ouyang, B. Li, J. Wang, Z. Wang, Marangoni effect on the bubble departure and CHF in subcooled flow boiling of pure water and surfactant solutions, Int. Commun. Heat Mass 153 (2024) 107351.

[220] Y. Zhang, W. Chen, Heat transfer study on flowing liquid film of SiO_2-water nanofluid with surfactant confined by metallic foam, Int. J. Energ. Res. 45 (2021) 6015-6031.

[221] L. Cheng, D. Mewes, A. Luke, Boiling phenomena with surfactants and polymeric additives:

A state-of-the-art review, Int. J. Heat Mass Tran. 50 (2007) 2744-2771.

[222] H. Jia, L. Xu, X. Xiao, K. Zhong, Study on boiling heat transfer of surfactant solution on grooved surface, Int. J. Heat Mass Tran. 181 (2021) 121876.

[223] B. M. Gasanov, Boiling of disperse-phase droplets in a forced flow of emulsion in a minichannel, Int. J. Heat Mass Tran. 142 (2019) 118454.

[224] Z. Rui, H. Sun, J. Ma, H. Peng, Experimental study and prediction on the thermal management performance of SDS aqueous solution based microchannel flow boiling system, Energy 282 (2023) 128747.

[225] J. Zhang, X. Luo, L. Wang, Z. Feng, T. Li, Combined effect of electric field and nanofluid on bubble behaviors and heat transfer in flow boiling of minichannels, Powder Technol. 408 (2022) 117743.

[226] J. Zhang, X. Luo, Z. Feng, Compound effect of EHD and nanofluid on flow boiling characteristics in minichannels, Powder Technol. 442 (2024) 119895.

[227] S. Mohammadi, F. Hormozi, E. H. Rad, Effects of surfactants on thermal performance and pressure drop in mini-channels- An experimental study, J. Taiwan Inst. Chem. E. 128 (2021) 430442.

[228] D. Deng, R. Chen, Y. Tang, L. Lu, T. Zeng, W. Wan, A comparative study of flow boiling performance in reentrant copper microchannels and reentrant porous microchannels with multi-scale rough surface, Int. J. Multiphas. Flow 72 (2015) 275-287.

[229] F. Li, Q. Ma, G. Xin, J. Zhang, X. Wang, Heat transfer and flow characteristics of microchannels with solid and porous ribs, Appl. Therm. Eng. 178 (2020) 115639.

[230] X. Yu, J. Xu, G. Liu, X. Ji, Phase separation evaporator using pin-fin-porous wall

microchannels: Comprehensive upgrading of thermal-hydraulic operating performance, Int. J. Heat Mass Tran. 164 (2021) 120460.

[231] B. Li, Y. Cui, G. Li, H. Jiang, Numerical analysis on thermal-hydraulic performance of optimized microchannel heat sink with slant ribs and quatrefoil rib-elliptical groove complex structures, Appl. Therm. Eng. 240 (2024) 122165.

[232] Y. Sun, F. Liang, Y. Tang, H. Tang, X. Xi, S. Yang, T. Fu, Effect of stagger angle on capillary performance of microgroove structures with reentrant cavities, Sci. China Technol. Sc. 64(7) (2021) 1436-1446.

[233] J. C. Chen, Correlation for boiling heat transfer to saturated fluids in convective flow, Indust. Eng. Chem. - Process Des. Develop. 5 (1966) 322-329.

[234] D. Steiner, J. Taborek, Flow boiling heat transfer in vertical tubes correlated by an asymptotic model, Heat Transfer Eng. 13 (1992) 43-69.

[235] N. Kattan, J. R. Thome, D. Favrat, Flow boiling in horizontal tubes: part-3: development of a new heat transfer model based on flow patterns, ASME J. Heat Transfer, 120 (1998) 156-165.

[236] L. Wojtan, T. Ursenbacher, J. R. Thome, Investigation of flow boiling in horizontal tubes: part I - a new diabatic two-phase flow pattern map, Int. J. Heat Mass Tran. 48 (2005) 2955-2969.

[237] L. Wojtan, T. Ursenbacher, J. R. Thome, Investigation of flow boiling in horizontal tubes: part II - development of a new heat transfer model for stratified-wavy, dryout and mist flow regimes, Int. J. Heat Mass Tran. 48 (2005) 2970-2985.

[238] L. Cheng, G. Ribatski, J. Moreno Quibén, J. R. Thome, New prediction methods for CO_2

evaporation inside tubes: part I - a two-phase flow pattern map and a flow pattern based phenomenological model for two-phase flow frictional pressure drops, Int. J. Heat Mass Tran. 51 (2008) 111-124.

[239] L. Cheng, G. Ribatski, J. R. Thome, New prediction methods for CO_2 evaporation inside tubes: part II - an updated general flow boiling heat transfer model based on flow patterns, Int. J. Heat Mass Tran. 51 (2008) 125-135.

[240] J. Moreno Quibén, L. Cheng, R. J. da Silva Lima, J. R. Thome, Flow boiling in horizontal flattened tubes: part I - two-phase frictional pressure drop results and model, Int. J. Heat Mass Tran. 52 (2009) 3634-3644.

[241] J. Moreno Quibén, L. Cheng, R. J. da Silva Lima, J. R. Thome, Flow boiling in horizontal flattened tubes: part II - flow boiling heat transfer results and model, Int. J. Heat Mass Tran. 52 (2009) 3645-3653.

[242] J. R. Thome, V. Dupont, A. M. Jacobi, Heat transfer model for evaporation in microchannels. Part I: presentation of the model, Int. J. Heat Mass Tran. 47 (2004) 3375-3385.

[243] V. Dupont, J. R. Thome, A. M. Jacobi, Heat transfer model for evaporation in microchannels. Part II: comparison with the database, Int. J. Heat Mass Tran. 47 (2004) 3387-3401.

[244] A. Cioncolini, J. R. Thome, Algebraic turbulence modeling in adiabatic and evaporating annular two- phase flow, Int. J. Heat Fluid Flow 32 (2011) 805-817.

[245] J. R. Thome, A. Cioncolini, Unified model suite for two phase flow, convective boiling and condensation in macro- and microchannel, Heat Transfer Eng. 37 (2016) 1148-1157.

[246] Y. Fang, D. Lu, W. Yang, H. Yang, Y. Huang, Saturated flow boiling heat transfer of R1233zdI in parallel mini-channels: Experimental study and flow-pattern-based prediction,

Int. J. Heat Mass Tran. 216 (2023) 124608.

[247] Z. Liu, R. H. S. Winterton, A general correlation for saturated and subcooled flow boiling in tubes and annuli, based on a nucleate pool boiling equation, Int. J. Heat Mass Tran. 34 (1991) 2759-2766.

[248] W. Li, Z. Wu, A general correlation for evaporative heat transfer in micro/mini-channels, Int. J. Heat Mass Tran. 53 (2010) 1778-1787.

[249] X. Fang, Q. Wu, Y. Yuan, A general correlation for saturated flow boiling heat transfer in channels of various sizes and flow directions, Int. J. Heat Mass Tran. 107 (2017) 972-981.

[250] X. Ma, X. Ji, C. Hu, X. Yang, Y. Zhang, J. Wei, S. H. Godasiaei, Saturated/subcooled flow boiling heat transfer inside micro/mini-channels: A new prediction correlation and experiment evaluation, Int. J. Heat Mass Tran. 210 (2023) 124184.

[251] X. Cheng, J. Wu, Geometry-metrics-dependent flow boiling characteristics in rectangular microchannels, Int. J. Heat Mass Tran. 218 (2024) 124733.

[252] A. Koşar, C.-J. Kuo, Y. Peles, Boiling heat transfer in rectangular microchannels with reentrant cavities, Int. J. Heat Mass Tran. 48 (2005) 4867-4886.

[253] D. Žalec, M. Može, M. Zupančič, I. Golobič, Elucidating the effects of surface wettability on boiling heat transfer using hydrophilic and hydrophobic surfaces with laser-etched microchannels, Case Stud. Therm. Eng. 57 (2024) 104357.

[254] A. Aboubakri, V. E. Ahmadi, S. Celik, A. K. Sadaghiani, K. Sefiane, A. Koşar, Effect of surface biphilicity on FC-72 flow boiling in a rectangular minichannel, Front. Mech. Eng. 7 (2021) 755580.

[255] A. Hadžić, M. Može, M. Zupančič, I. Golobič, Superbiphilic laser-microengineered surfaces

with a self-assembled monolayer coating for exceptional boiling performance, Adv. Funct. Mater. 34 (2024) 2310662.

[256] T. Alam, W. Li, W. Chang, F. Yang, J. Khan, C. Li, A comparative study of flow boiling HFE-7100 in silicon nanowire and plainwall microchannels, Int. J. Heat Mass Tran. 124 (2018) 829-840.

[257] A. Ateş, S. Çelik, V. Yağcı, M. Ç. Malyemez, M. Parlak, A. K. Sadaghiani, A. Koşar, Flow boiling of dielectric fluid HFE – 7000 in a minichannel with pin fin structured surfaces, Appl. Therm. Eng. 223 (2023) 120045.

[258] Y. Zhang, W. Fan, Z. Zhang, J. Li, T. Zhai, W. Liu, Z. Liu, Developing a stable microchannel flow boiling heat sink with a venting membrane, Int. Commun. Heat Mass 158 (2024) 107896.

[259] B. He, X. Luo, F. Yu, T. Li, Z. Feng, J. Zhou, Enhanced flow boiling performance of interconnected bi-porous minichannel, Int. Commun. Heat Mass 157 (2024) 107770.

[260] N. Shah, H. B. Mehta, J. Banerjee, Experimental investigations on a novel instability suppression mechanism for subcooled flow boiling in microchannel heat sink, Appl. Therm. Eng. 239 (2024) 122006.

[261] G. Xia, Y. Lv, D. Ma, Y. Jia, Experimental investigation of the continuous two-phase instable boiling in microchannels with triangular corrugations and prediction for instable boundaries, Appl. Therm. Eng. 162 (2019) 114251.

[262] G. Xia, Y. Lv, L. Cheng, D Ma, Y. Jia, Experimental study and dynamic simulation of the continuous two-phase instable boiling in multiple parallel microchannels, Int. J. Heat Mass Tran. 138 (2019) 961-984.

[263] G. Xia, Y. Cheng, L. Cheng, Y. Li, Heat transfer characteristics and flow visualization during flow boiling of acetone in semi-open multi-microchannels, Heat Transfer Eng. 40(16) (2019) 1349-1362.

[264] S. Wang, H.-H. Chen, C.-L. Chen, Enhanced flow boiling in silicon nanowire-coated manifold microchannels, Appl. Therm. Eng. 148 (2019) 1043-1057.

[265] W. Tang, J. Li, Z. Wu, J. Lu, K. Sheng, A numerical investigation of the thermal-hydraulic performance during subcooled flow boiling in MMCs with different manifolds, Appl. Therm. Eng. 236 (2024) 121820.

[266] H. Huang, J. R. Thome, An experimental study on flow boiling pressure drop in multi-microchannel evaporators with different refrigerants, Exp. Therm. Fluid Sci. 80 (2017) 391-407.

[267] W. Li, Two-phase heat transfer correlations in three-dimensional hierarchical tube, Int. J. Heat Mass Tran. 191 (2022) 122827.

[268] A. Priy, I. Ahmad, A. Ranjan, M. Pathak, M. K. Khan, Flow boiling characteristics in a microchannel heat sink with a condensing cover plate, Therm. Sci. Eng. Prog. 53 (2024) 102707.

Nomenclature

A_{cs} cross-sectional area of a micro/mini-channel, mm^2

Bd Bond number

CHF critical heat flux, W/m^2

Co Confinement number

c_p specific heat at constant pressure, J/(kgK)

D length scale, mm

D_h hydraulic diameter, mm

HTC heat transfer coefficient, $W/(m^2K)$

h_{fg} latent heat of vaporization of liquid, J/kg

IGBT insulated gate bipolar transistor

G mass flux, $kg/(m^2s)$

g gravitational acceleration, m/s^2

L Laplace number

MEMS micro-electromechanical systems

m mass flow rate, kg/s

Q heat exchange capacity, W

q heat flux, W/m^2

T temperature, °C

UAV unmanned aerial vehicle

V volume, m^3

W width of the micro/mini-channel

We Webber number

x vapor quality

Subscripts

C constant

Cu copper

h hydraulic diameter

eff effective

f fluid

g gas

HL heated length of the micro/mini-channel

in inlet

i local location in channels

l liquid

m mass

p constant pressure

Greek symbols

δ mass difference, kg

μ dynamic viscosity, kg/(s m)

ρ density, kg/m^3

φ porosity, %

σ surface tension, N/m

List of table captions

Table 1. Selected studies of flow boiling and two-phase flow in enhanced micro/mini-channels with microstructures or coatings.

Authors	Fluids	Heat sink material	Mass fluxes ($kg/(m^2s)$)	Enhancement techniques	Obtain results
Zhang et al. [76]	Deionized water	Copper	142	Sintering porous heat sink	Making the peak critical heat flux over 160 W/cm^2 at the mass flux of 142 $kg/(m^2s)$ and existing the explosive boiling process at some conditions.
Kim et al. [98]	Water	-	100-800	Heterogeneous wetting surface	An optimal proportion of hydrophobic area in parallel pattern and dotted pattern is approximately 32% gave the best heat transfer performance, while this in crosswise pattern is only about 16.5%.
Lin et al. [99]	Deionized water	Silicon	200-500	Heterogeneous wetting surface	The HTC on heterogeneous wetting surface with perpendicular stripes was enhanced by about 40%.
Tan et al. [100]	Deionized water	Copper	400	Bionic gradient wetting surface	Improving the HTC by over 50%.
Lioger-Arago et al. [101]	HFE-7100	Aluminum	140/390/648	Biphilic surface and porous surface	Increasing the CHF use the biphilic surface at the low mass flux is only 0.25 times of the porous coating surface.
Semenic et al. [102]	R245fa refrigerant	C1100 copper	-	Porous coating	The HTC with porous coating had on average 1.5 times higher than uncoated, maximum 2.5 times, and the CHF was 1.5 to 2 times.
Mao et al. [104]	Deionized water	Copper	-	Sintering porous heat sink	The impact of sintered particle diameter on flow boiling is significant, and the main mechanism of phase transition is thin liquid film boiling.
Sarwar et al. [107]	Water	-	100-300	Porous coating	The particle size and coating thickness have a significant impact on enhancing heat transfer. The CHF enhancement by 25% for Al_2O_3 coated surface, and TiO_2 coated surface is about 20%.
Ahn et al. [109]	Water	-	62/83/104	Multiwalled carbon nanotube channel	Effective separation of vapor and liquid in the channel has been achieved.

Table 2. Selected studies of enhanced flow boiling heat transfer performance in micro/mini-channels with surface modification techniques.

Authors	Fluids	D_h (mm)	Mass fluxes (kg/(m^{2}s))	Treatment techniques	Materials	Enhancement of CHF	Enhancement of HTC
Khanikar et al. [73]	Water	-	86/228/368	Chemical vapor deposition	CNTs and Copper	CHF was obvious enhanced and degraded following repeated tests at high mass fluxes.	
Lim et al. [81]	Water	~ 1.67	400/800/1200	Laser etching	Copper	Over 30% (Max)	-
Kumar et al. [112]	De-mineralized water	-	283/348/427	Chemical vapor deposition	CNT coatings and Copper	21.6% (Max)	-
Kousalya et al. [113]	Water	-	38	Chemical vapor deposition	CNT coatings and Copper	Heterogeneous wetting surface exhibit higher heat transfer coefficients at 0.66 and 0.85 superhydrophilic area fraction.	
Sia et al. [114]	Water	2	42/83/146	Thermal curing	GNPs/epoxy coatings and Copper	59.5% (Max)	64.9% (Max)
Sia et al. [115]	Water	0.8	57/83/ 122/167	Thermal curing	GNPs/epoxy coatings and Copper	134% (SPHO) 71.8% (SPHI)	135% (SPHO) 68.8% (SPHI)
Gupta et al. [116]	Deionized water	~ 2.6	53/113/187 268/361	Electrochemical deposition	Cu-TiO_2 coating	92% (Max)	94% (Max)
Gupta et al. [117]	Deionized water	~ 2.6	53/113/ 268/361	Electrochemical deposition + Single-step sintering	Cu-TiO_2 coating	~ 143% (Max)	~ 153% (Max)
Gupta et al. [118]	Deionized water	~ 2.6	53/113/187 268/361	Single-step electrodeposition	Cu-Al_2O_3 coating	86%	84%
Gupta et al. [119]	Deionized water	~ 2.6	53/113/ 268/361	Electrodeposition + Sintering	Cu-Al_2O_3 coating	~ 176% (Max)	~ 200% (Max)
Gupta et al.	Deionized water	~ 2.6	53-361	Electrochemical	Cu-Al_2O_3	93%	90%

[120]				deposition	coating		
Aravinthan et al. [134]	Deionized water	3	100-650	Electroless galvanic deposition	Nano silver	-	Over 20 % (Max)
Zhang et al. [135]	Deionized water	~ 0.98	150/275/400	Sintering	Copper	53.2% (Max)	114.5% (Max)
He et al. [142]	R141b	~ 1.33	255	Sintering	Copper woven tapes	-	261% (Max)
Yin et al. [143]	Deionized water	~ 0.53	151.5-551.1	Sintering	Copper	-	200%(Max)

Notes: SPHO is superhydrophobic surface and SPHI is superhydrophilic surface, D_h represents hydraulic diameter.

Table 3. Selected studies of enhanced flow boiling heat transfer performance in micro/mini-channels with enhanced structures.

Authors	Fluids	Mass fluxes ($kg/(m^2s)$)	Enhancement types	Materials	Enhancement of CHF	Enhancement of HTC
Fu et al. [151]	Deionized water	76-408	Copper foam fin channel	Copper	25% (Max)	80% (Max)
Ahmadi et al. [155]	Deionized water	140-340	Gradient wick channel	Woven copper meshes	60% (Max)	300% (Max)
Li et al. [156]	R141b	50-150	Metal foam channel	-	The bubble is small in channels filled with metal foam, and increases the fluid mixing frequency to improve heat transfer.	
Nam et al. [161]	R245fa	133-300	Metal foam filling	Copper foam	HTC in the dense-array spanwise pattern was higher than that in the sparse-array model.	
Gao et al. [164]	R134a	264-1213	Copper foam fin channel	Copper	-	~ 60% (Max)
Hong et al. [165]	Deionized water	26.5-110.5	Copper foam layer	Copper	-	~ 170%
Li et al. [166]	HFE-7100	-	Channel geometrical structure (Micro-pinfin fences)	Silicon	~ 80%	~ 170%
Li et al. [167]	HFE-7100	231-1155	Channel geometrical structure (Reentry cavities and micronozzles)	Silicon	37% (Compared to FP) 70% (Compared to PR)	208% (Compared to FP) -
Han et al. [168]	Deionized water	50-300	Channel geometrical structure (Saw-tooth shape)	Copper	~ 87% (Max)	~ 110.7% (Max)
Han et al. [169]	Deionized water	60-360	Channel geometrical structure (Tesla-type shape)	Copper	88.4% (Max)	86.8% (Max)
Hajialibabaei et al. [170]	Distilled water	-	Channel geometrical structure (Wavy shape)	Aluminum	The maximum reduction of highest temperature decreased is 7.84%.	
Lin et al. [176]	Water	500	Channel geometrical structure	Silicon	-	~ 62%

			(Micro-fin and micro-cavity surface)			
Lan et al. [188]	Distilled water	120.7/210.5	Channel geometrical structure (Twisted tape)	Oxygen-free copper	-	80.9% (Max)
Priy et al. [189]	Deionized water	206-335.49	Channel geometrical structure (Secondary flow path)	PDMS and copper	-	32%
Zhou et al. [192]	Deionized water	-	Channel geometrical structure (Micro pin fins manifold)	Chrome-zirconium copper	-	87% (Max)
Rui et al. [198]	HFE-7100	488.3-856.7	Channel geometrical structure (Tesla-type shape and sector bump shape)	Copper	Heat transfer coefficient with sector bump shape is approximately 45 % higher than that with tesla-type shape in average.	

Notes: FP is the four-nozzle plain-wall microchannels. PR is the plain microchannels with inlet restrictors.

Table 4. Selected studies of enhanced flow boiling heat transfer using surfactants in micro/mini-channels.

Authors	Surfactants	Optimal concentration	Enhancement types	Enhancement of CHF	Enhancement of HTC
Kumar et al. [216]	SDS	4 wt.%	surfactant + ZnO-Al_2O_3 composite coating	44.6%	29.7%
Wang et al. [217]	SDS	2‰	surfactant + deionized water or R113	70%	140%
Wang et al. [218]	CTAC/NaSal	0.1‰	surfactant aqueous solution	26%	36%
Zhang et al. [220]	SDBS	0.05‰ (SDBS)/0.1‰ (SiO_2)	surfactant + SiO_2 nanofluid	18% (Max)	-
Zhang et al. [225]	SDBS, CTAB, Span80	-	surfactant + Al_2O_3/R141b nanofluid	-	over 30% (SDBS)

Notes: Enhancement types include the combination of surfactants and coatings, and the combination of surfactants and working fluids.

List of figure captions

Fig. 1. Various passive heat transfer enhancement techniques: (a) Triangular groove shape channels [25]; (b) Twisted tape channels [26]; (c) Embowed groove shape channels [31]; (d) Pin-fin rib channels [33]; (e) Wavy shape channels [41] and (f) Longitudinal vortex generator array channels [42]. [(a), (b), (d), (e) and (f), copyright obtained from Elsevier; (c) CC-BY license.]

Fig. 2. Surface topology and SEM images of various porous coating structures: (a) Micro-structured surfaces and micro-nano-hierarchical-structured surfaces by PDMS coatings [51]; (b) Etched surface and rose petal surfaces [52] and (c) Nanoscale structures on the microporous coatings [53]. [Copyright obtained from Elsevier.]

Fig. 3. The enhanced flow boiling heat transfer performance in composite microchannel heat sink [54]. [Reproduction and copyright obtained from Elsevier.] (a) Comparison of heat transfer performance between base surface and enhanced surface. (b) Schematic of the surface boiling curves.

Fig. 4. Comparison of the channel classification criteria A by Mehendale and Jacobi [62] and criteria B by Kandlikar and Grande [63].

Fig. 5. Classification of flow boiling heat transfer enhancement techniques: (a) Spraying process [71]; (b) Chemical vapor deposition [73]; (c) Sintering process [76, 77]; (d) Laser etching [81]; (e) Chemical etching [82]; (f) Hot embossing [84] and (g) Electrochemical deposition [119]. [Reproduction and copyright obtained from Elsevier.]

Fig. 6. Comparison of non-uniform wetting patterns [98]. [Copyright obtained from Elsevier.]

Fig. 7. SiOC coating non-uniform wetting surface [101]. [Reproduction and copyright obtained

from Elsevier.]

Fig. 8. Surface structure of the copper particle sintered porous structure coating with different particle sizes [76]. [Copyright obtained from Elsevier.]

Fig. 9. Comparison of the copper particle sintered porous structure coating porosity and heat transfer with different particle sizes. Experimental conditions in this figure: the inlet temperature is 60 ℃ and the mass flux is 142 kg/(m^2s) [76]. [Reproduction and copyright obtained from Elsevier.]

Fig. 10. Comparison between Al_2O_3 microporous coating and TiO_2 microporous coating [107]. [Copyright obtained from Elsevier.]

Fig. 11. SEM images of CNPs coatings. [Copyright obtained from Elsevier.] (a) SEM image of different CNTs coating microstructure [73]. The left image shows the CNTs coating before the experiment, while the right image shows the CNT cellular and the unique “fish scale” shape coating formed after multiple experiments. (b) SEM image of sandblasted copper and CNTs coating microstructure [112]. The image on the left is the sand blasted copper surface, the middle is the diamond coated surface, and the right is the CNTs coating surface. In addition, there is also an inset of the contact angle in the bottom left corner of each image. (c) Coating microstructure and the alternating non-uniform wetting surface [113]. The two images in the upper layer show the non-uniform CNTs coating surface and the uniform CNTs coating surface, respectively; the middle layer is Teflon-coated GPCNTs and GPCNT coating after exposure to O_2 plasma; the lower layer is a wetting surface composed of parallel and alternating superhydrophobic and superhydrophilic regions.

Fig. 12. The trend of enhanced heat transfer of CNTs coatings with various mass flux [112].

[Reproduction and Copyright obtained from Elsevier.]

Fig. 13. Mechanism and comparison of enhanced heat transfer of graphene coatings [114]: (a) Liquid permeation dynamic process of GNPs/SE coating; (b) Liquid permeation dynamic process of GNPs/CE coating. In this figure: superhydrophilic surface GNPs/SE(I) (the GNPs/SE coating was cured at 300 ◦C for 40 min, ultrafast water permeability), superhydrophilic surface GNPs/SE(II) (the GNPs/SE coating was cured at 250 ◦C for 40 min), superhydrophobic surface GNPs/CE(I) (the GNPs/CE coating was cured with Kapton polyimide tape at 300 ◦C for 40 min), hydrophobic surface GNPs/CE(II) (the GNPs/CE coating was cured at 180 ◦C for 5 h). [CC-BY license.] (a) GNPs/SE coating. (b) GNPs/CE coating.

Fig. 14. The dynamics of bubbles during the flow boiling process (the pressure-induced wetting transition process) [115]: (a) Conventional superhydrophobic surface; (b) Superhydrophobic GNPs-coated surface. [CC-BY license.]

Fig. 15. Comparison of the SEM images of the surface microstructure of Cu-TiO_2 coatings prepared with two electrochemical deposition techniques [116]: (a) Bare copper surface; (b) Two-step electrochemical deposition porous coating surface. [Copyright obtained from Elsevier.]

Fig. 16. Comparison of the SEM images Cu-Al_2O_3 porous coating surface micropores with two current densities [119]. The left is higher current density (150 mA/cm^2) and the right is lower current density (50 mA/cm^2). [Copyright obtained from Elsevier.]

Fig. 17. Comparison of the CHF enhancement and porosity with different Cu-Al_2O_3 porous coatings [118-120]. [Reproduction and copyright obtained from Elsevier.]

Fig. 18. Microstructures and boiling of the laser-induced surfaces [81]. [Copyright obtained

from Elsevier.] (a) Surface microstructure and wettability. (b) Comparison of the bubble nucleation and growth processes at the heat flux of 50 W/cm^2 and the mass flux of 400 kg/(m^{2}s).

Fig. 19. Improvement rate of the CHF in minichannels of the laser-induced surfaces at the mass flux of 400 kg/(m^{2}s) [81]. [Reproduction and copyright obtained from Elsevier.]

Fig. 20. Differences in porous coatings with different particle sizes [135]. [Reproduction and copyright obtained from Elsevier.] (a) SEM image of porous coatings and corresponding binary method image. (b) Change in porosity of porous coatings.

Fig. 21. Porous copper woven tape structure [77, 142]. [Reproduction and copyright obtained from Elsevier.] (a) Schematic diagram of porous structure. (b) Comparison of bubble diameter at G = 253 kg/(m^{2}s) and q_{eff} = 11.2 kW/m^2.

Fig. 22. Structure and nucleation mechanism of solid channels and porous channels [143]. The left image is solid copper substrate heat sink and the right is sintering porous substrate heat sink. [Copyright obtained from Elsevier.]. (a) Comparison of microstructure. (b) Bubble nucleation process.

Fig. 23. Comparison of the HTC enhancement with different Cu-Al_2O_3 coatings formed by various techniques [118-120]. [Reproduction and copyright obtained from Elsevier.]

Fig. 24. Comparison of flow patterns between hydrophilic and hydrophobic surfaces [148]. [Copyright obtained from Elsevier.]

Fig. 25. Flow boiling in minichannels with a heat flux of 380 kW/cm^2 and a mass flux of 42 kg/(m^{2}s) [114]: (a) Uncoated surface; (b) GNPs/SE (I) surface; (c) GNPs/SE (II) surface; (d) GNPs/CE (I) surface and (e) GNPs/CE (II) surface. [CC-BY license.]

Fig. 26. SEM images of the microstructures of textured surfaces formed by laser etching

techniques [150]. [Copyright obtained from Elsevier.]

Fig. 27. Gradient wick minichannel heat sink [155]: (a) Schematic of a possible liquid-vapor interface; (b) Schematic of the structure. In this figure: “T.F.E.”, “S. Ph.” and “T. Ph.” stand for thin film evaporation, single-phase, and two-phase, respectively. [Copyright obtained from Elsevier.]

Fig. 28. The structure of secondary flow path based on hydrophobic porous PDMS [189]. [Copyright obtained from Elsevier.]

Fig. 29. The structures and flow patterns of aluminum-based porous rib minichannels [208]. [Copyright obtained from Elsevier.] (a) Schematic diagram of mini-channel structure. (b) Comparison of nucleation and boiling development processes at a mass flux of 115.5 kg/(m^{2}s) and an inlet temperature of 60 ℃.

Fig. 30. Different flow patterns in foam copper microchannels [151]: (a) and (b) bubbly flow (G = 205 kg/(m^{2}s), q_{eff} = 296 W/cm^2, x = 0.007); (c) and (d) slug flow (G = 68 kg/(m^{2}s), q_{eff} = 17 W/cm^2, x = 0.04); (e) and (f) churn flow (G = 102 kg/(m^{2}s), q_{eff} = 56 W/cm^2, x = 0.09); (g) and (h) annular flow (G = 68 kg/(m^{2}s), q_{eff} = 117 W/cm^2, x = 0.53) and (i) and (j) wispy-annular flow (G = 409 kg/(m^{2}s), q_{eff} = 297 W/cm^2, x = 0.19). [Copyright obtained from Elsevier.]

Fig. 31. Influence of twisted tapes on flow patterns. [Copyright obtained from Elsevier.] (a) The high-speed images and reconstructed images for the plain minichannel heat sink, the minichannel heat sinks with twisted tape lengths of 100 mm (STTI-100) and the minichannel heat sinks with twisted tape lengths of 150 mm (FTTI-150) at q_{eff} = 142.4 kW/m^2, G = 120.7 kg/(m^{2}s) and T_{in} = 80 °C [188]. (b) Flow images for distinct flow patterns during R134a convective flow boiling at p = 550 kPa and twist ratio is 4 [213].

Fig. 32. Flow pattern snapshot at T_{in} = 20 °C, m = 2.93 g/s [198]: (a) Tesla-type structure at q_{eff} = 12.97 W/cm^2; (b) Sector bump structure at q_{eff} = 12.84 W/cm^2. [Copyright obtained from Elsevier.]

Fig. 33. The nucleation sites on heating surface at different CTAC/NaSal aqueous solution concentrations [218]: (a) The heat flux is 1.7 × 10^5 W/m^2; (b) The heat flux is 2.9 × 10^5 W/m^2. [Copyright obtained from Elsevier.]

Fig. 34. Sequential images of the flow patterns in channels at q = 2.9 × 10^5 W/m^2 (G = 152 kg/(m^{2}s), $\Delta T_{sub,\ in}$ = 20 K) [218]: (a) Water; (b) 0.1‰ CATC/NaSal solution. [Copyright obtained from Elsevier.]

Fig. 35. Comparison of the flow pattern in straight microchannels [224]: (a) Without surfactant SDS; (b) With surfactant SDS. [Copyright obtained from Elsevier.]

Fig. 36. Schematic diagram in formation of composite enhanced structures.

Fig. 37. An ideal heat transfer mechanism for composite enhanced heat transfer techniques.

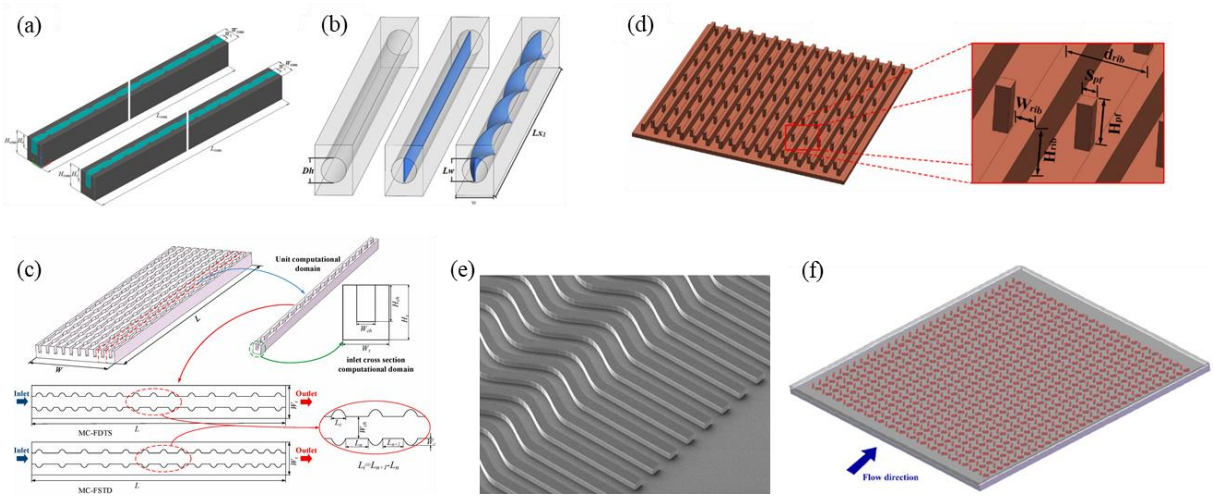

Fig. 1. Various passive heat transfer enhancement techniques: (a) Triangular groove shape channels [25]; (b) Twisted tape channels [26]; (c) Embowed groove shape channels [31]; (d) Pin-fin rib channels [33]; (e) Wavy shape channels [41] and (f) Longitudinal vortex generator array channels [42]. [(a), (b), (d), (e) and (f), copyright obtained from Elsevier; (c) CC-BY license.]

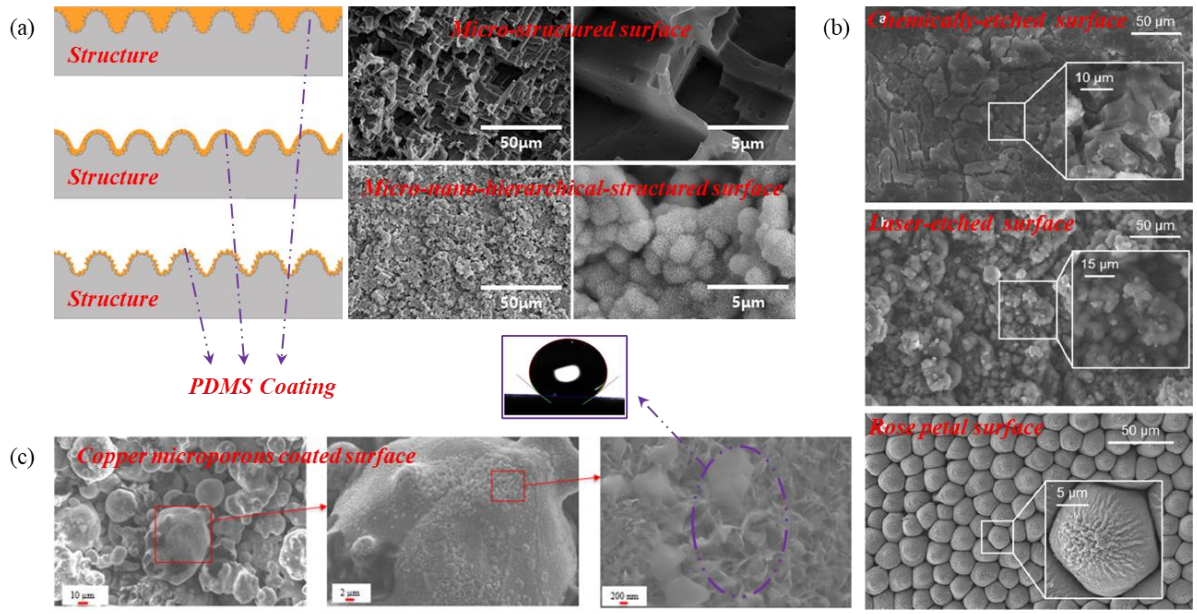

Fig. 2. Surface topology and SEM images of various porous coating structures: (a) Micro-structured surfaces and micro-nano-hierarchical-structured surfaces by PDMS coatings [51]; (b) Etched surface and rose petal surfaces [52] and (c) Nanoscale structures on the microporous coatings [53]. [Copyright obtained from Elsevier.]

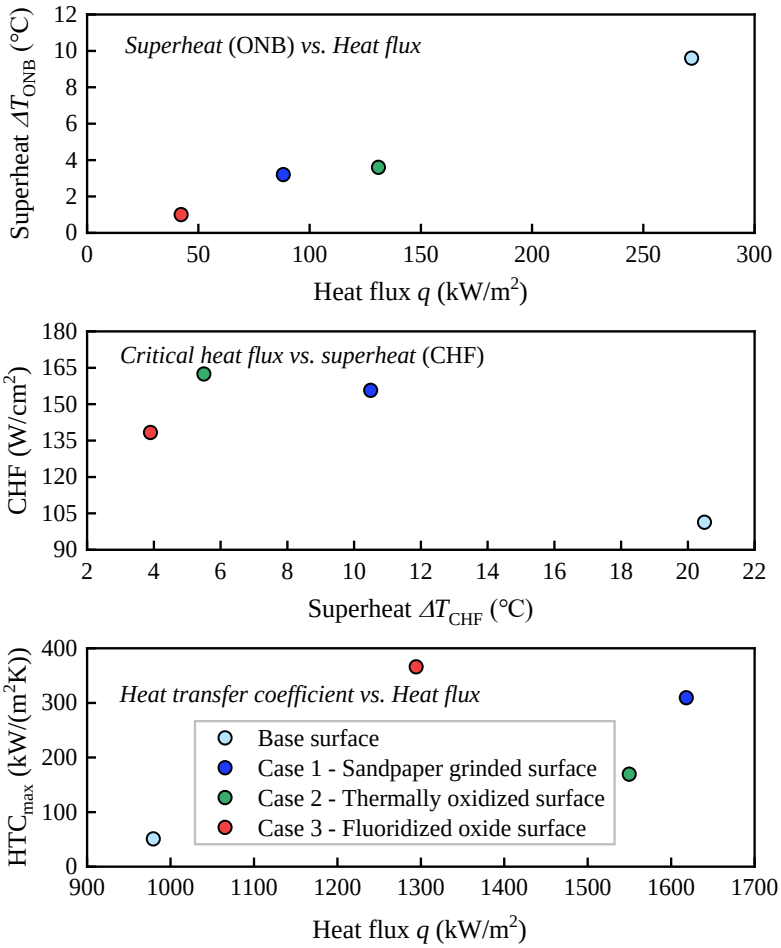

(a) Comparison of heat transfer performance between base surface and enhanced surface.

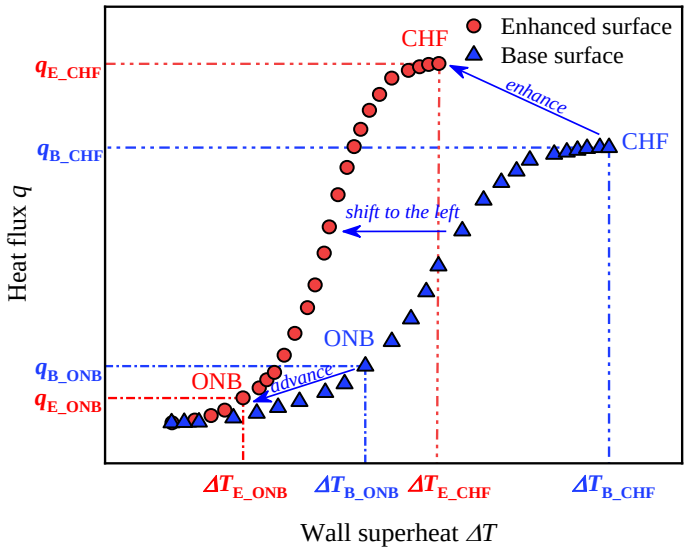

(b) Schematic of the surface boiling curves.

Fig. 3. The enhanced flow boiling heat transfer performance in composite microchannel heat sink [54]. [Reproduction and copyright obtained from Elsevier.]

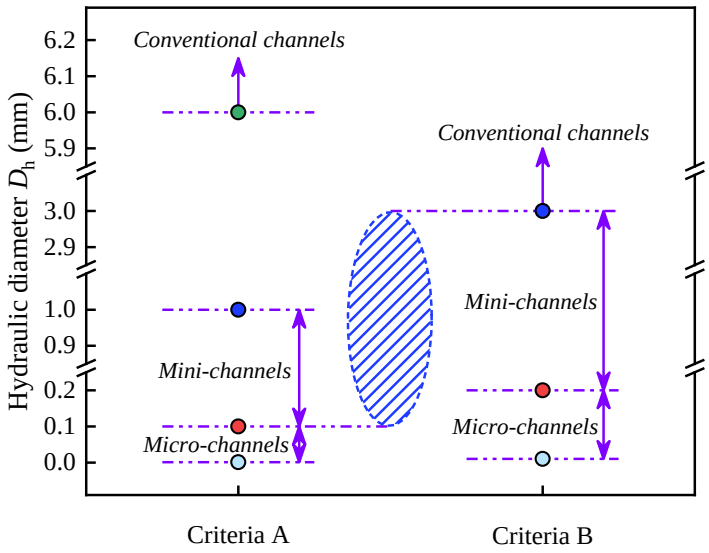

Fig. 4. Comparison of the channel classification criteria A by Mehendale and Jacobi [62] and criteria B by Kandlikar and Grande [63].

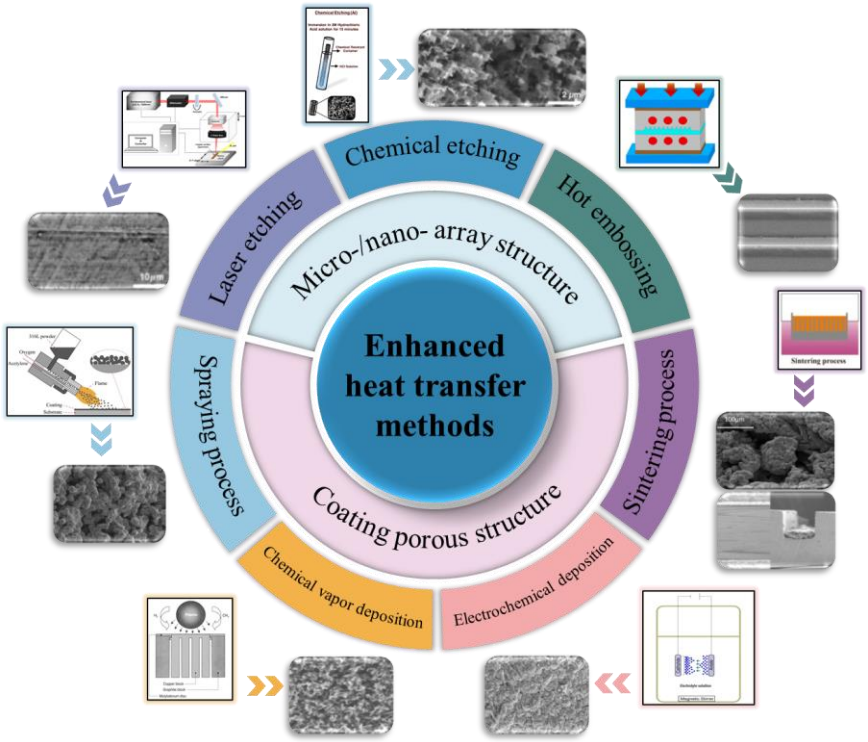

Fig. 5. Classification of flow boiling heat transfer enhancement techniques: (a) Spraying process [71]; (b) Chemical vapor deposition [73]; (c) Sintering process [76, 77]; (d) Laser etching [81]; (e) Chemical etching [82]; (f) Hot embossing [84] and (g) Electrochemical deposition [119]. [Reproduction and copyright obtained from Elsevier.]

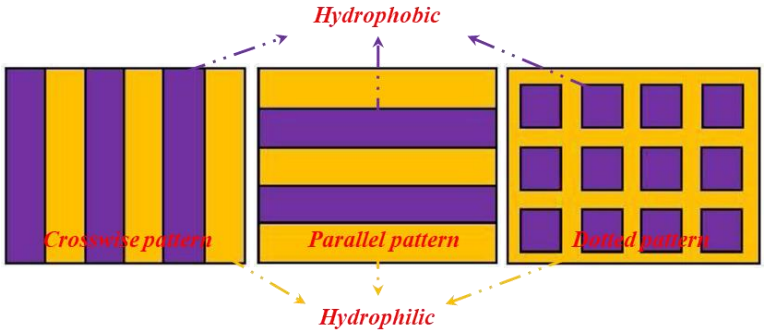

Fig. 6. Comparison of non-uniform wetting patterns [98]. [Copyright obtained from Elsevier.]

Fig. 7. SiOC coating non-uniform wetting surface [101]. [Reproduction and copyright obtained from Elsevier.]

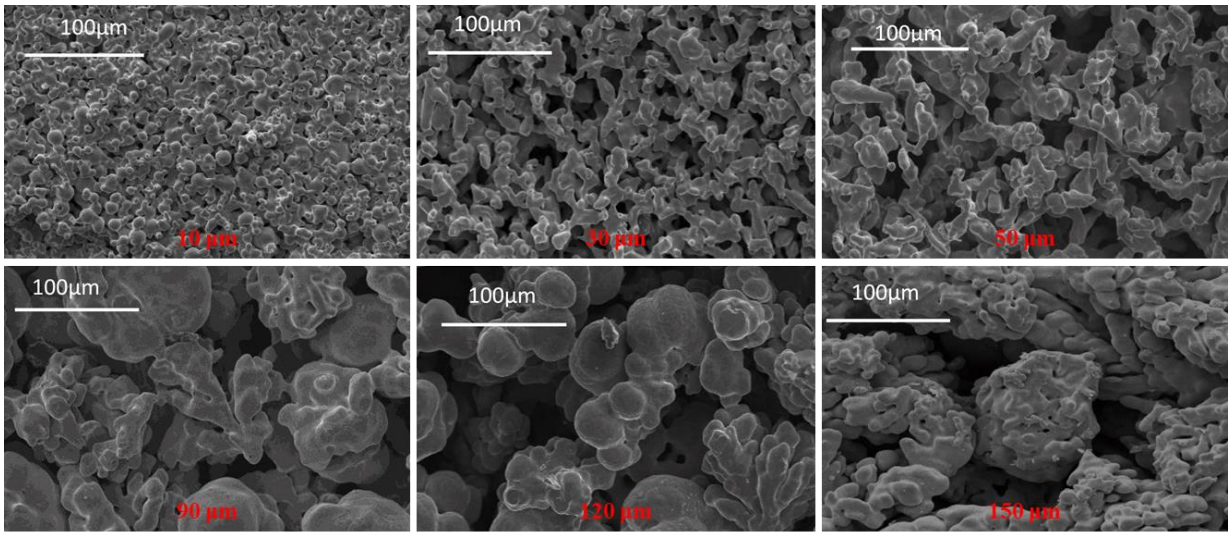

Fig. 8. Surface structure of the copper particle sintered porous structure coating with different particle sizes [76]. [Copyright obtained from Elsevier.]

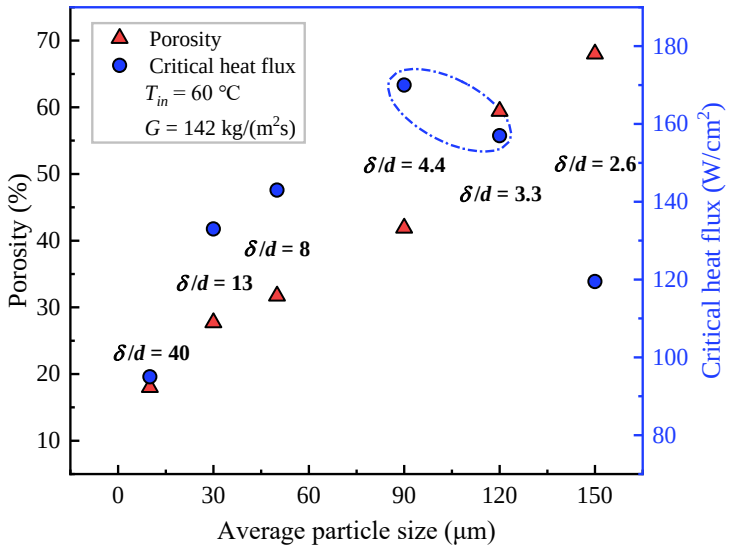

Fig. 9. Comparison of the copper particle sintered porous structure coating porosity and heat transfer with different particle sizes. Experimental conditions in this figure: the inlet temperature is 60 ℃ and the mass flux is 142 kg/(m^{2}s) [76]. [Reproduction and copyright obtained from Elsevier.]

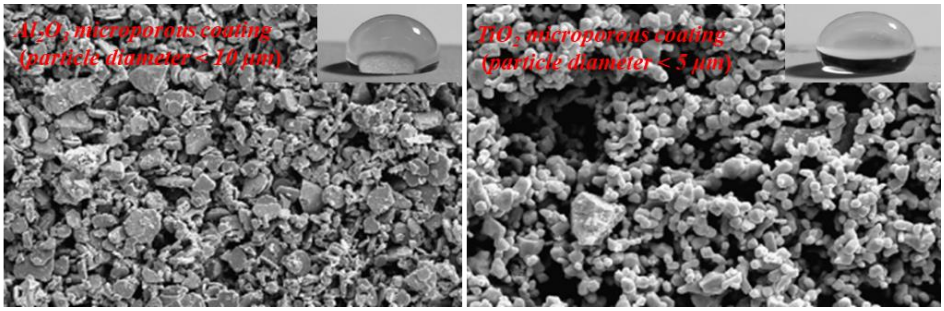

Fig. 10. Comparison between Al_2O_3 microporous coating and TiO_2 microporous coating [107].

[Copyright obtained from Elsevier.]

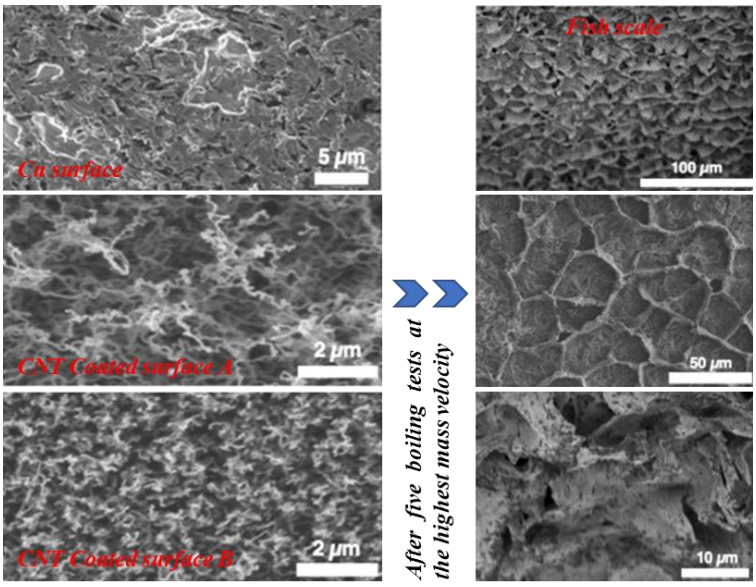

(a) SEM image of different CNTs coating microstructure [73]. The left image shows the CNTs coating before the experiment, while the right image shows the CNT cellular and the unique "fish scale" shape coating formed after multiple experiments.

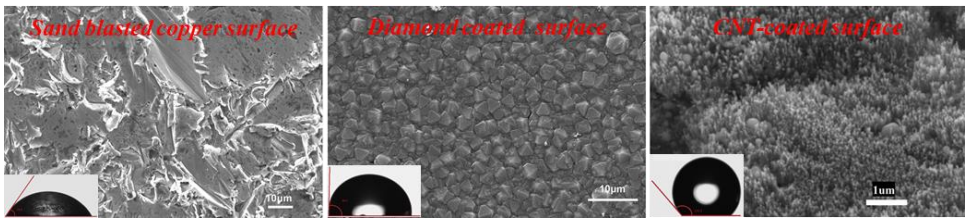

(b) SEM image of sandblasted copper and CNTs coating microstructure [112]. The image on the left is the sand blasted copper surface, the middle is the diamond coated surface, and the right is the CNTs coating surface. In addition, there is also an inset of the contact angle in the bottom left corner of each image.

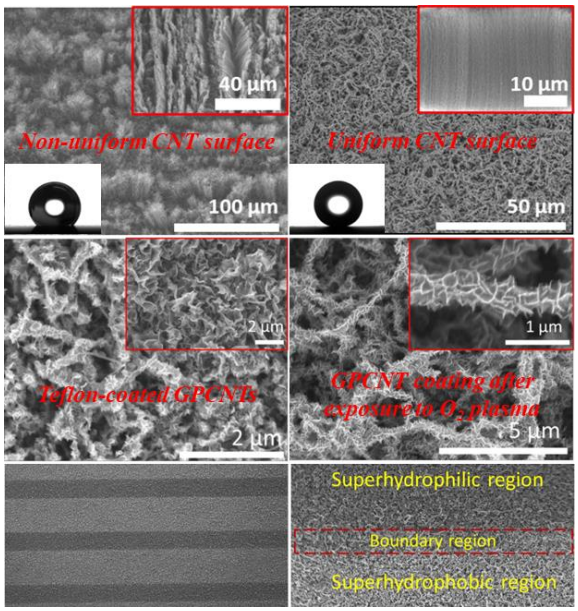

(c) Coating microstructure and the alternating non-uniform wetting surface [113]. The two images in the upper layer show the non-uniform CNTs coating surface and the uniform CNTs coating surface, respectively; the middle layer is Teflon-coated GPCNTs and GPCNT coating after exposure to O_2 plasma; the lower layer is a wetting surface composed of parallel and alternating superhydrophobic and superhydrophilic regions.

Fig. 11. SEM images of CNPs coatings. [Copyright obtained from Elsevier.]

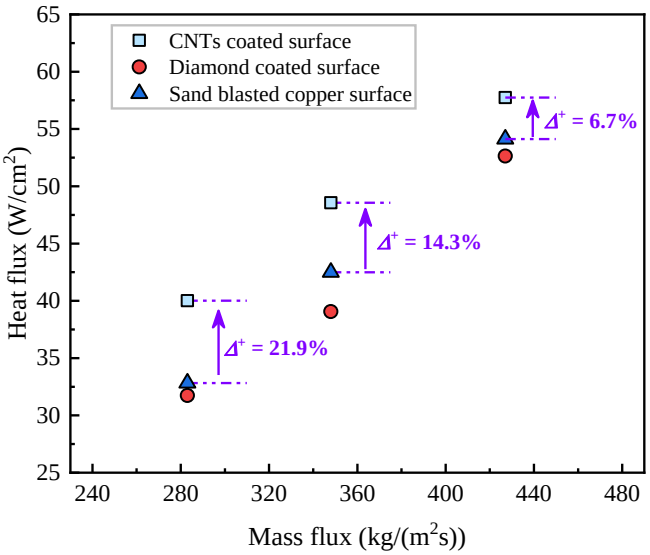

Fig. 12. The trend of enhanced heat transfer of CNTs coatings with various mass flux [112].

[Reproduction and Copyright obtained from Elsevier.]

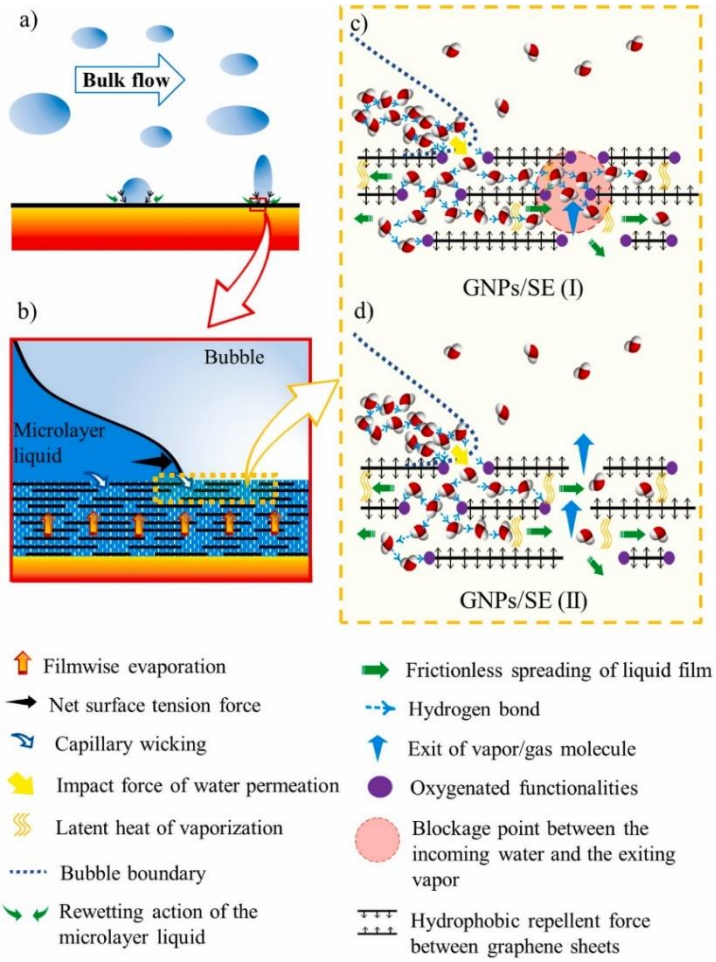

(a) GNPs/SE coating.

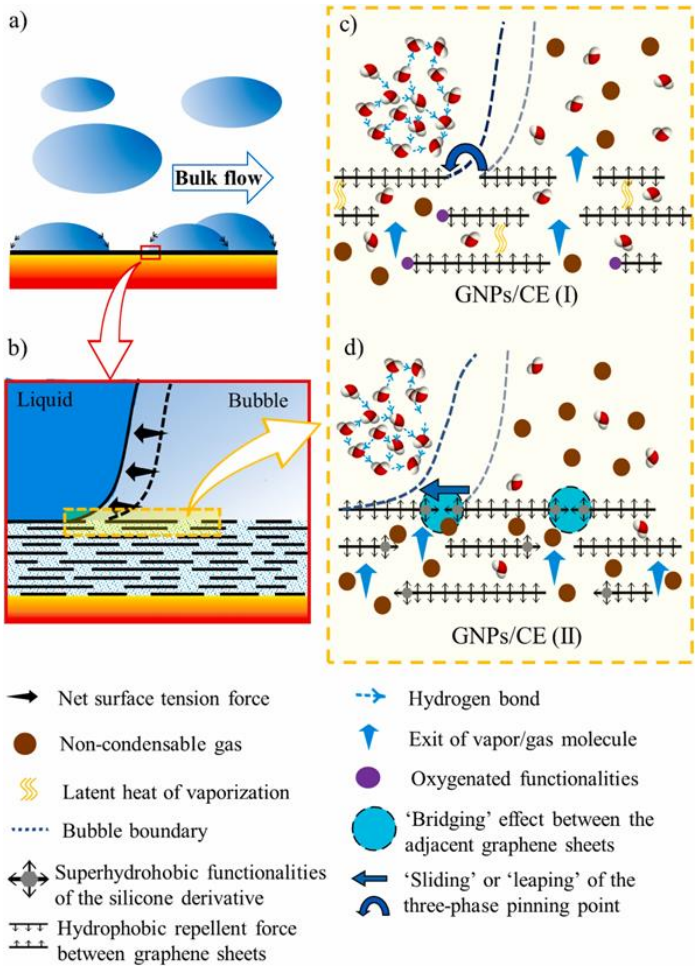

(b) GNPs/CE coating.

Fig. 13. Mechanism and comparison of enhanced heat transfer of graphene coatings [114]: (a) Liquid permeation dynamic process of GNPs/SE coating; (b) Liquid permeation dynamic process of GNPs/CE coating. In this figure: superhydrophilic surface GNPs/SE(I) (the GNPs/SE coating was cured at 300 ◦C for 40 min, ultrafast water permeability), superhydrophilic surface GNPs/SE(II) (the GNPs/SE coating was cured at 250 ◦C for 40 min), superhydrophobic surface GNPs/CE(I) (the GNPs/CE coating was cured with Kapton polyimide tape at 300 ◦C for 40 min), hydrophobic surface GNPs/CE(II) (the GNPs/CE coating was cured at 180 ◦C for 5 h). [CC-BY license.]

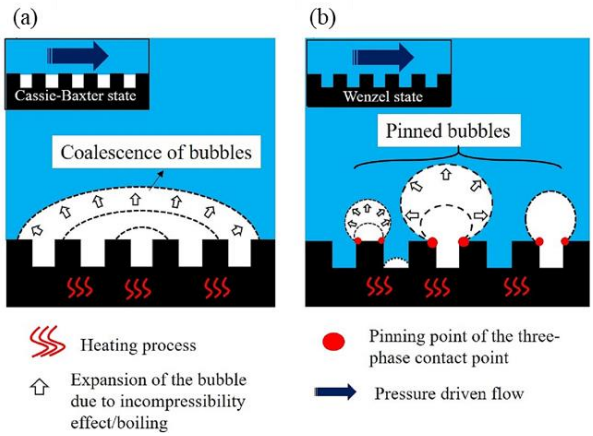

Fig. 14. The dynamics of bubbles during the flow boiling process (the pressure-induced wetting transition process) [115]: (a) Conventional superhydrophobic surface; (b) Superhydrophobic GNPs-coated surface. [CC-BY license.]

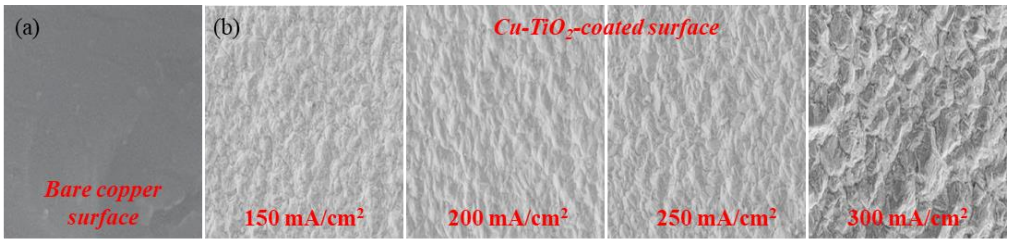

Fig. 15. Comparison of the SEM images of the surface microstructure of Cu-TiO_2 coatings prepared with two electrochemical deposition techniques [116]: (a) Bare copper surface; (b) Two-step electrochemical deposition porous coating surface. [Copyright obtained from Elsevier.]

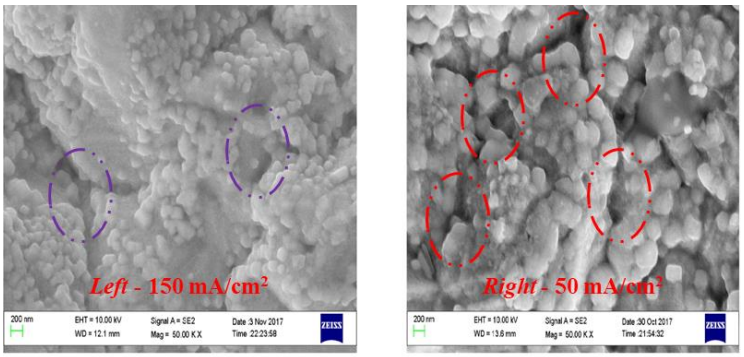

Fig. 16. Comparison of the SEM images Cu-Al_2O_3 porous coating surface micropores with two current densities [119]. The left is higher current density (150 mA/cm^2) and the right is lower current density (50 mA/cm^2). [Copyright obtained from Elsevier.]

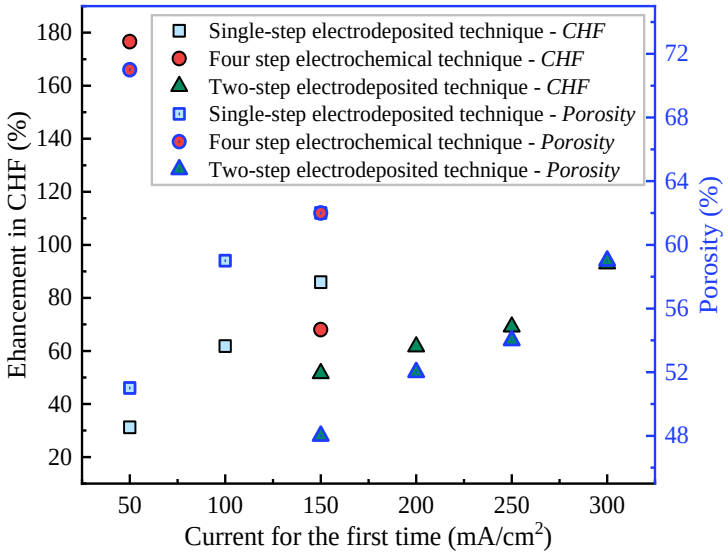

Fig. 17. Comparison of the CHF enhancement and porosity with different Cu-Al_2O_3 porous coatings [118-120]. [Reproduction and copyright obtained from Elsevier.]

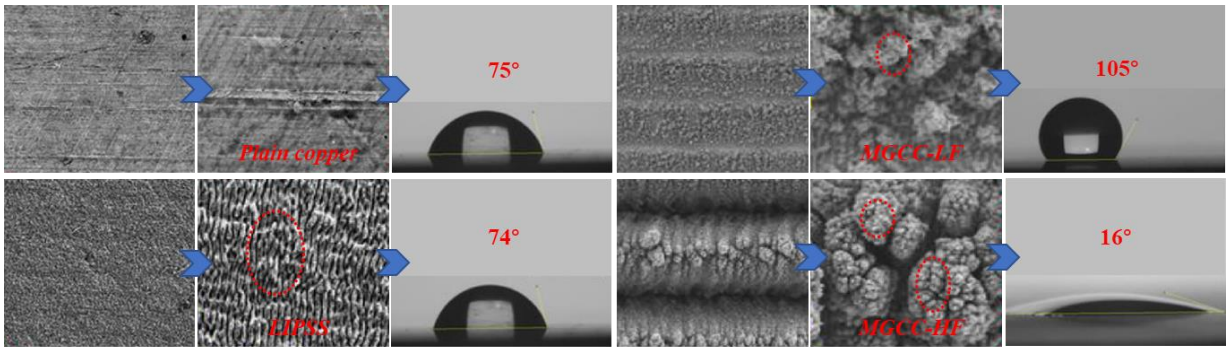

(a) Surface microstructure and wettability.

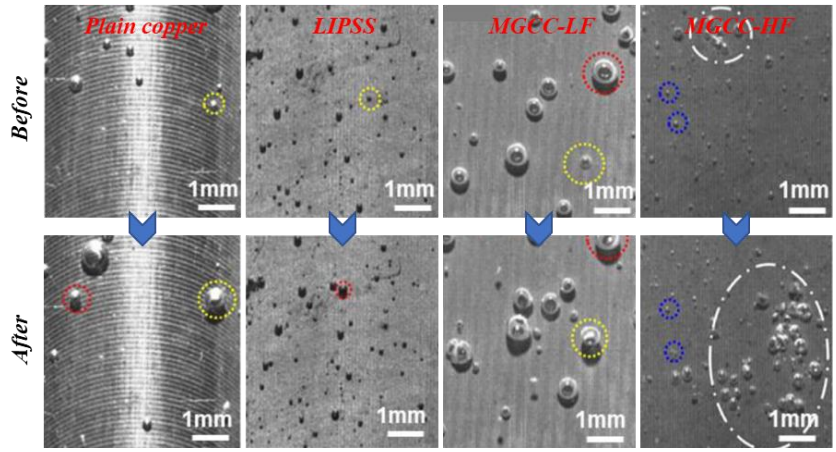

(b) Comparison of the bubble nucleation and growth processes at the heat flux of 50 W/cm^2 and the mass flux of 400 kg/(m^{2}s).

Fig. 18. Microstructures and boiling of the laser-induced surfaces [81]. [Copyright obtained from Elsevier.]

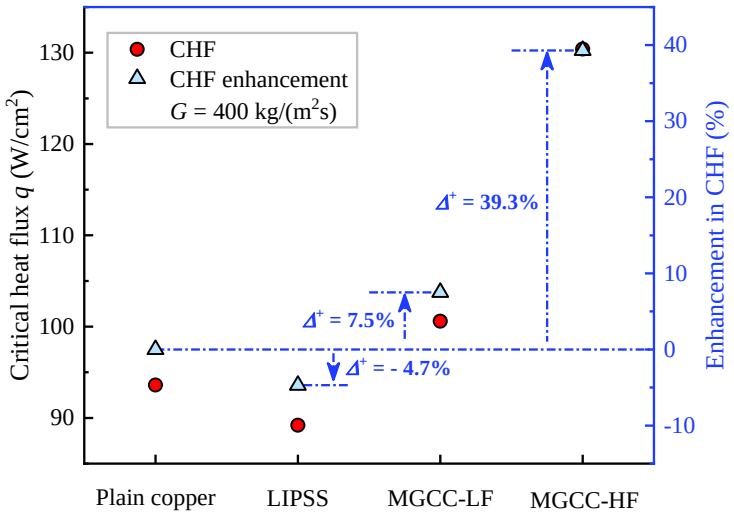

Fig. 19. Improvement rate of the CHF in minichannels of the laser-induced surfaces at the mass flux of 400 kg/(m^{2}s) [81]. [Reproduction and copyright obtained from Elsevier.]

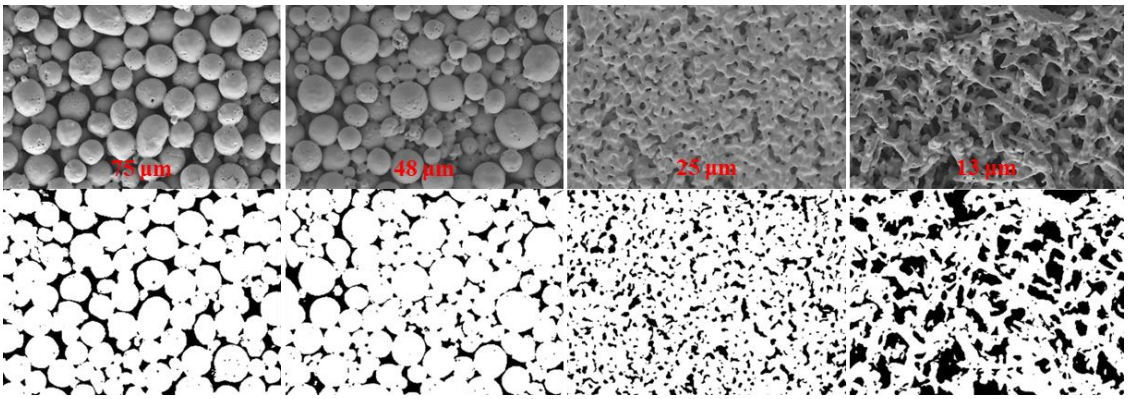

(a) SEM image of porous coatings and corresponding binary method image.

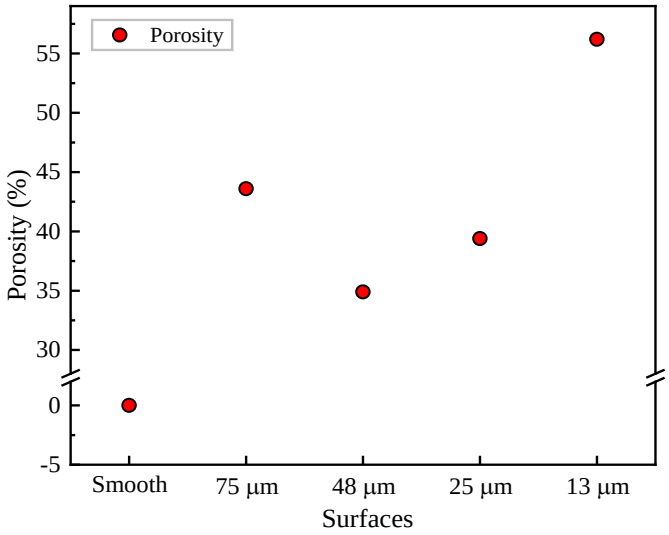

(b) Change in porosity of porous coatings.

Fig. 20. Differences in porous coatings with different particle sizes [135]. [Reproduction and copyright obtained from Elsevier.]

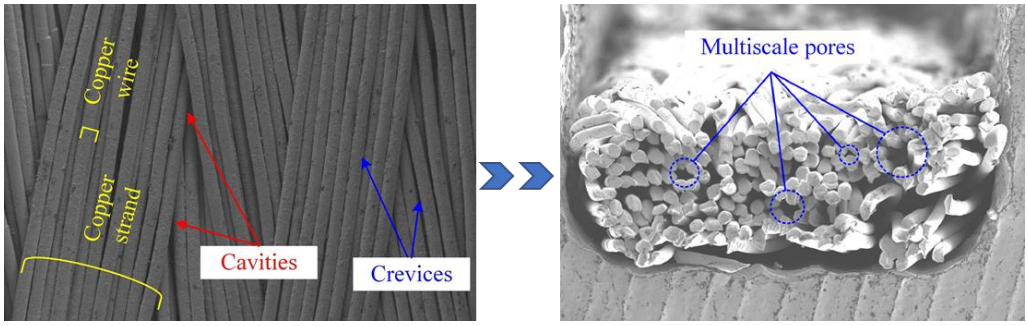

(a) Schematic diagram of porous structure.

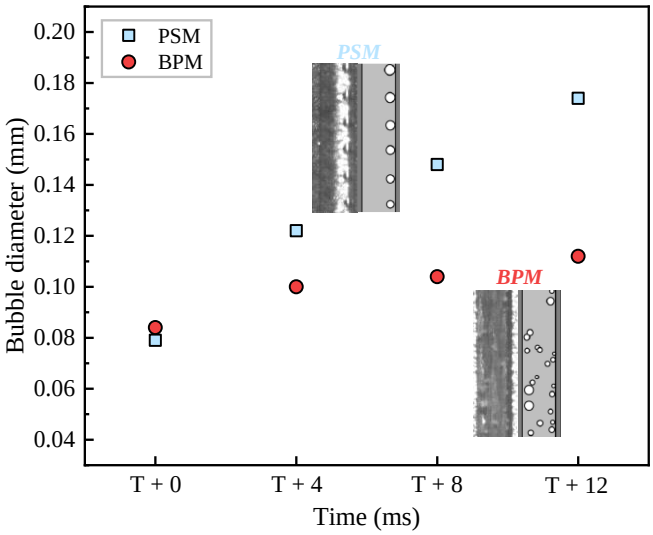

(b) Comparison of bubble diameter at $G = 253$ kg/(m^{2}s) and $q_{eff} = 11.2$ kW/m^2.

Fig. 21. Porous copper woven tape structure [77, 142]. [Reproduction and copyright obtained from Elsevier.]

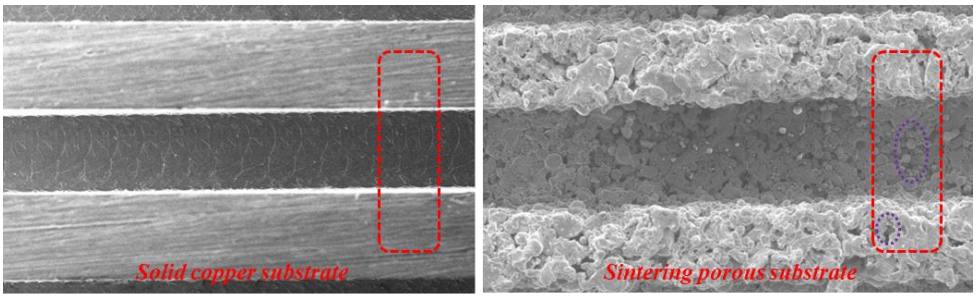

(a) Comparison of microstructure.

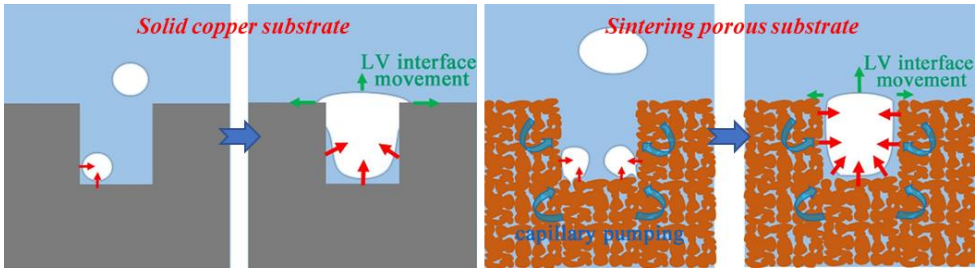

(b) Bubble nucleation process.

Fig. 22. Structure and nucleation mechanism of solid channels and porous channels [143]. The left image is solid copper substrate heat sink and the right is sintering porous substrate heat sink. [Copyright obtained from Elsevier.].

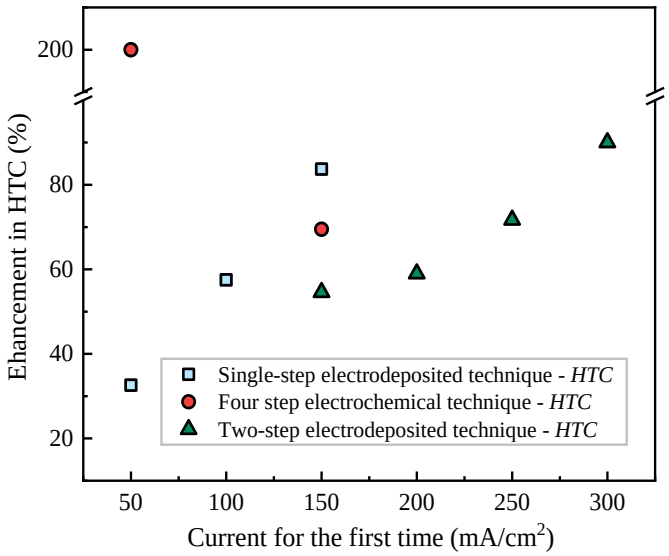

Fig. 23. Comparison of the HTC enhancement with different Cu-Al_2O_3 coatings formed by various techniques [118-120]. [Reproduction and copyright obtained from Elsevier.]

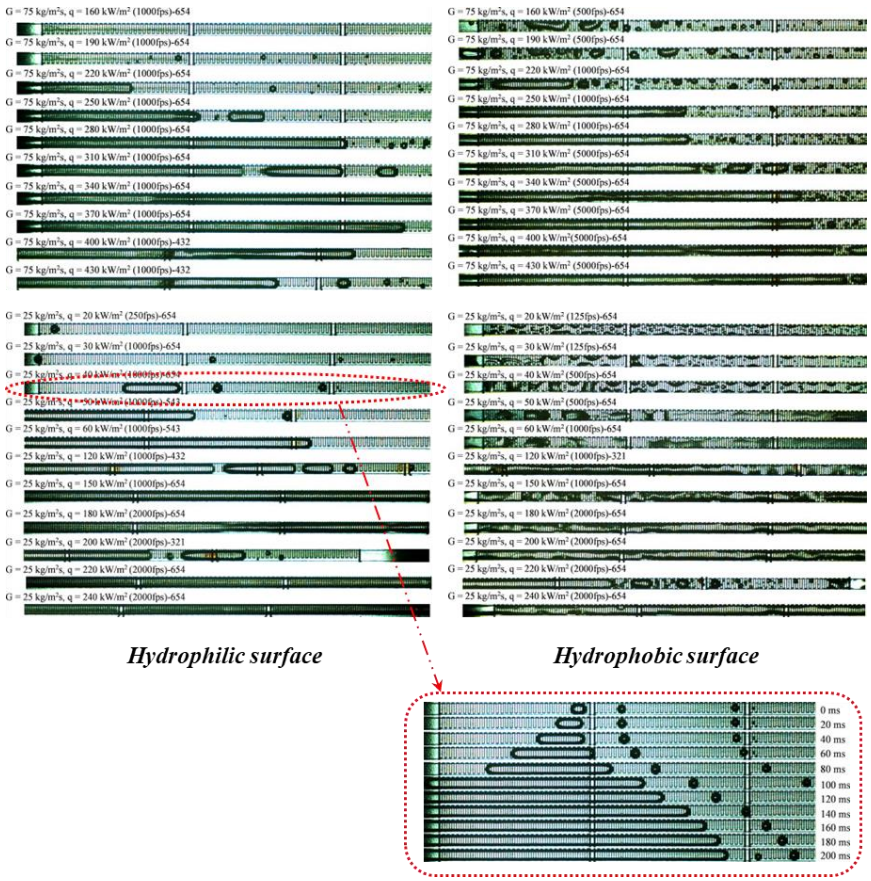

Fig. 24. Comparison of flow patterns between hydrophilic and hydrophobic surfaces [148].

[Copyright obtained from Elsevier.]

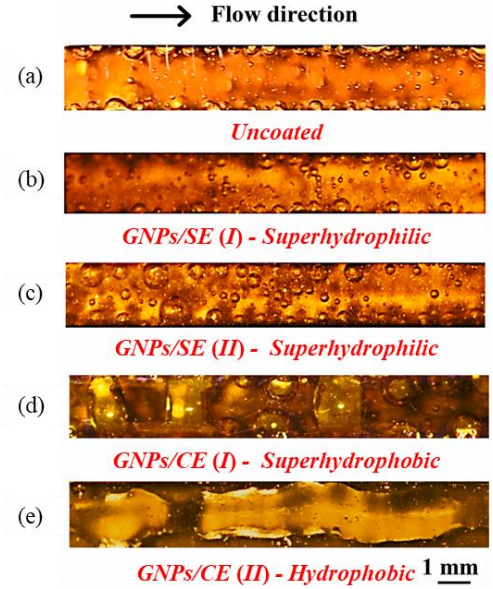

Fig. 25. Flow boiling in minichannels with a heat flux of 380 kW/cm^2 and a mass flux of 42 kg/(m^{2}s) [114]: (a) Uncoated surface; (b) GNPs/SE (I) surface; (c) GNPs/SE (II) surface; (d) GNPs/CE (I) surface and (e) GNPs/CE (II) surface. [CC-BY license.]

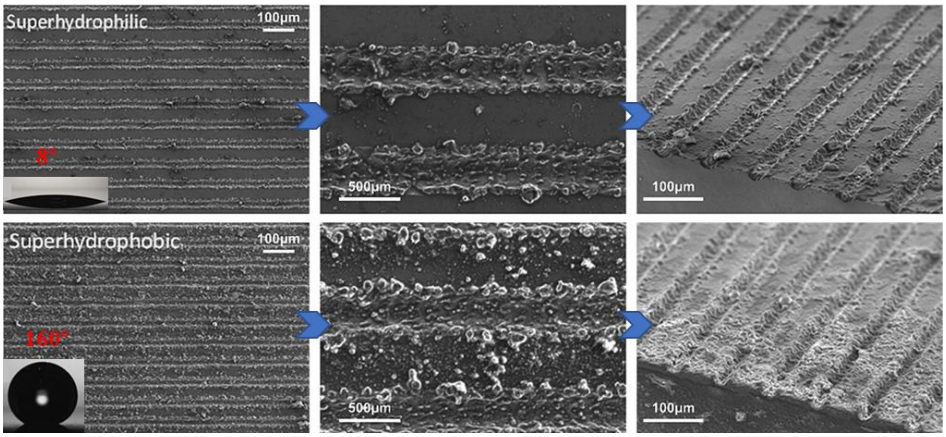

Fig. 26. SEM images of the microstructures of textured surfaces formed by laser etching techniques [150]. [Copyright obtained from Elsevier.]

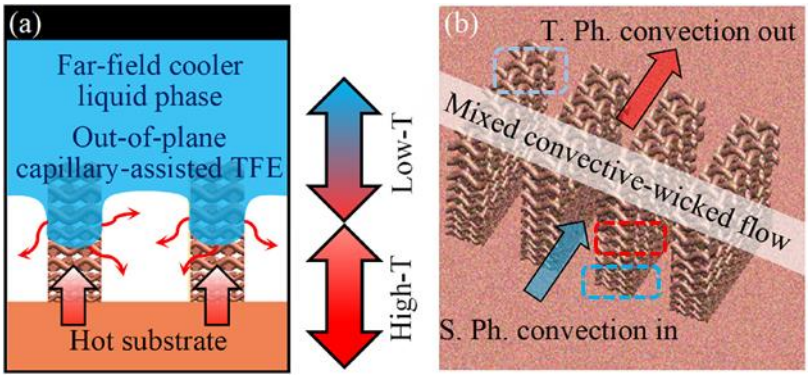

Fig. 27. Gradient wick minichannel heat sink [155]: (a) Schematic of a possible liquid-vapor interface; (b) Schematic of the structure. In this figure: “T.F.E.”, “S. Ph.” and “T. Ph.” stand for thin film evaporation, single-phase, and two-phase, respectively. [Copyright obtained from Elsevier.]

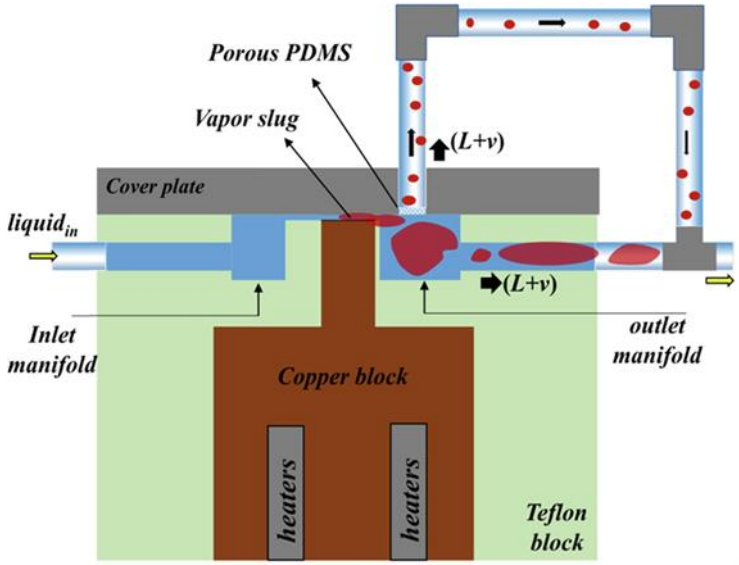

Fig. 28. The structure of secondary flow path based on hydrophobic porous PDMS [189]. [Copyright obtained from Elsevier.]

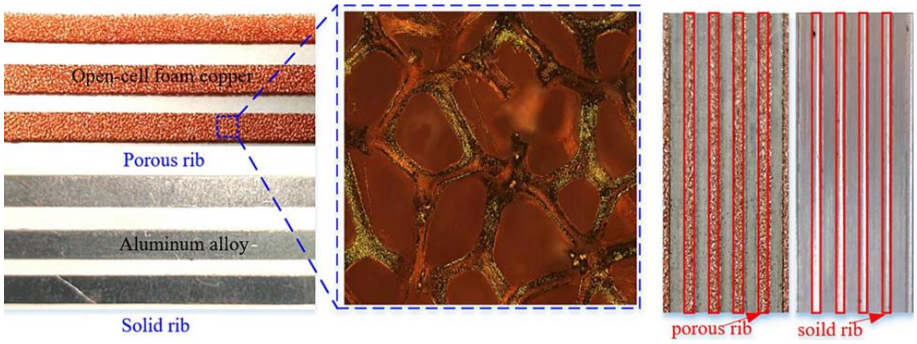

(a) Schematic diagram of mini-channel structure.

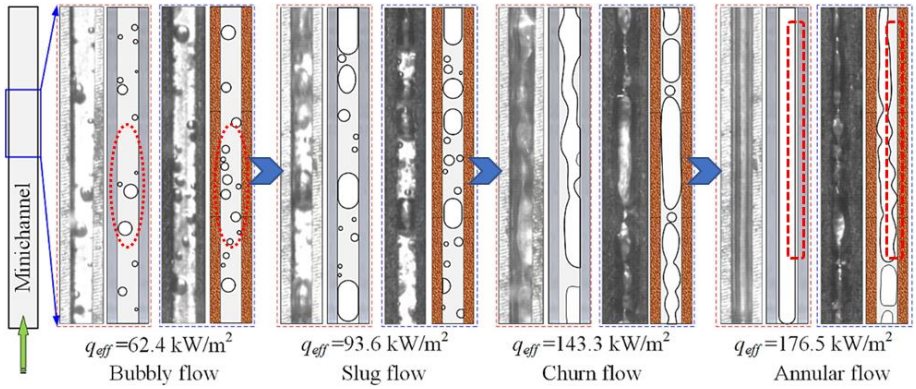

(b) Comparison of nucleation and boiling development processes at a mass flux of 115.5 kg/(m^{2}s) and an inlet temperature of 60 ℃.

Fig. 29. The structures and flow patterns of aluminum-based porous rib minichannels [208]. [Copyright obtained from Elsevier.]

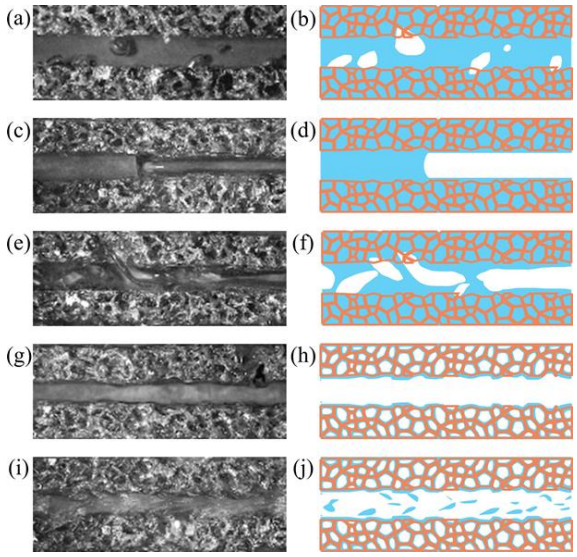

Fig. 30. Different flow patterns in foam copper microchannels [151]: (a) and (b) bubbly flow (G = 205 kg/(m^{2}s), q_{eff} = 296 W/cm^2, x = 0.007); (c) and (d) slug flow (G = 68 kg/(m^{2}s), q_{eff} = 17 W/cm^2, x = 0.04); (e) and (f) churn flow (G = 102 kg/(m^{2}s), q_{eff} = 56 W/cm^2, x = 0.09); (g) and (h) annular flow (G = 68 kg/(m^{2}s), q_{eff} = 117 W/cm^2, x = 0.53) and (i) and (j) wispy-annular flow (G = 409 kg/(m^{2}s), q_{eff} = 297 W/cm^2, x = 0.19). [Copyright obtained from Elsevier.]

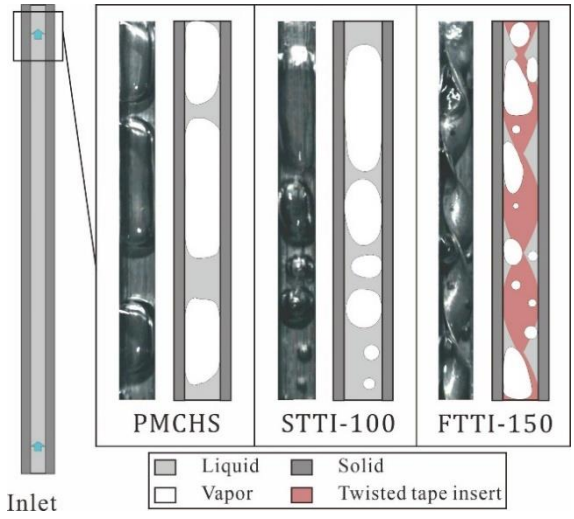

(a) The high-speed images and reconstructed images for the plain minichannel heat sink, the minichannel heat sinks with twisted tape lengths of 100 mm (STTI-100) and the minichannel heat sinks with twisted tape lengths of 150 mm (FTTI-150) at q_{eff} = 142.4 kW/m^2, G = 120.7 kg/(m^{2}s) and T_{in} = 80 °C [188].

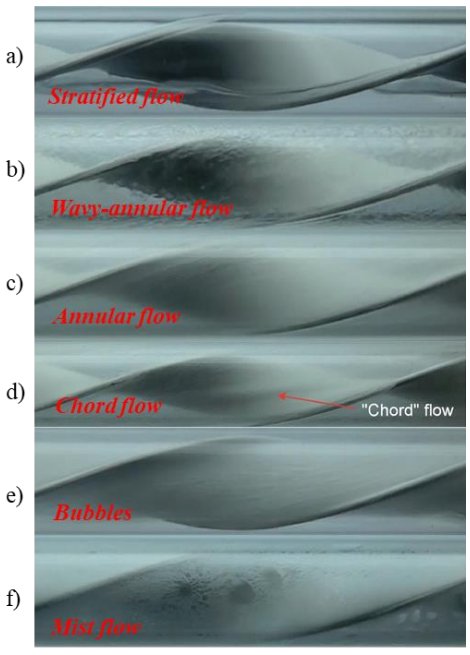

(b) Flow images for distinct flow patterns during R134a convective flow boiling at p = 550 kPa and twist ratio is 4 [213].

Fig. 31. Influence of twisted tapes on flow patterns. [Copyright obtained from Elsevier.]

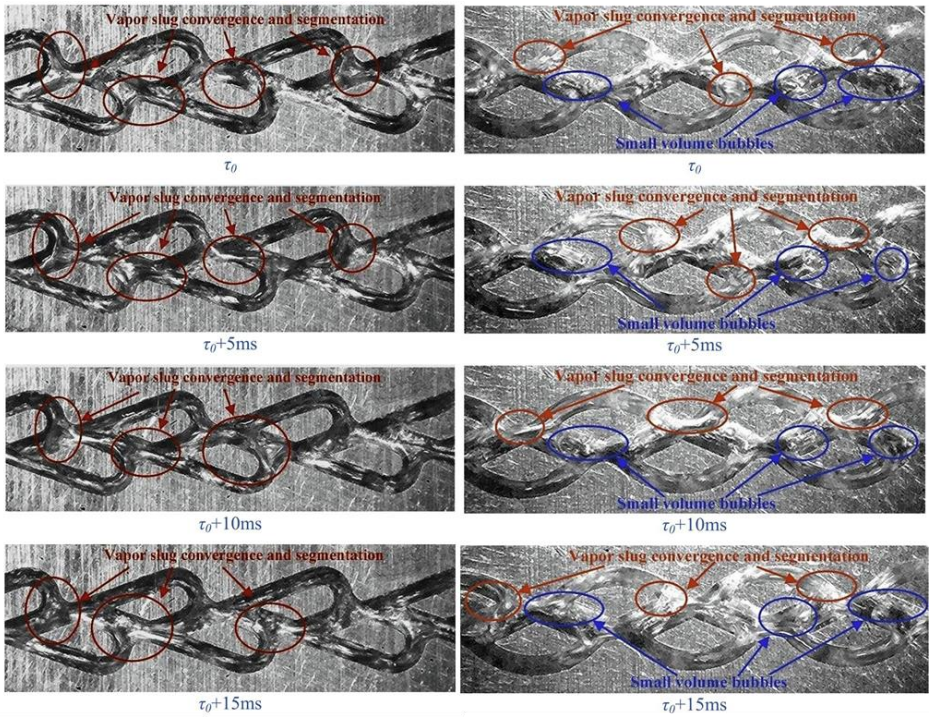

Fig. 32. Flow pattern snapshot at T_{in} = 20 °C, m = 2.93 g/s [198]: (a) Tesla-type structure at q_{eff} = 12.97 W/cm^2; (b) Sector bump structure at q_{eff} = 12.84 W/cm^2. [Copyright obtained from Elsevier.]

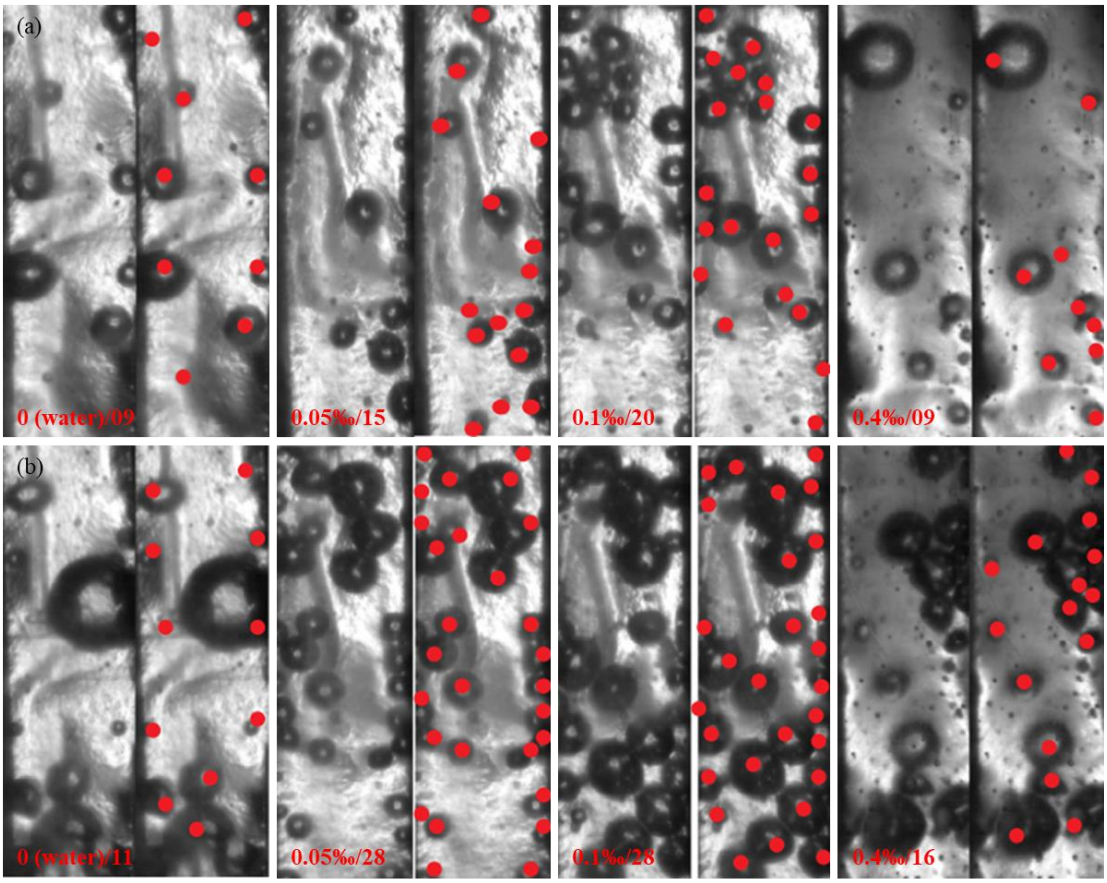

Fig. 33. The nucleation sites on heating surface at different CTAC/NaSal aqueous solution concentrations [218]: (a) The heat flux is 1.7×10^5 W/m^2; (b) The heat flux is 2.9×10^5 W/m^2. [Copyright obtained from Elsevier.]

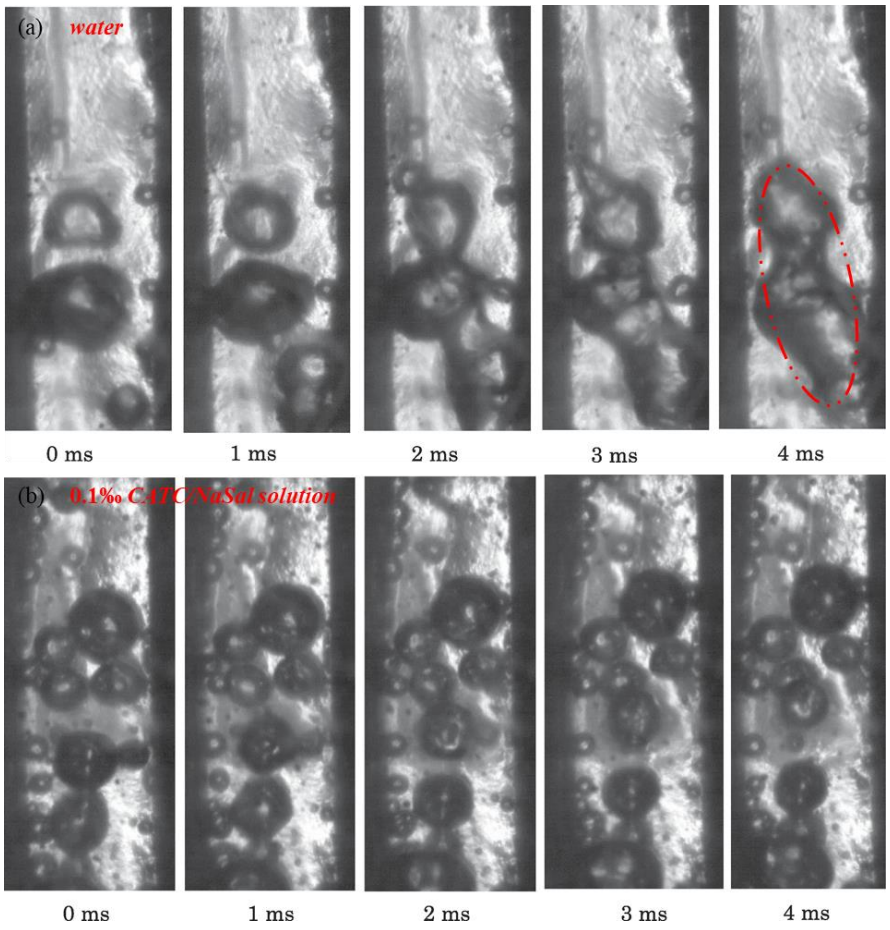

Fig. 34. Sequential images of the flow patterns in channels at q = 2.9 × 10^5 W/m^2 (G = 152 kg/(m^2s), $\Delta T_{sub,\ in}$ = 20 K) [218]: (a) Water; (b) 0.1‰ CATC/NaSal solution. [Copyright obtained from Elsevier.]

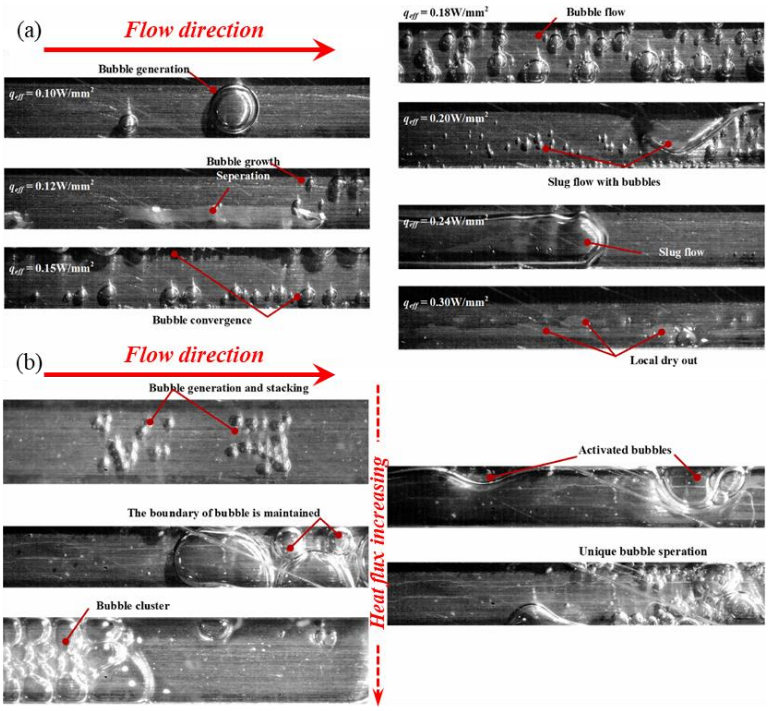

Fig. 35. Comparison of the flow pattern in straight microchannels [224]: (a) Without surfactant SDS; (b) With surfactant SDS. [Copyright obtained from Elsevier.]

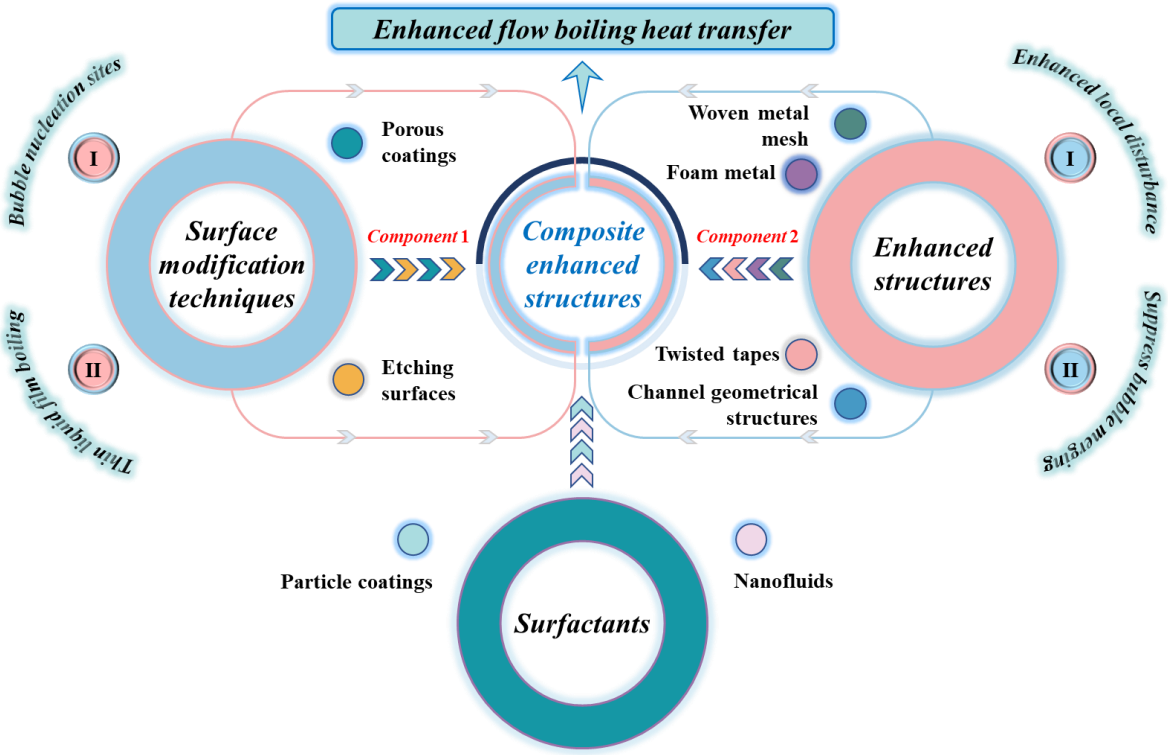

Fig. 36. Schematic diagram in formation of composite enhanced structures.

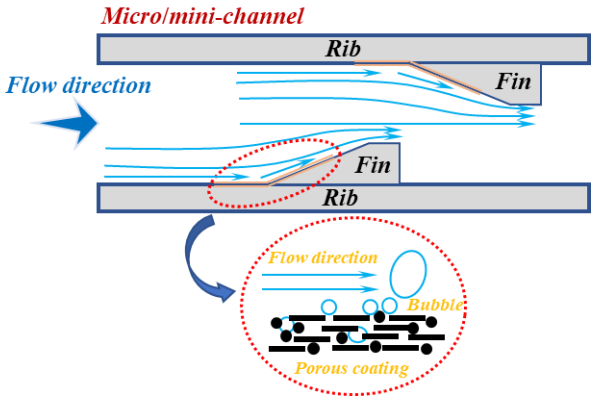

Fig. 37. An ideal heat transfer mechanism for composite enhanced heat transfer techniques.